8-2015

# Designing a Minimal-Knowledge Controller to Achieve Fast, Stable Growth for Recombinant Escherichia coli Cultures

Matthew E. Pepper
*Clemson University*

# Designing a Minimal-Knowledge Controller to Achieve Fast, Stable Growth for Recombinant Escherichia coli Cultures

---

A Dissertation
Presented to
the Graduate School of
Clemson University

---

In Partial Fulfillment
of the Requirements for the Degree
Doctor of Philosophy
Electrical Engineering

---

by
Matthew E. Pepper
August 2015

---

Accepted by:
Dr. Richard Groff, Committee Chair
Dr. Sarah Harcum
Dr. Yongqiang Wang
Dr. Adam Hoover

# Abstract

The biopharmaceutical industry is constantly developing new recombinant *Escherichia coli* strains to bring new products to market. In early stages of development, small scale bioreactors are used to make the product and explore different growth protocols. Researchers spend significant time finding a feed rate profile that will give fast growth and low byproduct accumulation. The objective for the controller presented in this work is to achieve fast growth and low acetate accumulation for an *E.coli* fermentation. The controller does not rely on previous characterization data or models but on fundamental metabolic relationships between oxygen and glucose as dictated by the Crabtree effect. The controller senses metabolic state using an online oxygen uptake rate ($OUR$) estimate and pushes the culture to the boundary of oxidative and overflow metabolism (BOOM). A simulated *E.coli* culture and bioreactor were constructed to test controller performance. Fermentation experiments compared the BOOM controller to an Exponential feed and a DO-stat controller. Using minimal knowledge about the strain, the BOOM controller kept an induced *E.coli* MG1655 pTVP1GFP strain growing near the boundary of oxidative and overflow metabolism. The BOOM controller produced more recombinant protein than the Exponential feed controller and the DO-stat controller, even though the growth rate used by the Exponential feed controller was extensively researched by a previous group. In another fermentation, the temperature was lowered to incur a fast change

in the *E.coli* metabolism. In all experiments, the BOOM controller demonstrated it could maintain fast growth and avoid inhibitory acetate concentrations while requiring minimal knowledge of the*E.coli* MG1655 pTVP1GFP strain. For laboratories which deal with many different strains and proteins, the BOOM controller would maximize protein production and speed up protocol development.

# Dedication

I dedicate this work to God, who blessed me throughout my graduate school career with amazing people, opportunties, and great success. The character change that I sought was always there in Jesus, but it took this path to fully realize that. I dedicate this to my parents who were a great support and an unwavering source of acceptance, love,and encouragement. Also, to my grandparents and family, whose prayers bless me more than I will ever know in this life. I have been blessed to have been surrounded by a great cloud of witnesses in Clemson. I will treasure these relationships for the rest of my life and into eternity. Thank you.

I dedicate this work to my advisors, without whom I would not have gotten to do so much collaborative work. My graduate career has been an journey into the uncharted, I appreciate the freedom I was given to make my own path. Dr. Groff, you were always available and ready to brainstorm, the best ideas came from our impromptu meetings. Dr. Harcum, your enthusiam kept me motivated and made me believe that an electrical engineer could do valuable work in this field. Thanks for your trust and for giving me free reign in your lab. Tom, for your great patience in dealing with a lab of electrical engineers. You were always ready with a helpful answer to our endless questions. To Li, Ajay, Shahin, Mayyan, Aswini, and Nick, I can't thank you enough for your great work and many hours of support during our experiments. This dissertation is a direct result of our collaboration.

# Table of Contents

# List of Tables

# List of Figures

# Chapter 1

# Introduction

The commercialization of therapeutic products cultivated and harvested from microorganisms began with *pencillin* in the late 1940s. The modern era of biotechnology began in the late 1970s when the procedures of Stanley Cohen with *Escherichia coli* (*E.coli* ) were translated into the industrial production of recombinant proteins. Currently, the biopharmaceutical industry depends heavily on *Saccharomyces cerevisiae* , *E.coli* , and Chinese hamster ovary (CHO) cells to produce recombinant proteins. *E.coli* are used to produce over half the recombinant protein entities [Jayaraj and Smooker, 2009]. *E.coli* is used for these products because it is easy to grow, grows quickly, and scales up easily for large production [Jayaraj and Smooker, 2009]. Also *E.coli* can grow on a variety of feed stocks, can tolerate relatively large pH and temperature ranges, and has a fully sequenced genome. *E.coli* is insensitive to shear effects, in contrast to animal cells, which can be damaged at high speeds [Simon and Karim, 2001].

In order to produce a biopharmaceutical, first researchers examine the growth of the organism to be used in special vessels, known as bioreactors or fermenters. Researchers interpret the behavior of the organism to different temperature, pH, oxygen

and substrate concentrations. They also identify desired ranges of growth and develop feeding procedures, a.k.a. protocols. These early fermentation studies, to date, have focused on maintaining set conditions in the fermenter. Having the capability to control cell behavior directly could reduce fermenter protocol development times. In both yeast and *E.coli* fermentations where biopharmecutical production is the goal, fast growth and low waste production is desired because waste product accumulation can cause the culture to become inefficient at producing the biopharmaceutical. Fast growth with low waste accumulation is the best way to maximize biomass, which maximizes overall recombinant protein production. Unfortunately, controlling a fermenter is not straightforward because real-time measurement of biomass and metabolite concentrations in the culture is currently expensive and not possible for all metabolites.

The objective of this study was to design a controller that would control the behavior of an *E.coli* culture in a fermenter. The controller guides the culture to fast growth while avoiding waste concentrations which could hinder biopharmaceutical production. The controller uses only real-time sensors which are low cost, publically available, and industrially accepted. The controller does not depend explicitly on a predefined culture growth model, but instead depends on the interaction of fundamental metabolic relationships, as seen in [Akesson et al., 1997]. The controller depends heavily on the input of an oxygen uptake rate (OUR) estimator, which constructs a real-time OUR signal from the dissolved oyxgen (DO) probe and exhaust-gas sensor. The controller applies periodic ramp functions to the feed rate in order to detect metabolic state and drive the culture toward fast efficient growth. A simulation of the *E.coli* culture and fermenation system was constructed in order to test the controller. The controller was used to control both induced and uninduced *E.coli* cultures. Experimental results show that the controller successfully achieved fast, efficient growth in fermentations undergoing either fast (temperature) or slow (in-

duction) metabolic shifts. In experiments measuring the total recombinant protein production, the controller was compared to an exponential and DO stat controller. Protein production was 10% higher than the exponential feed rate protocol tuned using past data. Protein production was 50% higher than the DO stat controller.

This dissertation is structured as follows. Chapter 2 reviews the relevant literature of *E.coli* metabolism, fermentation modelling and recombinant protein prodcution and advance control techniques. Chapter 3 describes the hardware-in-the-loop models used for simulating and deploying the control algorithm. Chapter 4 describes the online OUR estimator that eliminates measurement latency of the exhaust-gas sensor. Chapter 5 describes the metabolic state sensing algorithm. Chapter 6 describes the materials and methods used to validate the algorithm. Chapter 7 assess the algorithm under fed-batch fermentation conditions and compares the outcomes to two more common use control algorithms used in *E.coli* recombinant protein production. Chapter 8 summarizes this work and suggests future work.

# Chapter 2

# Literature Review: *E.coli* Metabolism, Fermenter Modelling, and Advanced Control

In this chapter, a basic overview of *E.coli* metabolism will be presented. The simulation models for growth rate and the mass-balance in the bioreactor are presented. Lastly, a review of the estimation and control algorithms found in literature is presented.

## 2.1 *Escherichia coli*

The *E.coli* metabolism is the rate ($\mu$) in which the cell takes in substrate and produces biomass (X), modeled in (2.1). The rate at which the biomass grows (2.2) is determined by the three phases of *E.coli* metabolism: oxidative ($\mu_1$), overflow ($\mu_2$),

and metabolite consumption ($\mu_3$).

$$X = X_0 \, exp(\mu \, t) \tag{2.1}$$

$$\mu = \mu_1 + \mu_2 + \mu_3 \tag{2.2}$$

Glucose is processed during all three metabolic phases and it's removal from the culture represents the Glucose Uptake Rate (GUR). The reactions presented below follow glucose as it is processed in the cell and reflect the understanding of *E.coli* metabolism adapted from [Wolfe, 2005, Vemuri et al., 2006], see Figure 2.1. The effects of protein production via induction are not included.

#### 2.1.0.1 Oxidative Metabolism, $\mu_1$

The reactions in the oxidative metabolism represent the main source of glucose processing and energy production for the cell. It is important to remember that the rate of glucose absorption by the cell is driven by the glucose concentration in the culture, $S$. As glucose is transported through the cell membrane, it enters glycolysis and is converted into pyruvate; this occurs regardless of surrounding oxygen.

$$\text{glucose} \rightarrow 2 \text{ pyruvate} + 2 \; H^+ + 2 \; ATP + 2 \; H_2O \tag{2.3}$$

The pyruvate undergoes pyruvate decarboxylation and yields acetyl Coenzyme A (Acetyl-CoA).

$$\text{pyruvate} + CoA \rightarrow \; \text{Acetyl-CoA} + H^+ + CO_2 \tag{2.4}$$

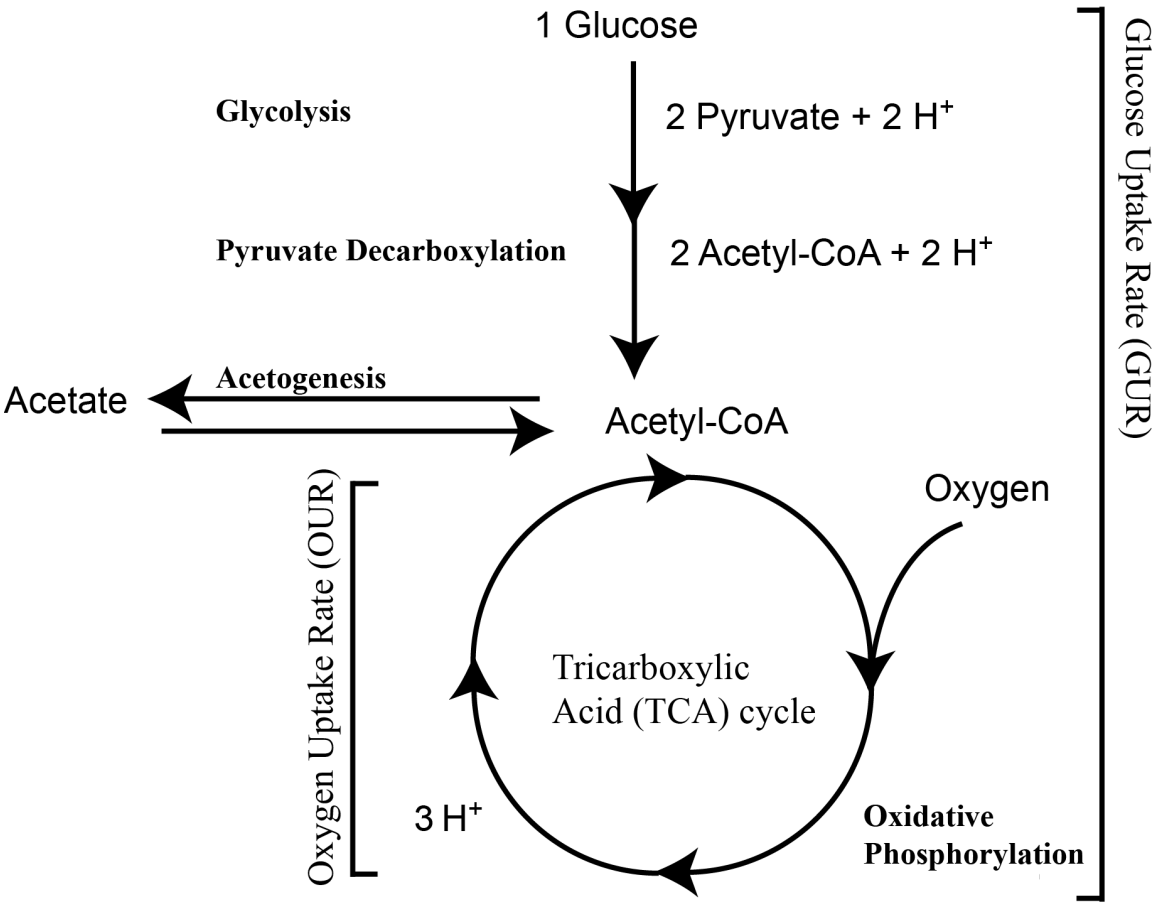


**Acid Contribution per Metabolic Phase:**

Oxidative: 1 Glucose = 10 $H^+$

Overflow: 1 Glucose = 4 $H^+$ + 2 $H^+$ (Acetate)

Metabolite Consumption: 1 Acetate = 3 $H^+$

Figure 2.1: Major reactions that involve the processing of glucose in *E.coli* metabolism. The TCA cycle needs the products produced via oxidative phosphorylation to process the Acetyl-CoA.

Acetyl-CoA is the main carbon input to the tricarboxylic acid (TCA) cycle.

$$\text{Acetyl-CoA} + 3\ NAD^+\ PO_4^{-3} \rightarrow\ \text{CoA} + 3\ NADH + 3\ H^+ + 2\ CO_2 \qquad (2.5)$$

The TCA cycle indirectly uses oxygen to process Acetyl-CoA. Absorbed oxygen is used in a parallel process called oxidative phosphorylation. Oxidative phosphorylation regulates the TCA cycle by accepting electrons from $NADH$, forming $NAD^+$, and releasing them later to help form ATP [Akesson et al., 1999a].

#### 2.1.0.2 Overflow Metabolism, $\mu_2$

If the GUR exceeds the maximum rate of the TCA cycle and the oxidative phosporylation process [Johnston et al., 2003], Acetyl-CoA concentration inside the cell increases. When a certain threshold concentration of Acetyl-CoA is reached, the cell begins to convert Acetyl-CoA to acetate by acetogenesis. Acetogenesis is a reaction that does not require oxygen, decreases the pool of Acetyl-CoA, and provides some $ATP$. The concentration of glucose which forces the *E.coli* into acetogenesis is called the acetate threshold.

#### 2.1.0.3 Metabolite Consumption Metabolism, $\mu_3$

As the glucose concentration outside the cell decreases, the GUR slows down. When the excess Acetyl-CoA inside the cell is depleted by the TCA cycle and acetogenesis, extracellular acetate is absorbed along with glucose where it is converted back into Acetyl-CoA. In this case, the TCA cycle is processing Acetyl-CoA derived from both glucose and acetate.

#### 2.1.0.4 Metabolism and Biomass

Gycolysis and pyruvate decarboxylation are catabolic reactions, meaning these reactions break down complex molecules into simpler ones. The TCA cycle is both catabolic and anabolic; the intermediates produced catabolically by the TCA cycle are used anabolically for the assembly of larger molecules, in this case, additional biomass [Xu et al., 1999]. Oxidative metabolism contributes the most toward the growth rate of a culture. Overflow metabolism and metabolite consumption only generate a small amount of biomass while active. The most efficient use of glucose and the best condition for fast growth is to drive the growth rate to the boundary of oxidative and overflow metabolism (BOOM). When a culture is in the BOOM region, it is maximizing oxidative metabolism and minimizing overflow metabolism.

## 2.2 *E.coli* Growth Rate Model Selection

It is important to choose a growth rate model representative of the microorganism when modeling a bioreactor system. There are more than fifty different types of growth rate models found in the literature. One of the most popular growth rate models is the Monod model, developed in 1942 to describe microorganism growth data [Bastin and Dochain, 1990]. One example of a Monod growth model is

$$\mu(S) = \frac{S}{K_s + S} \tag{2.6}$$

where $\mu$ is the growth rate (1/h), $S$ the substrate concentration (g/L), and $K_s$, the saturation (or half growth-rate) constant. The saturation constant, $K_s$, represents the substrate concentration at which growth is at half the maximum growth rate. In (2.7), the growth rate is also a function of the substrate concentration, but here

additional polynomials have be added to account for chemicals that cause growth rate inhibition. In [Mohseni et al., 2009], the authors added a term which inhibits the growth rate as the acetate concentration, $A$, increases.

$$\mu(S, A) = \left(\frac{S}{K_s + S}\right)\left(\frac{K_i}{K_i + A}\right) \tag{2.7}$$

The inhibition constant, $K_i$, represents the concentration of acetate which limits the growth rate to half its maximum rate. Two other popular growth rate models are: 1) the Haldane model, which describes inhibition due to high substrate concentration 2) the Contois model, which describes inhibition due to high biomass concentration [Bastin and Dochain, 1990, Rahman et al., 2010].

The Monod model does not represent all the phases of *E.coli* metabolism. There is no provision for the transition from oxidative to overflow metabolism, nor the consumption of extracellular acetate. Several models in literature extend the single Monod model to a series of Monod equations that control the fluxes of glucose, oxygen, and acetate into the cell. Those fluxes are constrained by the current state of the metabolism and combined to form the growth rate. These growth models are not continuous like a single Monod expression, but piecewise continuous, meaning the growth rate model changes based upon the current metabolic phase [Pomerleau and Perrier, 1990, Bastin and Dochain, 1990, Akesson et al., 1997, Xu et al., 1999, Rocha and Ferreira, 2002, Karakuzu et al., 2006]. These types of growth rate models are more metabolically accurate.

### 2.2.1 The Xu Growth Rate Model

The growth rate model selected for this project is piecewise continuous and taken from [Xu et al., 1999]. The metabolic parameters for this model were fitted

based on experiments using the *E.coli* W3110 strain. This model was selected as the growth rate model for the simulation and testing of control algorithms for this project because it's behavior is similar to the *E.coli* MG1655 pTVP1GFP strain. The growth rate, $\mu$, calculation for the Xu model begins with the glucose flux into the cell:

$$qS = \left(\frac{qS_{max}}{1 + A/K_{i,S}}\right)\left(\frac{S}{S + K_s}\right) \tag{2.8}$$

The total substrate flux is limited by $qS_{max}$ . This limit is scaled by the acetate concentration, which has been shown to have an inhibitory affect at levels exceeding 2 g/L [Babaeipour et al., 2007]. As shown in Section 2.1, glycolysis and pyruvate decarboxylation turn all glucose into Acetyl-CoA. Acetyl-CoA can follow two separate metabolic paths: oxidative or overflow metabolism.

$$qS = qS_{ox} + qS_{of} \tag{2.9}$$

The processing rate of Acetyl-CoA due to the oxidative metabolism is $qS_{ox}$. The processing rate of Acetyl-CoA due to overflow metabolism via acetogenesis is $qS_{of}$. Oxygen is used to process Acetyl-CoA in two ways, in the TCA cycle to make energy and in the anabolism to make biomass. $qS_{ox}$ is split into two parts, one part representing the processing rate of Acetyl-CoA for anabolism, $qS_{ox,an}$, the other for the TCA cycle, $qS_{ox,en}$.

$$qS_{ox} = qS_{ox,an} + qS_{ox,en} \tag{2.10}$$

These magnitude of $qS_{ox,an}$ is calculated by examining the carbon mass balance equa-

tions:

$$\begin{aligned} &\text{carbon flux to anabolism} = qS_{ox,an}C_S \\ &\text{carbon flux converted to biomass} = (qS_{ox} - q_m)Y_{X/S_{ox}}C_X \end{aligned} \tag{2.11}$$

where $C_S$ represents the carbon content of glucose (mol/g), $Y_{X/S_{ox}}$ the yield coefficient exclusive of maintenance ($q_m$), and $C_X$ the carbon content of biomass (mol/g). Equation 2.11 defines the same process in two different ways; $qS_{ox,an}$ can be solved for by setting the two equations equal to each other. The anabolic rate is:

$$qS_{ox,an} = (qS_{ox} - q_m)Y_{X/S_{ox}}\frac{C_X}{C_S} \tag{2.12}$$

and the rate of the TCA cycle is calculated from the remainder.

$$qS_{ox,en} = qS_{ox} - qS_{ox,an} \tag{2.13}$$

The total oxygen flux into the cell is

$$qO = qO_S + qA_{c,en}Y_{O/A} \tag{2.14}$$

In oxidative metabolism, the rate of oxygen used by the TCA cycle is

$$qO_S = qS_{ox,en}Y_{O/S} \tag{2.15}$$

In low glucose concentrations this value stays below the maximum rate, limited by $qO_{max}$:

$$qO_S \leq \frac{qO_{max}}{(1 + A/K_{i,O})} \tag{2.16}$$

Note the inhibition constant, $K_{i,O}$, tied to the acetate concentration in the criteria calculation. It has been shown that as acetate concentration increases, OUR decreases,

slowing down the TCA cycle [Xu et al., 1999]. As the producton of Acetyl-CoA rises due to increasing glucose concentration, the amount of oxygen needed also increases. When $qO$ reaches $qO_{max}$, $qS_{ox}$ cannot increase. When the rate of Acetyl-CoA production exceeds the ability of the anabolism and the TCA cycle to process it, $qS > qS_{ox}$, overflow metabolism begins. In order to calculate $qS$, $S_{ox}$ must be calculated using the new criteria below:

$$\begin{aligned} qO_S &= \frac{qO_{max}}{(1 + A/K_{i,O})} \\ (qS_{ox,en})_{qO_{max}} &= \frac{qO_{max}}{(1 + A/K_{i,O})} \frac{1}{Y_{O/S}} \end{aligned} \tag{2.17}$$

When the culture is not in overflow metabolism, it is assumed that the entire glucose flux is processed oxidatively, $qS_{ox} = qS$. If $qS_{ox,en}$ has a fixed size based on $qO_S$, then the $qS_{ox,an}$ and $qS_{ox}$ values must be resized. This is done by first calculating the $qS_{ox,en}$ assuming $qS_{ox} = qS$. A ratio is formed using this ideal flux value, $(qS_{ox,en})_{qS=qS_{ox}}$ and the value according to $qO_{max}$. This is then used to resize the other two fluxes:

$$ratio = \frac{(qS_{ox,en})_{qO_{max}}}{(qS_{ox,en})_{qS=qS_{ox}}} \tag{2.18}$$

$$(qS_{ox,an})_{qO_{max}} = ratio \quad qS_{ox,an} \tag{2.19}$$

$$(qS_{ox})_{qO_{max}} = (qS_{ox,an})_{qO_{max}} + (qS_{ox,en})_{qO_{max}} \tag{2.20}$$

The value for $qS_{of}$ represents flux for the excess glucose and is now calculated:

$$qS_{of} = qS - (qS_{ox})_{qO_{max}} \tag{2.21}$$

The Acetyl-CoA flux in the overflow metabolism is calculated similarly to oxidative metabolism, with a portion going to anabolism and the rest processed via acetogen-

esis.

$$\begin{aligned} qS_{of,an} &= qS_{of} Y_{X/S_{of}} \frac{C_X}{C_S} \\ qS_{of,en} &= qS_{of} - qS_{of,an} \end{aligned} \tag{2.22}$$

The acetate production rate (APR) is then:

$$qA_p = qS_{of,en} Y_{A/S} \tag{2.23}$$

When the glucose concentration lowers, the excess Acetyl-CoA begins to deplete. When $qO_S < \frac{qO_{max}}{(1+A/K_{i,O})}$, overflow mtabolism ceases. The total consumption of acetate is governed by

$$qA_c = qA_c \frac{A}{A + K_A} \tag{2.24}$$

where $K_A$ is the half-rate constant for acetate consumption. It is divided into two parts.

$$\begin{aligned} qA_{c,an} &= qA_c Y_{X/A} \frac{C_X}{C_A} \\ qA_{c,en} &= qA_c - qA_{c,an} \end{aligned} \tag{2.25}$$

The total oxygen flux into the cell is

$$qO = qO_S + qA_{c,en} Y_{O/A}$$

and $qA_{c,en}$ represents the portion of the TCA cycle that can process Acetyl-CoA

converted from extracellular acetate.

$$qA_{c,en}Y_{O/A} = \frac{qO_{max}}{(1 + A/K_{i,O})} - qO_s \tag{2.26}$$

$$(qA_{c,en})_{qO_{max}} = (\frac{qO_{max}}{(1 + A/K_{i,O})} - qO_s)\frac{1}{Y_{O/A}} \tag{2.27}$$

To ensure that the rate of acetate consumption is properly scaled to occupy the gap between $qO_S$ and the boundary condition. $qA_c$ and $qA_{c,an}$ are rescaled similarly to the substrate flux (2.18).

$$(qA_c)_{qO_{max}} = (qA_{c,en})_{qO_{max}} + (qA_{c,en})_{qO_{max}} \tag{2.28}$$

The total oxygen consumption rate for all 3 metabolic regimes is shown in (2.29) and the total growth rate is shown in (2.30), with the corresponding metabolic regimes.

$$qO = qO_S + qA_{c,en}Y_{O/A} \tag{2.29}$$

$$\mu = \underbrace{(qS_{ox} - q_m)\ Y_{X/S,ox}}_{oxidative} + \underbrace{qS_{of}\ Y_{X/S,of}}_{overflow} + \underbrace{qA_c\ Y_{X/A}}_{metabolite\ \ consumption} \tag{2.30}$$

## 2.3 Mass-balance Model

Once a form for $\mu$ is chosen, it is incorporated into a set of ordinary differential equations defining the mass-balance dynamics of the bioreactor. Equation 2.31 represents the mass-balance equations for biomass, substrate, and acetate concentration

Table 2.1: Parameter definitions and values for the Xu model

| Symbol | Parameter | Value | Units |
|---|---|---|---|
| $C_A$ | mol C per g Acetate | 1/30 | mol $g^{-1}$ |
| $C_S$ | mol C per g Glucose | 1/30 | mol/g |
| $C_X$ | mol C per g Biomass | 0.04 | mol/g |
| $K_A$ | Half rate Acetate Consumption | 0.05 | g/L |
| $K_{i,O}$ | OUR Inhibition by Acetate | 4 | g/L |
| $K_{i,S}$ | GUR Inhibition by Acetate | 5 | g/L |
| $K_S$ | Half rate Glucose Uptake | 0.05 | g/L |
| $qA_{Cmax}$ | max Acetate Consumption | 0.2 | g/(g · h) |
| $q_m$ | maintenance | 0.04 | g/(g · h) |
| $qO_{max}$ | max OUR | 0.429 | g/(g · h) |
| $qS_{max}$ | max GUR | 1.25 | g/(g · h) |
| $Y_{A/S}$ | g A produced per g S | 0.667 | g/g |
| $Y_{O/A}$ | g O consumed per g A | 1.067 | g/g |
| $Y_{O/S}$ | g O consumed per g S | 1.067 | g/g |
| $Y_{X/A}$ | g X produced per g A | 0.4 | g/g |
| $Y_{X/S_{of}}$ | g X produced per g S | 0.15 | g/g |
| $Y_{X/S_{ox}}$ | g X produced per g S | 0.51 | g/g |

dynamics in a fed-batch reactor:

$$\frac{d}{dt}\begin{bmatrix} X \\ S \\ A \end{bmatrix} = \begin{bmatrix} 1 & 0 & 0 \\ -Y_{S/X} & 0 & 0 \\ Y_{A/X} & 0 & 0 \end{bmatrix} \mu X - \frac{F}{V}\begin{bmatrix} 0 \\ S - S_{in} \\ 0 \end{bmatrix} \tag{2.31}$$

with substrate yield coefficient $Y_{S/X}$ (g/g) and acetate yield coefficient $Y_{A/X}$ (g/g) representing grams consumed per gram biomass. Acetate concentration $A$ (g/L), feed flow rate $F$ (L/h), volume $V$ (L), and glucose feed concentration $S_{in}$ (g/L) are also represented. The relationships between states are dictated by the growth rate times the yield coefficients times the biomass. For this model, the growth rate is a

simple Monod expression and affects every state equally:

$$\mu(S, A) = \left(\frac{S}{K_s + S}\right)\left(\frac{K_i}{K_i + A}\right) \tag{2.32}$$

The mass-balance model for a system with a piecewise continous growth rate is structured slightly differently. As stated in Section 2.1, *E.coli* have 3 distinct metabolic phases: oxidative ($\mu_1$), overflow ($\mu_2$), and metabolite consumption ($\mu_3$). Santos shows how these reactions relate to the states [Santos et al., 2010]:

$$k_1\ S + k_5\ O \xrightarrow{\mu_1} \quad X \tag{2.33}$$

$$k_2\ A + k_6\ O \xrightarrow{\mu_2} \quad X \quad +k_3\ A \tag{2.34}$$

$$k_4\ A + k_7\ O \xrightarrow{\mu_3} \quad X \tag{2.35}$$

where the $k_i$'s represent the yield coefficients. The model in 2.36 is from [Santos et al., 2010]:

$$\frac{d}{dt}\begin{bmatrix} X \\ S \\ A \\ C \end{bmatrix} = \begin{bmatrix} 1 & 1 & 1 \\ -k_1 & -k_2 & 0 \\ 0 & k_3 & -k_4 \\ -k_5 & -k_6 & -k_7 \end{bmatrix} \begin{bmatrix} \mu_1 \\ \mu_2 \\ \mu_3 \end{bmatrix} X - \frac{F}{V}\begin{bmatrix} X \\ S - S_{in} \\ A \\ 0 \end{bmatrix} + \begin{bmatrix} 0 \\ 0 \\ 0 \\ OTR \end{bmatrix} \tag{2.36}$$

For this model, the growth rates are defined:

$$\mu_1 = \min(q_S, q_{S,crit})/k_1 \tag{2.37}$$

$$\mu_2 = \max(0, q_S - q_{S,crit})/k_2 \tag{2.38}$$

$$\mu_3 = \begin{cases} \max(0, q_A)/k_4 & \text{if } q_S k_{OS} + q_A k_{OA} \leq q_O. \\ \max(0, (q_O - q_S k_{OS})/k_{OA})/k_4 & \text{otherwise.} \end{cases} \tag{2.39}$$

where $q_S$ is the glucose flux into the cell, $q_{S,crit}$ is the maximum glucose flux, $q_A$ is the acetate flux in to the cell, and $k_{OS}$ is the oxygen substrate yield coefficient. Further definitons can be found in (3) of [Santos et al., 2010]. In (2.36), note how $\mu_1$ and $\mu_2$ both consume substrate but $\mu_2$ produces acetate while $\mu_3$ consumes it. These growth rates more accurately reflect the different metabolic phases. The different phases affect the different states based on how they are multiplied with the different yield coefficients.

For the growth rate model found in [Xu et al., 1999], the mass-balance model is slightly different. Only the biomass is scaled by the growth rate while the other states are affected by their corresponding fluxes:

$$\begin{aligned} \frac{d}{dt}\begin{bmatrix} X \\ S \\ A \\ C \end{bmatrix} &= \begin{bmatrix} \mu \\ -qS \\ (qA_p - qA_c) \\ -qO \end{bmatrix} X - \frac{F}{V}\begin{bmatrix} X \\ S - S_{in} \\ A \\ 0 \end{bmatrix} + \begin{bmatrix} 0 \\ 0 \\ 0 \\ OTR \end{bmatrix} \\ \frac{dV}{dt} &= F - F_{sample} \\ \mu &= (qS_{ox} - q_m)Y_{X/S,ox} + qS_{of}Y_{X/S,of} + qA_cY_{X/A} \end{aligned} \tag{2.40}$$

The flux calculations were described in Section 2.2.1. All the fluxes ($q$, g/g-h) and yield coefficients ($Y$, g/g) for the Xu model can be found in Table 2.1.

To completely model a bioreactor system, the hardware, software, and constraints of the physical system must be also studied. Depending on the states of the mass-balance model, the administration of substrate and oxygen and even acid and base need to be characterized. The methods and resolution in which these solutions are added to the bioreactor affect how a control algorithm interacts with the mass-balance and growth rate models. The full description of that work for this project can be found in Section 3.1.

## 2.4 Advanced Bioreactor Controls

This section will describe the different types of on-line sensors, estimators and controllers found in the literature.

### 2.4.1 Motivation

In 2004, the United States Food & Drug Administration (FDA) presented their report, "'Guidance for Industry Process Analytical Technology (PAT) - a Framework for Innovative Pharmaceutical Development, Manufacturing, and Quality Assurance"', known as the PAT Initiative [Food and Association, 2004]. The purpose of the PAT initiative was to present non-binding recommendations to the biopharmaceutical industry. The PAT Initiative highlights the lack of technological advancement in the biopharmaceutical industry with regards to its process development and manufacturing methods; a state which was "undesirable from a public health standpoint". The FDA urged the use of small-scale fermentation systems for process understanding and the use of online sensors to monitor their processes more closely. The FDA stated

that using both together would provide "increased insight and understanding for process development, optimization, scale-up, technology transfer, and control" [Food and Association, 2004]. Better online measurements improves growth rate control, which leads to more biomass, and ultimately more product [Babaeipour et al., 2007].

The biopharmaceutical industry invests between 16 to 20% of its earnings back into research and manufacturing changes for new products. Research and development may cost from $800 million to $1.7 billion and take up to 10 years to bring a new product to market [Mosier and Ladisch, 2009]. The product development process goes hand-in-hand with process scale-up in the biopharmaceutical industry. One area where the industry can be accelerated is the early stages of drug development. Due to the lack of sensing or understanding, the current protocols for small scale systems are predefined using no or simple feedback control. More accurate sensing solutions coupled with new control algorithms could deliver fast, stable growth, which would maximize protein production, speed up protocol development, and increase product yield during this critical time.

### 2.4.2 Online Sensors

The FDA report urged companies to monitor their processes more closely through the use of online sensors. Using online and offline sensors together would provide "increased insight and understanding for process development, optimization, scale-up, technology transfer, and control" [Food and Association, 2004]. The most common on-line sensors for benchtop fermentation systems are pH, temperature, and dissolved oxygen (DO) probes, and exhaust-gas sensors. These sensors provide control algorithms with the real-time data necessary to control culture behavior.

### 2.4.3 Software Sensors

Software sensors rely on known relationships between the measurable and the unmeasurable states of mass-balance culture models. Software sensors take on-line sensor measurements and generate signals that can be used by controller algorithms. The two main types of software sensors found in literature are state estimators and neural networks.

In a state estimator, the mass-balance model is used to relate unknown states, such as the biomass, to known states, such as the oxygen. Models like (2.36) are used to create observer-based estimates for both the growth rate and biomass using standard dissolved oxygen and exhaust gas sensors. The observer-based estimators are usually formed around Luenberger observers. An observer-based estimator can even estimate growth rate without assuming a growth rate model for the culture [Bastin and Dochain, 1990]. This means it can be used for many different organisms. Convergence properties and tuning rules have been thoroughly studied for these estimators [Pomerleau and Perrier, 1992]. A different version of this estimator based on OUR was studied extensively by Lubenova [Lubenova et al., 1993, V., 1996, Ljubenova and Ignatova, 1994]. This estimator has performed well in many actual culture experiments, mostly involving bakers yeast and *E.coli* [Pomerleau and Perrier, 1992, Charbonnier and Cheruy, 1994, Montesinos et al., 1995, V., 1996, Tatiraju et al., 1998, Levisauskas et al., 1999, Perrier et al., 2000, Simon and Karim, 2002, Rocha et al., 2008, Veloso et al., 2009].

The major assumption for all observer-based estimators is that the yield coefficients in the model are known and static. For many models in literature, the origin of the yield coefficients is not stated or the yield coefficients are derived from similar previous experiments [Montesinos et al., 1995, Dowd et al., 1999, Perrier et al.,

2000, Oliveira et al., 2002, Jenzsch et al., 2006a, Pinsach et al., 2006, Rocha et al., 2006, Hocalar and Turker, 2010]. Controllers depend on the estimates to make decisions, but the quality of the estimation is dependent directly on the validity of the model [Montesinos et al., 1995]. Observer-based estimators are adaptive and can handle some parameter drift and process-model-mismatch, but any new organism or strain would require new characterization experiments to be performed. In general, observer-based estimators are not used in experiments involving induction. Induction produces a severe metabolic burden on the cells and drastically changes the yield coefficients, making the estimator inaccurate [Akesson et al., 1999a, Babaeipour et al., 2007]. There were two papers which did use these estimators on induced cultures but in one the model coefficients came from post-induction experiments [Montesinos et al., 1995]and in the other the authors noted the organisms metabolism only slightly changed with induction [Pinsach et al., 2006]. Overall, the implementation of observer-based estimators would require months of characterization experiments to find yield and model coefficents. This type of method would only be appropriate for a known culture operating in a narrow set of conditions and would not be appropriate for use with an unknown culture in which the cells change behavior.

Several groups have used neural networks (NN) to control cell cultures [Psichogios and Ungar, 1992, Keulers, 1993, Levisauskas et al., 1999, Simon and Karim, 2002, Karakuzu et al., 2006, Jenzsch et al., 2006a, Kiran and Jana, 2009]. Neural networks try to establish complex relationships between the designated inputs-outputs of a culture by analyzing training data and assigning weights between these relationships. Just like observer-based estimators, NNs are used to determine the relationships between on-line sensors like OUR and biomass concentration or growth rate. In [Jenzsch et al., 2006a], the authors explore a variety of estimation techniques for biomass estimation such as polynomial regression, auto-associative artificial neural

networks (ANNs), and principle component analysis. They concluded that ANNs worked the best in estimating biomass from OUR, CPR, BASE, and DO. In [Simon and Karim, 2002], NNs are used to predict the amount of dead cells in the culture in order that they would be minimized using a model predictive controller. In [Kiran and Jana, 2009], they used NNs to estimate the specific growth rate combined with a model predictive controller to keep the yeast cells in a specific metabolic state. In [Jenzsch et al., 2006b], an ANN is used to estimate total biomass and a feedback controller was used to keep the biomass on a set profile. Neural networks are very effective but they require dozens of experiments to train for one particular set of conditions [Kiran and Jana, 2009]. Collecting this data could take months. Also, Neural networks tend to exhibit poor performance when the process exhibits off-nominal behavior. Like observer-based estimators, neural networks would not be helpful to implement in a research environment which studies a broad range of cells and culture conditions.

### 2.4.4 Control Methods

Bioreactor control literature contains a wide variety of experimentally validated control methods. Most of these experiments were performed on benchtop systems with vessel sizes from 2 L up to 10 L, while a few used much larger tanks, 200 L in [Voisard et al., 2002] and 16000 L in [Hocalar and Turker, 2010]. The level of sophistication ranged from P, PI, and PID feedback algorithms to heuristic control to model predictive control algorithms. The standard sensor configuration found in most bioreactor control papers consisted of exhaust gas, DO, pH, temperature, and weight sensors. The set of sensors available to the system made a large difference as to the type of control that was implemented. For example, there were a small number

of papers which used systems with very specialized on-line sensors for biomass [Cornet et al., 1993, Dabros et al., 2010] or for metabolite concentration [Karakuzu et al., 2006, Hocalar and Turker, 2010]. About half of the papers used software sensors to create estimators for their controllers.

The control methods described in the literature break into two main methodologies. The first set presented controllers which forced the culture to follow some predetermined setpoint or profile. The second set presented controllers which achieved a certain goal, such as maximizing biomass or minimizing waste.

#### 2.4.4.1 Setpoint Controllers

Most bioreactor controls papers use a setpoint control approach, where the culture was supposed to follow a predetermined growth rate or sensor profile. The objective of these setpoint based controllers was to reject disturbances and keep the process growing stably. In [Rocha et al., 2008], DO and off-gas sensors were used to estimate the biomass concentration used by an optimal controller to maintain a set growth rate. In [Schaepe et al., 2011], the temperature profile of a well behaved culture was used as a reference, and a reference tracking controller using only temperature sensors varied the feed rate to achieve a similar temperature profile. In [Aehle et al., 2011b], a similar approach was used but the controller was tracking an oxygen consumption profile. Similar schemes have been used by other research groups [Voisard et al., 2002, Jenzsch et al., 2006b]. The controller presented in [Aehle et al., 2012] maintained a growth rate setpoint by refitting the the growth model at different points throughout the experiment and then used the new model for future control decisions.

In most papers, growth rates are controlled within conservative ranges. In [Pico-Marco and Pico, 2003], the growth rate was kept at 0.05 $h^{-1}$ for yeast and in [Pinsach et al., 2006] to 0.09 and 0.16 $h^{-1}$ for *E.coli* . In [Dabros et al., 2010],

baker's yeast was held at a growth rate of 0.15 $h^{-1}$ when it's known maximum oxidative growth rate was 0.24 $h^{-1}$. Selecting conservative growth rates maintains the culture far from overflow metabolism and minimizes waste accumulation; however, culture times are extended, which might be harmful to recombinant protein products (1996Swartz) [Hocalar and Turker, 2010]. Conservative growth rates reflect the narrow set of conditions used to derive the models driving the controllers [Perrier et al., 2000, Pinsach et al., 2006, Rocha et al., 2008, Aehle et al., 2011b]. Consistent behavior is important for the accuracy of observer-based and neural network estimators. Only one paper attempted setpoint control before and after induction, however the organism choice was fairly unique and the induction did not cause a significant metabolic burden [Pinsach et al., 2006]. The metabolic burden due to induction has been shown to reduce the growth rate by fifty percent [Akesson et al., 1999a] to ninety percent in [Babaeipour et al., 2007]. There are several drawbacks to setpoint or profile controllers: 1) the models require extensive characterization 2) conservative growth rate setpoints require long fermentation times to reach high biomass levels 3) the control algorithms are not amiable to changes in metabolism during the culture [Simon and Karim, 2002, Levisauskas et al., 1999].

#### 2.4.4.2 Adaptive Controllers

Adaptive controllers modify the feed rate based on changes in the culture metabolism rather than force the culture to maintain an arbitrary growth rate. By monitoring metabolism, adaptive controllers can drive the culture to fast growth with low waste accumulation without requiring the researcher to spend time upfront characterizing the culture around different operating ranges. In [Cornet et al., 1993], the authors used an online sensor to detect waste concentration and adjust the feed rate to keep the growth rate on the boundary between oxidative and overflow metabolism;

ensuring high growth rate and the minimal waste. A similar method was followed in [Hocalar and Turker, 2010]. In [Levisauskas et al., 1999], the authors used previous experiments to train an ANN and an evolutionary programming technique to generate an optimal feed rate profile. In [Voisard et al., 2002], the authors derived an optimal heat profile which the controller followed using calorimeters. In [Simon and Karim, 2002], the authors used a neural network to estimate the number of apoptotic (dead) cells in the culture of CHO cells making proteins and minimized them with an MPC.

Some maximizing controllers were non-model based and did not assume a model structure for the culture when adjusting the feed rate. Feed rate control decisions were based on a heuristic set of rules based on the outcome of discrete inputs to the system [Akesson et al., 1999a, Akesson et al., 1999b, Akesson and Hagander, 2000, Johnston et al., 2002, Mare et al., 2005]. When a feed rate pulse was administered to the system, the DO probe was monitored. If the oxygen level dropped, the feed rate was increased according to the magnitude of the change using a PID controller. If the oxygen level remained steady, the culture was in overflow, oxidative metabolism was already maximized, and the feed rate was decreased. These model-free controllers were able to control different strains of *E.coli* cultures before and after induction achieving maximum bioreactor productivity [Akesson et al., 2001]. Model-free adaptive controllers have many advantages 1)there are no characterization experiments to perform 2) the algorithms work on a wide range of different organisms 3) they can handle different metabolic shifts during culture. Model-free adaptive controllers present the best solution for keeping cultures near the boundary of oxidative and overflow metabolism (BOOM). These controllers minimize protocol development time and maximize the protein production by maximizing biomass through fast growth [Babaeipour et al., 2007].

## 2.5 Industrial Controls

As stated by the PAT Initiative, the sophistication of controllers in industry is low. This section will review two popular bioreactor control methods: Exponential feed rate and DO/pH stat control.

### 2.5.1 Exponential Feed Rate Control

In the bipharmaceutical industry, predetermined feed rate control methods are widely used for fed-batch cultures. The substrate feed rate is set prior to the culture beginning. The feed rate (F) could be constant, exponential, or a series of discrete additions at pre-determined times, evenly or unevenly spaced [Riesenberg et al., 1990]. Exponential fed-batch strategies keep the culture at a growth rate high enough to reach high cell densities quickly but sufficiently low enough to avoid overflow metabolism [Korz et al., 1995]. In exponential feed rate control, the set growth rate ($\mu_{set}$) determines the substrate flow rate (F). The feed rate formula shown here is from [Durany et al., 2005]:

$$F = \frac{\mu_{set} X_0 V_0}{S_f Y_{X/S_{ap}}} \, exp(\mu_{set} t)$$

where $X_0$ and $V_0$ are the inital biomass and volumes, $\mu_{set}$ is the desired growth rate, $S_f$ is the feed glucose concentration, and $Y_{X/S_{ap}}$ is the subtrate to biomass yield coefficient. Based on the behavior of the dissolved oxygen, base flow rate, or off-line biomass or substrate, the health of the culture can be assessed. Additionally, responses to substrate change can be monitored, if overflow metabolism was suspected, the substrate feed can be cutoff, and the DO monitored. If it does not change, then the culture was in overflow, and the substrate is left off until the DO begins to change.

These intervening actions are common for setpoint control, especially following any type of culture stress such as recombinant protein induction, suspected prophage caused by cell lysis, or temperature changes.

### 2.5.2 DO/pH stat Control

DO/pH stat controllers are also used industrially for *E.coli* fermentations. This feed rate method is characterized by conservative culture growth [Chen et al., 1997]. The DO/pH stat control algorithm works by administering feed pulses based on thresholds for the dissolved oxygen and pH probes. If the DO goes above the DO threshold, the feed pulse turns on. When the DO goes below the DO threshold, the feed pulse turns off. The algorithm works the same for the pH threshold. The height of the feed rate pulse is set high and increases as the volume increases. The feed rate pulse is set high enough to provide enough glucose even when the culture reaches high cell densities. The DO/pH stat controller also has a custom dissolved oxygen controller. Rather than using a setpoint PID controller to maintain the DO level, the DO/pH stat DO controller stays constant unless the DO goes below a second lower DO threshold. When the DO gets too low, the DO/pH stat DO controller will increase the stir speed by a set percentage. The DO is only controlled to ensure that some minimum DO level is maintained, else the stir speed is constant, ensuring the $OTR$ is also constant. By having a constant $OTR$, the DO/pH stat algorithm uses the higher DO threshold for the glucose pulse to ensure the $OUR$ stays at some minimum level. The pH is controlled by base addition, but if the pH rises above some threshold because the culture have consumed all acidic byproducts in the media, then the glucose pulse is activated.

# Chapter 3

# Fermentation System Control & Simulation

In this chapter, the Hardware-In-the-Loop (HIL) design of the fermentation system used in this work will be discussed. In an HIL system, a complex real-time system is simulated for the purpose of testing control algorithms. A system's actuators and sensors are simulated as well as the control inputs. The control algorithms are then used to control the actual system. For this project, the growth rate model and mass-balance model were chosen from [Xu et al., 1999]. The fermenter is a BioStat B Digital Control Unit (DCU) (Sartorius Stedim, Bohemia, NY) with 5 L glass vessel. The physical constraints and resolution of systems in the DCU are modeled. The communication delays and behavior associated with the DCU, exhaust-gas, balances, and mass flow sensors are also modeled.

This following sections describe the development and implementation of two Matlab Simulink models, FermCtrl and FermSim. The FermSim model simulated the Biostat B fermentation system and was used to develop and refine different control algorithms. The FermCtrl model ran the different control algorithms and controlled

the Biostat B fermentation system during live culture experiments.

## 3.1 The BioStat B Fermentation System

The BioStat B Fermentation system is composed of a Digital Control Unit (DCU) housing 4 peristaltic pumps with power and data connections for a tempereature probe (Sartorius), a dissolved oxygen (DO) probe (OXYFERM 325, Hamilton (Reno, NV)), a pH probe (EASYFERM+ K8 325, Hamilton), and an electric motor, see Figure 3.1. The DCU communicates over RS-485 with the MFCS-win command software (Sartorius) running on a Windows computer. Using the Open Platform Communcations (OPC) standard, commands and data are sent and received every 15 seconds. The dissolved oxygen and pH PID control algorithms running on the DCU read the DO and pH probes every second. Implementing external PID controls using MFCS or Matlab reduces read times to 15 seconds. The motor for stir speed has a range of 0 to 1200 RPM. For *E.coli* experiments, the lower limit is set to 200 RPM to ensure homogeneity of the liquid. The stir speed also affects the oxygen transfer rate into the liquid. The stir motor is run by a PID controller which accepts setpoint commands directly from an outside source or from a dissolved oxygen controller on the DCU. The perstaltic pumps are separated into two groups. The bottom pair of pumps are controlled by the pH control system, one for base addition the other for acid addition. These pumps are not able to be commanded by any other means except by the pH PID controller. The top two pumps can be individually commanded. The pumps work on a six second duty cycle and commands are sent in terms of percentage, for example a 50% setpoint command would cause the pump to run for three out of every six seconds. The minimum resolution for these pumps is 2% and any whole or decimal command is rounded up or down to the nearest even number. All four

Table 3.1: Biostat B Fermenatation System Sensor Specifications

| **Name** | **Resolution** | **Range** | $T_s$ | **Comm** | $\tau$ |
|---|---|---|---|---|---|
| DO probe | $< 0.5\%$ | 10 ppb - 40 ppm | 15s | DCU | 10s |
| pH probe | $< 0.1$ pH | pH 0-14 | 15s | DCU | |
| Temp probe | | | 15s | DCU | |
| Balance | 0.1 g | 4000g | 5s | RS-232 | 1s |
| Mass Flow meter | $\pm$ 3.0% FS | 1 - 5 LPM | 5s | DAQ | $< 30$s |
| Mass Flow controller | $\pm$ 3.0% FS | 1 - 10 LPM | 5s | DAQ | $< 30$s |
| Exhaust-gas sensor | $\pm$ 2.0% FS | 0-50% $O_2$<br>0-25% $CO_2$ | 15s | RS-485<br>OPC | 55s |

pumps can be calibrated and their volumes tracked using the calibration pump rate (mL/min); the internal totalizer has a resolution of 0.05mL. In order to achieve fine resolution on substrate feeding, two pumps were used with different tubing diameters, Masterflex (Cole-Parmer (Vernon Hills, IL)) LS 12 (ID:0.01 mm Flow:0.133 mL/min, Mas) and LS14 (ID:0.06 mm Flow:5.6 mL/min), respectively. An exhaust-gas sensor (BlueInOne, BlueSens GmbH (Herten, Germany)), Mass flow sensors (FLR1006, Omega Eng Inc (Stamford, CT)) and balances (Scout Pro , Ohaus (Parsippany, NJ)) were added to track inputs and outputs to the bioreactor. The exhaust-gas sensor reports the relative humidity and percent composition of $CO_2$ and $O_2$ inside a 35 mL measurement chamber. In addition, the exhaust-gas sensor outputs chamber pressure and temperature. See Table 3.1 for details on the resolution, limits, sample times, and time constants for the Biostat B fermentation system and sensors.

## 3.2 Fermentation Control (FermCtrl) Model

The FermCtrl model is a Simulink (Matlab 2012a, Mathworks Inc (Natick, MA)) model that controls the Biostat B Fermentation system during a culture experiment. The Biostat B DCU has a 'Remote Mode', which allows an external program

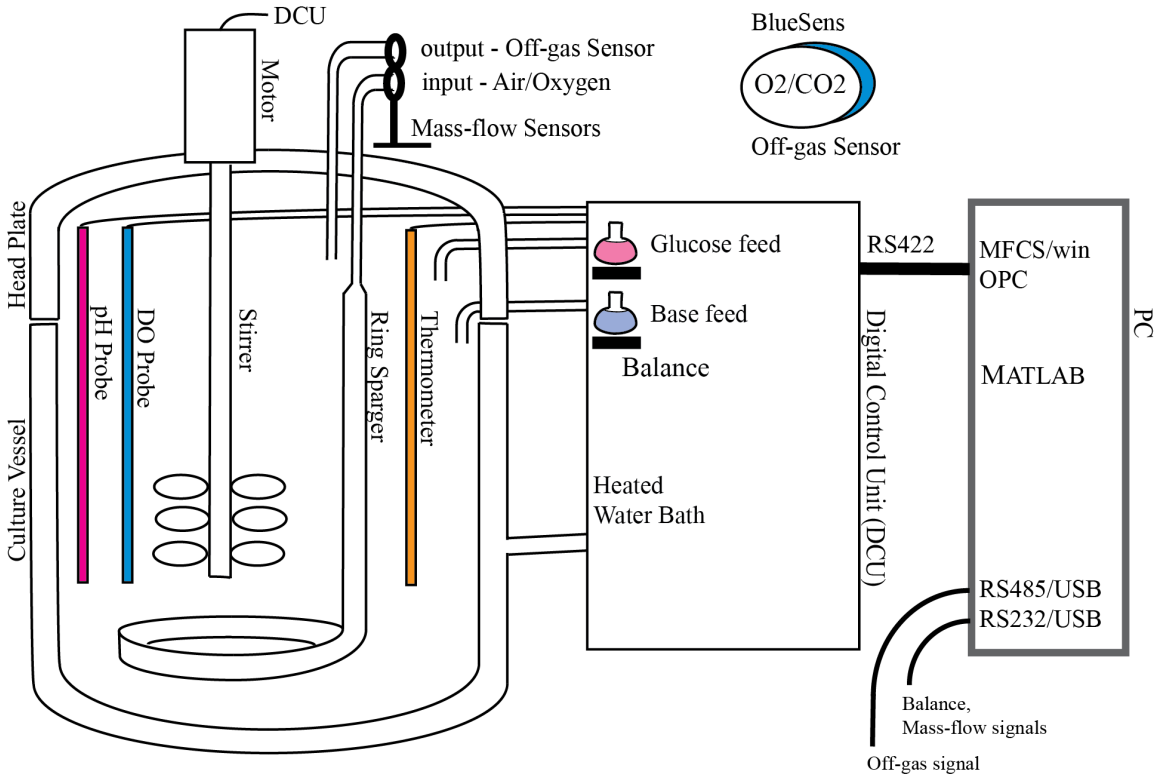


Figure 3.1: Biostat B Fermentation system setup, including an exhaust-gas sensor, balances for the glucose input and base input bottles, and standard sensor set.

to recieve data and issue commands through MFCS-win using the OPC protocol. Using this 'Remote' mode, all command and control of the Biostat B system was done externally using Matlab and the OPC toolbox. The FermCtrl contains three distinct sections. There is the MONITOR section which contains displays of all the different values coming from the estimator and controller as well as the DCU and its sensor values. The MONITOR section has areas to define the start of fed-batch phase, the initial volume of the fermenter, and to specify the names of the mat files, which save all data.

The CONTROL section of the model contains the blocks that control the fermentation system. This includes the feed rate controller as well as DO controller. A user may also specify gas mixture (GASMX) or pH setpoints in this section. The output of the feed rate blocks go to the 'Fs pump discretization' block located at the end of this section. The inputs into the 'Fs pump discretization' block are the two calibration values in mL/min for the L/S 14 and L/S 12 tubing based on a two minute flow rate test. The calibration value for the larger tubing is updated every experiment while the smaller tubing calibration is left static. It was measured once using a 10 minute flow rate test. The L/S 12 tubing is replaced every experiment.

The COMMAND section of FermCtrl contains all the OPC, User Datagram Protocol (UDP), and serial communcations blocks. The exhaust-gas sensor and the BioStat B DCU communicate with Matlab over OPC. The OPC Read blocks connect to the MFCS-win OPC servers and read the data from the DCU every 15 seconds. The OPC Write blocks send commands to the DCU for the stir speed, GASMX, pH, and substrate pumps. The balances send data over the COMM ports using RS-232 every 5 seconds. The mass flow sensors send data via UDP protocol after their voltages are read by the Analog IN ports on a Quanser Q4 DAQ card (Quanser (Markham, Ontario)). A mass flow controller (Omega FMA-A2409) accepts commands over

UDP and outputs the data over the Quanser's Analog OUT ports. The UDP data is updated every 5 seconds. All the relevant data, such as sensor, setpoint, signal, and command values are sent through rate transistion delays and recorded with the 'To File' block in the MONITOR section. The rate transistion delays are set to 15 seconds, which is the slowest sample time in the model, to ensure that all data is properly synced.

## 3.3 Fermentation Simulation (FermSim) Model

To test control algorithm theory and tunings, the COMMAND section of the FermCtrl model can be replaced with a simulation of the sensors, vessel specific characteristics, and the Xu culture model. The mass flow, balance, and exhaust-gas sensors are modeled by adding white noise in accordance with each instruments resolution and error specifications. An embedded simulink model acts as the fermentation system model. It is designed to represent the culture in the vessel and the operation of the DCU. It takes in the same inputs as the DCU, i.e. substrate commands and stir speed commands, and returns simulated outputs, such as DO percentage, exhuast-gas data, volume measurements for base and substrate, balance data, and mass flow data. In addition to simulating actual values, the embedded model returns actual state values such as biomass, acetate, and OUR. The Xu growth rate and mass-balance models were simulated and the performance verified by comparing the simulation outputs to the simulation results presented in [Xu et al., 1999]. The MONITOR section of the FermSim model still records the sim outputs into a mat file. Therefore, it is possible to use the same scripts to examine both simulation data and experiment data.

# Chapter 4

# On-line Oxygen Uptake Rate Estimator

Oxygen uptake rate (OUR) is an essential signal for tracking *E.coli* metabolism. An estimate of the oxygen transfer coefficient can be used to calculate OUR. The output from this estimator could be used by a control algorithm to estimate metabolic state of an *E.coli* culture. This chapter will give a brief overview of bioreactor oxygen transfer dynamics. The development of this estimator will be presented. This OUR estimate was completed in large part by a Masters student, Li Wang, and has been published [Pepper et al., 2013, Wang et al., 2014]. This work was rederived and different gains used for this work.

## 4.1 Oxygen Transfer in a Bioreactor System

Oxygen transfer is essential to the successful growth of any aerobic organism. The oxygen concentration dynamics are among the fastest in a bioreactor. Oxygen is most often provided to a bioreactor as air through a sparger, shown in Figure

4.1. If high oxygen content is needed, a mixture of air and oxygen can be used. The gas enters the bioreactor with an initial concentration, $b_0$. The gas exits the liquid with concentration $b_1$. The bubbles leaving the liquid mix with the gas in the headspace, which has concentration $b_2$. After leaving the bioreactor, the exhaust gas concentration is read either by a mass spectrometer or a dedicated off-gas sensor as $b_3$.

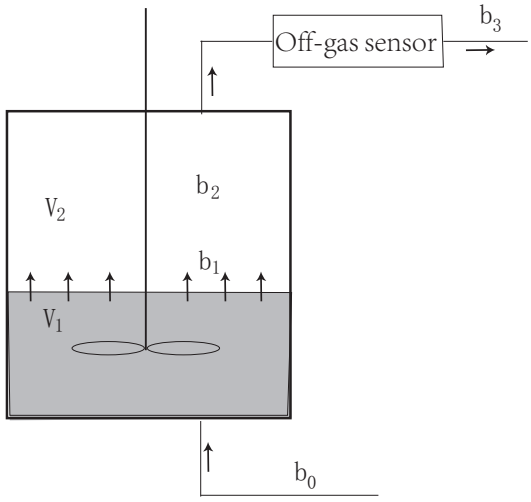


Figure 4.1: In a bioreactor, $b_0$, $b_1$, $b_2$, and $b_3$ correspond to oxygen gas concentrations entering the vessel, exiting the liquid, exiting the headspace, and read by an off-gas sensor.

The dynamics for oxygen in the the culture inside a bioreactor

$$\frac{d}{dt}C = OTR - OUR \tag{4.1}$$

where $C$ is the dissolved oxygen concentration, and $OTR$ is the oxygen transfer rate of the input air into the liquid. In order to calculate OUR, OTR must be calculated

$$OTR = \frac{M_f(b_0 - b_1)\rho_{o_2}}{V_1}, \tag{4.2}$$

where $M_f$ is the mass flow rate (L/min), $\rho_{o_2}$ is the oxygen density at $37^oC, 1\ atm$ $(g/L_{oxygen})$, and $V_1$ is the liquid volume of the culture. The $b_1$ concentration is unknown and cannot be directly measured. The DO probe only measures the concentration inside the liquid. The only sensor available to measure the oxygen concentration after that point is the off-gas sensor $b_3$. It is generally assumed that $b_3$ is equivalent to $b_1$; however, analysis of the mixing dynamics in the headspace and the measurement delays of the exhaust gas sensor show this to be false. The oxygen concentration dynamics for the bioreactor are

$$\frac{d}{dt}b_2 = \frac{M_f}{V_2}(b_1 - b_2) \tag{4.3}$$

$$\frac{d}{dt}b_3 = \frac{1}{\tau_2}(b_2 - b_3) \tag{4.4}$$

where the mixing in the headspace, $b_2$, is a filtered version of $b_1$ with a time constant $\tau_1 = V_2/M_f$, and $V_2$ is the headspace volume (L). The measurement delay of the off-gas sensor then filters the $b_2$ signal with time constant, $\tau_2$. Any $OUR$ signal using $b_3$ in the $OTR$ calculation (4.2) would be heavily filtered. The response of this $OUR$ signal would not be suitable for feedback control.

The OTR can be physically modeled as

$$OTR = k_L a\ (C^* - C) \tag{4.5}$$

where $k_L a$ is the oxygen transfer coefficient and represents the rate of diffusion of oxygen into the liquid, and $C^*$ represents the saturation concentration. The diffusion of oxygen into the liquid occurs across the liquid-gas interface of the sparged air bubbles. Increasing the stir speed increases $k_L a$. $k_L a$ is affected by numerous culture parameters, such as viscosity, pressure, temperature, and salinity [Dorresteijn et al.,

1994], some of which change during the course of a fermentation. The dependence of $k_La$ on stir speed is modeled as

$$k_La = \alpha_0 + \alpha_1 (N - N_0) \tag{4.6}$$

with $\alpha_0$ and $\alpha_1$ representing fitted parameters and N0 is a constant. Several sources indicate that as the biomass grows, the coefficients of $k_La$ change [Akesson et al., 1997,Simon and Karim, 2001,Schaepe et al., 2011]. One of the most obvious changes to the culture over time is its viscosity. Assuming constant values of $\alpha_0$ and $\alpha_1$ and using Equations 4.1, 4.5, and 4.6 to estimate $OUR$ would not be accurate over an entire fermentation.

The input signal to Equation 4.4, $b_1$, can be defined in terms of known variables using Equations 4.2, 4.5, and 4.6

$$b_1 = b_0 - \frac{V_1(C^* - C)}{M_f\rho_{o_2}}\alpha_0 - \frac{V_1(C^* - C)(N - N_0)}{M_f\rho_{o_2}}\alpha_1 \tag{4.7}$$

In state space form with $\bar{\mathbf{x}} = [b_2 \quad b_3]^T$, the oxygen concentration dynamics from (4.4) and (4.4) are

$$\dot{\bar{\mathbf{x}}} = \begin{bmatrix} -\frac{M_f}{V_2} & 0 \\ \frac{1}{\tau_2} & -\frac{1}{\tau_2} \end{bmatrix} \bar{\mathbf{x}} + \begin{bmatrix} \frac{M_f}{V_2} \\ 0 \end{bmatrix} b_1 \tag{4.8}$$

After substituting in the value of $b_1$ found in Equation 4.7, Equation 4.8 becomes

$$\begin{aligned} \dot{\bar{\mathbf{x}}} &= \bar{A}\bar{\mathbf{x}} + \bar{B}\bar{\mathbf{u}}, \\ y &= \bar{C}\bar{\mathbf{x}} \end{aligned} \tag{4.9}$$

where,

$$\bar{\mathbf{x}} = \begin{bmatrix} b_2 \\ b_3 \end{bmatrix}, \quad \bar{A} = \begin{bmatrix} -\frac{M_f}{V_2} & 0 \\ \frac{1}{\tau_2} & -\frac{1}{\tau_2} \end{bmatrix}, \quad \bar{B} = \begin{bmatrix} \alpha_0 & \alpha_1 & b_0 \\ 0 & 0 & 0 \end{bmatrix}, \quad \bar{C} = [0\ 1],$$

$$\bar{\mathbf{u}} = \begin{bmatrix} \frac{-V_1(C^*-C)}{V_2\rho_{o_2}} \\ \frac{-V_1(C^*-C)(N-N_0)}{V_2\rho_{o_2}} \\ \frac{M_f}{V_2} \end{bmatrix}$$

An accurate $b_1$ signal now only depends on the variation of $\alpha_0$ and $\alpha_1$ to be small. An adaptive observer algorithm is used to estimate unknown parameters in the system or input matrix [Kudva and Narendra, 1973]. The main requirement for convergence is that input signals into the system be persistently exciting, i.e. rich in frequency content. To formulate the observer, Equation 4.9 converted to observable canonical form. The transfer function of (4.9) is

$$\bar{G}(s) = \bar{C}(sI - \bar{A})^{-1}\bar{B} = \frac{1}{s^2 + (\frac{M_f}{V_2} + \frac{1}{\tau_2})s + \frac{M_f}{V_2\tau_2}} \begin{bmatrix} \alpha_0\ \alpha_1\ b_0 \end{bmatrix} \frac{1}{\tau_2} \tag{4.10}$$

The observable canonical realization of transfer function (4.10) is

$$\dot{\mathbf{x}} = A\mathbf{x} + B\mathbf{u}, \tag{4.11}$$

$$y = C\mathbf{x}, \tag{4.12}$$

$$\mathbf{x} = \begin{bmatrix} b_3 \\ \bar{b_2} \end{bmatrix}, \quad A = \begin{bmatrix} -\frac{M_f}{V_2} - \frac{1}{\tau_2} & 1 \\ -\frac{M_f}{V_2\tau_2} & 0 \end{bmatrix}, \quad B = \begin{bmatrix} 0 & 0 & 0 \\ \alpha_0 & \alpha_1 & b_0 \end{bmatrix}, \quad C = [1\ 0], \quad \mathbf{u} = \begin{bmatrix} u_0 \\ u_1 \\ u_2 \end{bmatrix} \frac{1}{\tau_2}$$

where the output of the system $y$ is the off-gas sensor measurement $b_3$, the input $\mathbf{u}$ to the system is a vector of functions of the DO level and stir speed signals, as defined in (4.9). The state $\bar{b_2}$ is a linear combination of $b_2$ and $b_3$.

Table 4.1: Parameters values for the $k_La$ estimator

| **Parameter** | **Value** |
|---|---|
| $\tau_2$ | 55 s |
| $\Gamma$ | 0.5 |
| $\Lambda$ | $50e^{-3}$ |
| $d_1$ | 1 |
| $d_2$ | 1/30 |

## 4.2 Adaptive $k_La$ Estimator

The estimator equation is

$$\dot{\hat{\mathbf{x}}} = A\hat{\mathbf{x}} + \hat{\mathbf{b}}(t)u + \mathbf{w} + \mathbf{r}, \tag{4.13}$$

$$\hat{\mathbf{y}} = C\hat{\mathbf{x}}, \tag{4.14}$$

where $\hat{\mathbf{x}}$ is the estimate of $[b_3 \quad \bar{b_2}]$, and $\hat{\mathbf{b}}$ is the unknown parameter estimates for the input function $\mathbf{u}$. For adaptive estimator stability, two feedback signals, $\mathbf{w}$ and $\mathbf{r}$, are added. $\mathbf{w}$ and $\mathbf{r}$ must tend to 0 as $t \to \infty$. The full system is shown below

$$\dot{\hat{\mathbf{x}}} = A\hat{\mathbf{x}} + \begin{bmatrix} 0 \\ \hat{\alpha_0} \end{bmatrix} \frac{u_1}{\tau_2} + \begin{bmatrix} 0 \\ \hat{\alpha_1} \end{bmatrix} \frac{u_2}{\tau_2} + \begin{bmatrix} 0 \\ b_0 \end{bmatrix} \frac{u_3}{\tau_2} + \mathbf{w} + \mathbf{r}, \tag{4.15}$$

$$\hat{y} = C\hat{\mathbf{x}}, \tag{4.16}$$

$$u_1 = \frac{-V_1(C^* - C)}{V_2\rho_{o_2}}, \quad u_2 = \frac{-V_1(C^* - C)(N - N_0)}{V_2\rho_{o_2}}, \quad u_3 = \frac{M_f}{V_2}$$

The auxiliary terms $\mathbf{w}$ and $\mathbf{r}$ are defined as

$$\mathbf{w} = -e_1 \begin{bmatrix} 0 \\ \mathbf{v}^T \Gamma A_2 \mathbf{v} \end{bmatrix} \tag{4.17}$$

$$\mathbf{r} = -e_1 \begin{bmatrix} 0 \\ \mathbf{q}^T \Lambda A_2 \mathbf{q} \end{bmatrix} \tag{4.18}$$

$$A_2 = \begin{bmatrix} 0 & d_2 \\ 0 & d_1 \end{bmatrix} \tag{4.19}$$

in terms of signals $\mathbf{v}$ and $\mathbf{q}$, where $\mathbf{v}$ and $\mathbf{q}$ are constructed by passing $u_1$ and $u_2$ through two filters

$$\mathbf{v} = G_1(s)u_1(t) \tag{4.20}$$

$$\mathbf{q} = G_2(s)u_2(t) \tag{4.21}$$

$$G_1(s) = \frac{s}{d_1 s + d_2} \tag{4.22}$$

$$G_2(s) = \frac{1}{d_1 s + d_2} \tag{4.23}$$

The estimated $k_L a$ parameters, $\hat{\alpha_0}$ and $\hat{\alpha_1}$, are updated according to

$$\dot{\hat{\alpha_0}} = -\Gamma e_1 \mathbf{v} \tag{4.24}$$

$$\dot{\hat{\alpha_1}} = -\Lambda e_1 \mathbf{q} \tag{4.25}$$

The estimated $k_L a$ parameters are used to generate

$$\hat{OTR} = (\hat{\alpha_0} + \hat{\alpha_1}(N - N0))(C^* - C) \tag{4.26}$$

$$\hat{OUR} = \hat{OTR} - \dot{C} \tag{4.27}$$

# Chapter 5

# Controller

## 5.1 Algorithm Development

The goal for this work was to design a controller that was based on non-specific organism knowledge. The control algorithm would keep an *E.coli* culture growing on the boundary of oxidative and overflow metabolism (BOOM) using a minimum of prior knowledge of the strain. This type of controller is needed in industry and particularly in research laboratories. Research laboratories use a wide variety of cell types, ranging from *E.coli* to yeasts to mammalian cells. A large knowledge base is necessary to correctly run different protocols required by each organism and strain. When a new strain needs to be grown, researchers have to rely on previous knowledge as a starting point for developing a new protocol. This process can be slow and labor intensive. Automatic culture control is one of the benefits of this proposed algorithm. The BOOM controller would automatically change the feed rate to maximize the oxidative metabolism, requiring less resources to monitor and manually adjust or override setpoint feed rates. The BOOM controller will be able to handle off-nominal situations such as shifts in metabolism due to expected and unexpected events.

Keeping the culture near the BOOM region will result in fast growth rate and low waste accumulation of *E.coli* cultures from batch through fed-batch phases. The BOOM controller is also capable of adjusting to the metbolic burden of recombinant Protein production during induction. In order to develop the BOOM controller, first the relationships between oxygen uptake and acetate production due to the Crabtree effect , i.e. overflow metabolism, had to be sensed. By pulsing glucose, it is theoretically possible to see if a culture is being underfed or overfed based on the DO response and exhaust-gas levels. In practice, a pulsing controller using only the DO probe works well in small volume tanks but is less stable in larger volume (>50L) tanks [Velut et al., 2007].

In this study, a controller uses a real-time OUR estimate to sense the boundary between oxidative and overflow metabolism using a series of periodic ramps in the feed rate. During each ramp event, the OUR is recorded and used to set the feed rate afterward. Throughout the experiment, the algorithm adjusts the ramp event height and length to account for the exponential growth of the biomass. The full designation for this controller is BOOM-OUR because it uses the OUR estimate, but it will referred to as the BOOM controller for simplification.

### 5.1.1 Boundary of Oxidative and Overflow Metabolism

Akesson demonstrated that maximizing oxidative metabolism and keeping a culture in the BOOM region depended on decoding the metabolic information hidden in the oxygen sensor data. Identifying overflow metabolism depends on an accurate assessment of the saturation of the TCA cycle and the oxidative phosphorylation reaction. In [Xu et al., 1999], the OUR during oxidative metabolism is modeled as:

$$OUR = qO_S \, X \tag{5.1}$$

where $qO_S$ represents the substrate dependent oxygen flux ($g_O$ consumed per $g_X$ per hour) into the cells, and is defined as:

$$qO_s = qS_{ox,en} Y_{O/S} \tag{5.2}$$

where $Y_{O/S}$ is the oxygen-to-substrate yield coefficient and $qS_{ox,en}$ the flux of substrate oxidized through the TCA cycle. When the *E.coli* enters overflow metabolism, the magnitude of the $qS_{ox,en}$ is dictacted by the $qO_{max}$, which is the maximum oxidation rate of the TCA cycle or maximum carbon flux through the TCA cycle. When $qO_S = qO_{max}$, the carbon from glucose is redirected into overflow metabolism.

If it was possible to obtain a real-time measurement of the biomass concentration, then maintaining the culture near the BOOM region would be trivial. The $qO_S$ signal would be found from $OUR/X$ and a controller would be designed to track and maximize $qO_S$ at all times. Since real-time biomass measurements are not reliably available, the value of $qO_S$ must be determined dynamically. Akesson applied this method; by using short pulses the change in $OUR$ could be assumed to be due to a change in $qO_S$ and not in $X$. Akesson kept OTR constant and the change in $OUR$ was determined from the change in the dissolved oxygen level, C:

$$\frac{d}{dt}C = OTR - OUR \tag{5.3}$$

.

As shown in [Velut et al., 2007], in larger volume tanks (>50L) the homogeneity of oxygen cannot be assumed and different placements of the DO probe result in different responses to feed rate pulses. These different responses require that the PID feed rate controller using the DO pulse reponses be readjusted significantly depending

on probe location. Also, dissolved oxygen PID controllers are not as stable in larger volumes and are more sensitive to tuning errors. A stable DO environment is essential to an algorithm based solely on the DO probe. Velut stated that integrating the $OUR$ calculation into the algorithm could increase stability [Velut et al., 2007]. Prior to the development of the OUR estimator, which eliminated OUR measurement latency, the $OUR$ response from a glucose pulse using the exhaust-gas sensor would have been too filtered to use in a real-time feedback controller.

In the BOOM controller, the $OUR$ is used directly to track $qO_S$. If a culture in oxidative metabolism is subjected to a quick change in feed rate, the glucose concentration will rise, causing a change in $qS_{ox,en}$. The $qO_S$ responds by changing as well, which is reflected in $OUR$:

$$\frac{d}{dt}qS_{ox,en} \approx \frac{d}{dt}qO_S \approx \frac{d}{dt}OUR \tag{5.4}$$

When the culture enters overflow metabolism, the oxidative metabolism is maximized ($qO_S = qO_{max}$). As the culture crosses into overflow, the $OUR$, currently $\frac{d}{dt}OUR > 0$, suddenly stops changing, $\frac{d}{dt}OUR = 0$, due to saturation of the TCA cycle. To track the maximum oxidative metabolism, an accurate and fast $OUR$ signal is required. The $OUR$ estimator was constructed to eliminate latency by removing the filtering effects due to the head-space and the exhaust gas measurement delay.

The BOOM controller uses a sensitivity ratio, $SR$, to make control decisions. The $SR$ is composed of two signals $k_O$ and $k_F$. The $k_O$ term represents the rate of change of the $OUR$ estimate, $\frac{d}{dt}OUR_{est}$, normalized by $OUR_{est}$. The $k_S$ term

represents the rate of change of the $F_S$ normalized by $F_S$. The equations are:

$$\frac{d}{dt}OUR_{est} = k_O\ OUR_{est} \tag{5.5}$$

$$\frac{d}{dt}F_S = k_F\ F_S \tag{5.6}$$

$$k_O = \frac{\frac{d}{dt}OUR_{est}}{OUR_{est}} \tag{5.7}$$

$$k_F = \frac{\frac{d}{dt}F_S}{F_S} \tag{5.8}$$

$$SR = \frac{k_0}{k_F} \tag{5.9}$$

The $SR$ got its name from its similarity to the Bode' sensitivity test, in which the rate of change of the output is compared to the rate of change of the input. When a ramp event occurs, the $SR$ value represents how quickly $OUR$ is able to change in relation to the feed rate. An $SR$ value of 0.4 would mean the $OUR$ is changing at 40% the rate of the feed rate. In simulation and in practice, the $SR$ proved to be a more stable measurement than using $\frac{d}{dt}OUR$ to maintain the culture near the BOOM region. By examining simulation data, the oxidative threshold ($SR_{thresh}$=0.2) was identified as a good lower bound for the minimum change in $OUR$ during oxidative metabolism. If the culture never crosses the oxidative threshold during a ramp event, then the culture is in overflow metabolism.

### 5.1.2 Algorithm Walk-through

The BOOM controller is activated at the end of the batch phase of the fermentation. A ramp event will occur as often as dictated by the ramp frequency parameter. Briefly, the algorithm checks to make sure a ramp isn't already taking place and starts a timer. The initial feed rate and current OUR values are captured, $F_{init}$ and $OUR_{init}$ respectively. For a set amount of time, the controller will increase

the feed rate command by the initial slope, this value is multipled by a second term named step, which is initially set to one. While the timer is running, the controller is giving the system time to respond to the ramp and constantly monitoring rate of change of the $OUR$ of the culture through the $SR$ variable. During the ramp, the controller records the maximum $OUR_{est}$ value and sets that value equal to $OUR_{max}$. The controller also checks to see if the $SR$ reading has exceeded the oxidative threshold If the threshold is breached, a 'goodRamp' flag is set. The timer elapses when the number of seconds is reached equal to 'OverflowCkTimer'. The controller checks if the $SR$ value is above the threshold. If the $SR$ is below the threshold and the 'goodRamp' flag is off, the controller decides the culture was in overflow. The feed rate is changed according to the feed rate law,

$$F_{new} = \frac{OUR_{max}}{OUR_{init}} F_{init} \tag{5.10}$$

and the ramp indicator is turned off. If the $SR$ value is above the oxidative threshold, then the ramp continues. During this extra time, the controller increases the 'step' variable by some value 'stepDot'. Since 'slope' and 'step' are multiplied together, the increase in 'step' increases the overall ramp slope. The culture should enter overflow more quickly and drive the $SR$ value below the oxidative threshold, which will stop the ramp. The feed rate will be set by the feed rate law (5.10). The controller resets and waits for the next ramp time. Pseudocode for the controller can be found in the Appendix in Section C.

#### 5.1.2.1 OUR-driven Ramp Adaptation

Besides using the $SR$ to detect the BOOM region, the controller also uses the $SR$ to dictate the steepness of the ramp slope. As stated above, if the $SR$ ratio is

above the oxidative threshold after 'OFckTimer' seconds, then the controller begins to increase the 'step' variable by 'stepDot', which was by the parameter 'deltaStep'. The 'step' variable is initially set to 1, thus the initial ramp slope, defined as 'slope' times 'step', is just the 'slope'. As the ramp continues past 'OFckTimer', the ramp slope becomes steeper as 'step' grows. When the $SR$ detects that the culture has entered overflow metabolism, $SR < 0.2$, the ramp is stopped. It is important that the value of 'step' is retained and the ramp slope for the next ramp event reflects the steeper ramp slope. If the 'step' value was reset to one, each ramp event would continue to use the original 'slope'. Eventually the biomass would become large enough that the amount of glucose administered during each ramp would not be enought to change the $OUR$ to detect the BOOM region. The $SR$ would not be able to exceed the oxidative threshold and the feed rate would stagnate. The slope adaptation allows the ramp events to detect the BOOM region of an unknown amount of biomass. The controller will operate successfully as long on the initial 'slope' value is large enough to perturb the $OUR$ of the biomass at the end of batch phase.

#### 5.1.2.2 Feed rate selection

Feed rate selection was originally set by capturing the current feed rate whenever $SR$ would dip below the oxidative threshold during a ramp event. Examination of experimental growth rate curves and acetate results (data not shown) revealed the culture was still being overfed. The goal for the feed law in (5.10) was to choose a feed rate which would immediately stop the rise in glucose concentration due to the ramp event and prevent further growth of the overflow metabolism. The feed rate is kept constant between ramp events to allow the culture to process the excess acetate and come out of overflow metabolism, keeping the culture in the BOOM region. The feed law was derived by reexamining the terms in the original Xu model.

Using the mass-balance model in Xu, the substrate dynamics at feed rate $F_0$ and glucose concentration $S_0$ would be:

$$\frac{d}{dt}S = -qS(S_0)\ X + \frac{F_0}{V}(S_{IN} - S_0) \tag{5.11}$$

Before a ramp event, the feed rate is constant. Before the ramp starts, the rate of change of glucose is negative, but is assumed to be approximately zero:

$$\frac{d}{dt}S \approx 0 = -qS(S_0)\ X + \frac{F_0}{V}(S_{IN} - S_0) \tag{5.12}$$

Equation 2.8 and 2.9 are repeated here as 5.13 and 5.14. Equation 5.13 shows that the glucose flux has some maximum and (5.14) shows that $qS$ is split up into two terms:

$$qS = \left(\frac{qS_{max}}{1 + A/K_{i,S}}\right)\left(\frac{S}{S + K_s}\right) \tag{5.13}$$

$$qS = qS_{ox} + qS_{of} \tag{5.14}$$

When not in overflow, $qS_{of} = 0$. Using the assumption $S_{IN} \gg S_0$, (5.12) becomes:

$$qS_{ox}(S_0)\ X = \frac{F_0}{V}S_{IN} \tag{5.15}$$

The oxidative glucose flux, $qS_{ox}$, seen in (2.10) is split into two parts:

$$qS_{ox} = qS_{ox,an} + qS_{ox,en} \tag{5.16}$$

with the $qS_{ox,an}$ representing glucose going toward anabolism or biomass creation and $qS_{ox,en}$ representing glucose going toward oxidation in the TCA cycle. From Xu in

(2.17), the oxygen dynamics are:

$$\begin{aligned} qO_S &= qS_{ox,en} Y_{O/S} \\ qO_S &\leq \frac{qO_{max}}{(1 + A/K_{i,O})} \\ OUR &= qO_S \, X \end{aligned} \tag{5.17}$$

Then using (5.16), its parameter values yield:

$$\begin{aligned} qS_{ox,an} &\approx 0.58 \, qS_{ox} \\ qS_{ox,en} &\approx 0.42 \, qS_{ox} \end{aligned} \tag{5.18}$$

In (5.17)a, since $Y_{O/X} \approx 1$, then the $OUR$ at feed rate $F_0$ and glucose concentration $S_0$ is:

$$OUR_{S_0} = 0.42 \; qS_{ox}(S_0) \; X \tag{5.19}$$

After the ramp, the feed rate is at some value $F_1$, the culture is in overflow, and the new substrate dynamics are:

$$\dot{S} = -(qS_{ox}(S_1) + qS_{of}(S_1)) \; X + \frac{F_1}{V} S_{IN} \tag{5.20}$$

The goal for the feed rate $F_2$, is to select $F_2 < F_1$ which will appropriately set $\dot{S} = 0$, preventing $qS_{of}$ from growing and keeping $qS_{ox}$ at the maximum for oxidative metabolism.

$$\dot{S} = 0 = -(qS_{ox}(S_1) + qS_{of}(S_1)) \; X + \frac{F_2}{V} S_{IN} \tag{5.21}$$

As the ramp was running, $qS_{ox}(S_0) \rightarrow qS_{ox}(S_1)$ and $qO \rightarrow qO_{max}$. With the culture

in overflow, the $OUR$ at the current substrate concentration, $S_1$, using (5.19) is:

$$OUR_{S_1} = 0.42\ qS_{ox}(S_1) \tag{5.22}$$

The amount which the oxidative metabolism (the TCA cycle) changed can be approximated by:

$$\frac{OUR_{S_1}}{OUR_{S_0}} = \frac{0.42\ qS_{ox}(S_1)}{0.42\ qS_{ox}(S_0)} \tag{5.23}$$

$$qS_{ox}(S_1) = \frac{OUR_{S_1}}{OUR_{S_0}} qS_{ox}(S_0) \tag{5.24}$$

Substituting this result into (5.21) and rearranging yeilds:

$$\dot{S} = 0,\ \frac{F_2}{V} S_{IN} = (\frac{OUR_{S_1}}{OUR_{S_0}} qS_{ox}(S_0) + qS_{of}(S_1))\ X \tag{5.25}$$

Using the result from (5.15):

$$\dot{S} = 0,\ \frac{F_2}{V} S_{IN} = \frac{OUR_{S_1}}{OUR_{S_0}} \frac{F_0}{V} S_{IN} + qS_{of}(S_1)\ X \tag{5.26}$$

Dropping the substrate flux due to overflow, $qS_{of}(S_1)$,and solving for $F_2$ forces $\dot{S} \leq 0$, rearranged the equation becomes:

$$\dot{S} \leq 0, \frac{F_2}{V} S_{IN} = \frac{OUR_{S_1}}{OUR_{S_0}} \frac{F_0}{V} S_{IN} \tag{5.27}$$

$$\dot{S} \leq 0, F_2 = \frac{OUR_{S_1}}{OUR_{S_0}} F_0 \tag{5.28}$$

The new feed rate therefore should force the glucose concentration to immediately start to decrease, minimizing $qS_{of}$, and keeping the culture in the BOOM region. As

described previously, the estimated $OUR$ uses the exhaust-gas measurements to estimate the $k_La$ parameters and the DO probe for fast response. The adaptive controller requires OUR estimates without time delays or filtering, which are possible due to the $OUR$ estimator, which addresses system latency and the inherently variability of $k_La$.

## 5.2 Setting Controller Parameters

The FermSim model development and simulations were used to determined starting values for the slope, deltaStep, and muGS:

1. slope - the initial slope used when the controller begins
2. deltaStep - the rate at which the controller is allowed to change the 'slope'
3. muGS - an exponential rate that continuously grows 'slope' and 'deltaStep'

Table 5.1 lists the different values of 'slope', 'deltaStep', and 'muGs' that were evaluated using the BOOM controller and the FermSim model. Each simulation represents a 24 hour fermentation, with the initial conditions set close to the actual experimental conditions [Sharma et al., 2007]. The initial OD was 0.5 and batch phase ended around 5 hours. Each set of values was evaluated for overall ramp adaptation ($Step_{final}$), final feed rate ($Fs_{final}$), time to saturate the feed rate at 100% ($t_{Fsat}$), and final biomass OD. The simulations in set $A$ used a 15 minute ramp frequency for the BOOM controller ($\text{BOOM}_{15}$) and the culture grew according the Xu growth rate model, which had a maximum growth rate of 0.5. The simulations in set $B$ used $\text{BOOM}_{15}$ and an 'induced' Xu growth rate model, in which the $qO_{max}$ term was slowly decreased to simulate the metabolic burden that recombinant protein production causes on the growth rate. The 'induced' growth rate decreased from 0.5 $\text{h}^{-1}$ at 1 hour to below

0.2 $h^{-1}$after 24 hours. The simulations in set $C$ used a 30 minute ramp frequency ($BOOM_{30}$) and the 'induced' Xu growth rate model.

For the uninduced experiments, the BOOM controller was able to keep the culture in the BOOM region and produce large amounts of biomass using a wide range of values for 'slope', 'deltaStep', and 'muGS'. Analysis of these simulations indicated that setting the 'slope' value too high prevented proper ramp adaptation. In simulations A7 and A8, the lack of ramp adaptation is seen in the $Step_{final}$ value of 1, which indicated the initial slope was steep enough to drive the culture into overflow in the first 3 minutes during every ramp event. The different values of 'muGS' tested in these simulations has less effect in these simulations because the maximum growth rate of the culture was higher. The value of 'muGS' did have some effect. In simulation A1, the muGS was set very low, and the BOOM controller yielded low biomass. The value was slightly increased in simulation A2 and the controller converged to the BOOM region, yielding over twice the biomass of A1. The 'deltaStep' variable is the least sensitive parameter, but dictates how quickly the controller converges to the BOOM region more than the other two. The 'deltaStep' variable determines the rate of increase for the 'step' variable, which in turn increases the overall slope. Increasing the slope of the ramp allows the controller to quickly accelerate the process if the current growth rate and maximum growth rate are very different, such as right after the batch phase. Therefore, a higher 'deltaStep' value allows faster convergence of the grow rate to the BOOM region, increasing the overall biomass. Simulations A2 and A3, illustrate this effect, as the higher 'deltaStep' value in A3 caused faster convergence to the maximum oxidative metabolism and saturation of the feed rate 4 hours sooner than in A2.

For the induced simulations, the final biomass was more sensitive to the parameter values. Specifically, the 'slope' or 'muGS' variable slowed ramp adaptation

and caused unstable growth when set too high. In simulations B4 and B5 (data not shown), the 'slope' value was low, but the 'muGS' value was high. The 'muGS' prevented the adaptation of the ramp by passively increasing the slope at a rate close to the maximum 'induced' growth rate of the cells. In Figure 5.1, the results from simulation B15 are shown. The 'slope' selected was very aggressive, and ramp events at hours 13, 15, and 16 caused massive acetate spikes in Figure 5.1D. The ramp events were small enough that the culture processed the excess acetate and brought itself back into the BOOM region. However, the large 'muGS' value caused the ramp event at hour 17 to generate so much acetate that the culture could not process it before the next ramp event, and the culture failed due to acetate buildup. The 'muGS' represents a continual exponential growth of the values of 'slope' and 'deltaStep'. If the the growth rate of the culture is descreasing as in these simulations, a large value of 'muGS' will cause the culture to go unstable. The 'muGS' must be set far below the theoretical max growth rate of the culture value. In B15, the 'muGS' was 0.10 $h^{-1}$ and the 'induced' growth rate had dropped to 0.25 $h^{-1}$ when the culture became unstable. In Figure 5.2B, the $SR$ threshold correctly identified overflow between the hours of 13 and 16. The feed rate law (5.10) did not increase the feed rate while the culture was in overflow in Figure 5.2D. The feed rate was increased accordingly when the acetate was consumed, keeping the $qO$ near $qO_{max}$ and the culture in the BOOM region, see Figure 5.2C. In simulation B16 (data not shown), the 'muGS' variable was set to half its B15 value; the BOOM controller did not generate excess acetate and the culture achieved final biomass ($OD_{final}$) numbers similar to the other well performing simulations in $B$. In both B15 and B16, the 'slope' variable was set too high because the ramp never had to adapt ($Step_{final} = 1$).

In simulation B2, the effect of different values of the 'deltaStep' variable were examined. In B2, the slope, deltaStep, and muGS were set to low values. In this

simulation, seen in Figure 5.3 and 5.4, the final biomass is lower than the other simulations in B. The low value for 'deltaStep' slowed the BOOM controller's ability to push the culture into the BOOM region and converge to the maximum growth rate. The plot in Figure 5.4D indicates that the ramp events were able to keep the $SR$ value above the oxidative threshold long enough for the 'step' variable to change, but the small value of the 'deltaStep' variable meant that the 'step' could not change the ramp slope very quickly. Smaller ramp events meant small changes in $OUR$ and small ratios of the $OUR_{max}/OUR_{init}$, resulting in small changes in feed rate, see Figure 5.4D. The inability of the ramp event to increase the growth rate can be seen in Figure 5.4A. Ideally, just one ramp event should be able to drive the growth rate to it's maximum, see Figure 5.2A. When there is a larger gap between the actual and maximum growth rate, such as after batch phase, that may not be possible. The decreasing maximum growth rate due to 'induction' was the main reason the BOOM controller was able to converge around hour 10, see Figure 5.4. A larger value of 'deltaStep' allows the ramp slope to grow steeper more quickly and drive the growth rate to its maximum values. In simulations B6 through B9 in Table 5.1, the 'deltaStep' value is gradually increased, values of 60 and 100 yielded final biomass ($OD_{final}$) results 13% higher than B2.

The simulations in set $C$ were conducted used the BOOM controller with a half hour ramp frequency ($\text{BOOM}_{30}$) instead of the quarter hour ramp frequency. There was very little difference in the final biomass numbers using $\text{BOOM}_{30}$ versus $\text{BOOM}_{15}$, see Table 5.1. $\text{BOOM}_{30}$ was more sensitive to lower of values of 'deltaStep'. With ramp events occuring less frequently, it is more important to adapt the ramp slope quickly or the biomass could grow to large, as seen in B2. $\text{BOOM}_{30}$ was more tolerant of higher 'slope' values than $\text{BOOM}_{15}$, which is understable since a culture controlled by $\text{BOOM}_{30}$ has longer to process the acetate inbetween ramp events and

prevent excess acetate buildup.

These simulations demonstrated the relationships between the three main tuning variables for the ramp controller. The $BOOM_{15}$ controller is preferrable to the $BOOM_{30}$ controller due to stability, faster ramp adjustment, and overall higher average growth rate. For the *E.coli* represented by the Xu model, the 'slope' variable should be set to a low value, between 0.1 to 0.3, any higher and it will impede the ability of the 'deltaStep' to adapt the ramp slope to the culture. The controller has no way to decrease the 'slope', and if the 'slope' variable is too high, the stability can be adversely effected. Based on the simulations, the deltaStep value can be set from 10 to 100 depending on the maximum growth rate. The exact value of the deltaStep is much less important to overall stability, and setting it in the lower range will not significantly impact the final biomass. The muGS should be 1/4 to 1/5th the estimated maximum growth rate of the culture. muGS should be set conservatively if the culture is induced and the induced growth rate is unknown.

Table 5.1: Results of the simulated BOOM controller experiments

| **Sim** | **slope** | **deltaStep** | **muGS** | **Step**$_{final}$ | **Fs**$_{final}$ | $t_{Fs_{sat}}$ | **OD**$_{final}$ |
|---|---|---|---|---|---|---|---|
| A1 | 0.1 | 1 | 0.01 | | | | 78 |
| A2 | 0.1 | 1 | 0.05 | 5.1 | | 19 | 177 |
| A3 | 0.1 | 50 | 0.05 | 21 | | 15.2 | 187 |
| A4 | 0.1 | 100 | 0.05 | 26 | | 15.2 | 187 |
| A5 | 0.1 | 1 | 0.1 | 4.8 | | 16.5 | 184 |
| A6 | 0.9 | 30 | 0.1 | 2.5 | | 14.5 | 187 |
| A7 | 3 | 30 | 0.1 | 1 | | 14.5 | 188 |
| A8 | 5 | 50 | 0.1 | 1 | | 14.3 | 188 |
| B1 | 0.05 | 100 | 0.1 | 9 | 41 | | 100 |
| B2 | 0.1 | 1 | 0.05 | 2.45 | 56 | | 112 |
| B3 | 0.1 | 1 | 0.1 | 1.7 | 65 | | 119 |
| B4 | 0.1 | 1 | 0.2 | 1 | 76 | | 127 |
| B5 | 0.1 | 1 | 0.3 | 1 | 56 | | 120 |
| B6 | 0.1 | 10 | 0.05 | 4 | 63 | | 118 |
| B7 | 0.1 | 30 | 0.05 | 4.5 | 69 | | 122 |
| B8 | 0.1 | 60 | 0.05 | 5 | 75 | | 125 |
| B9 | 0.1 | 100 | 0.05 | 5.5 | 76 | | 127 |
| B10 | 0.1 | 100 | 0.1 | 5.8 | 75 | | 126 |
| B11 | 0.3 | 100 | 0.1 | 2.4 | 90 | | 137 |
| B12 | 0.5 | 10 | 0.05 | 1.14 | 87 | | 135 |
| B13 | 1 | 1 | 0.05 | 1 | 90 | | 137 |
| B14 | 0.9 | 30 | 0.1 | 1 | 91 | | 138 |
| B15 | 3 | 30 | 0.1 | 1 | 33 | | 100 |
| B16 | 3 | 30 | 0.05 | 1 | 84 | | 137 |
| C1 | 3 | 30 | 0.1 | 1 | 67 | | 126 |
| C2 | 0.1 | 1 | 0.05 | 2.2 | 34 | | 95 |
| C3 | 0.1 | 100 | 0.1 | 6 | 69 | | 122 |
| C4 | 0.9 | 30 | 0.1 | 1 | 72 | | 125 |

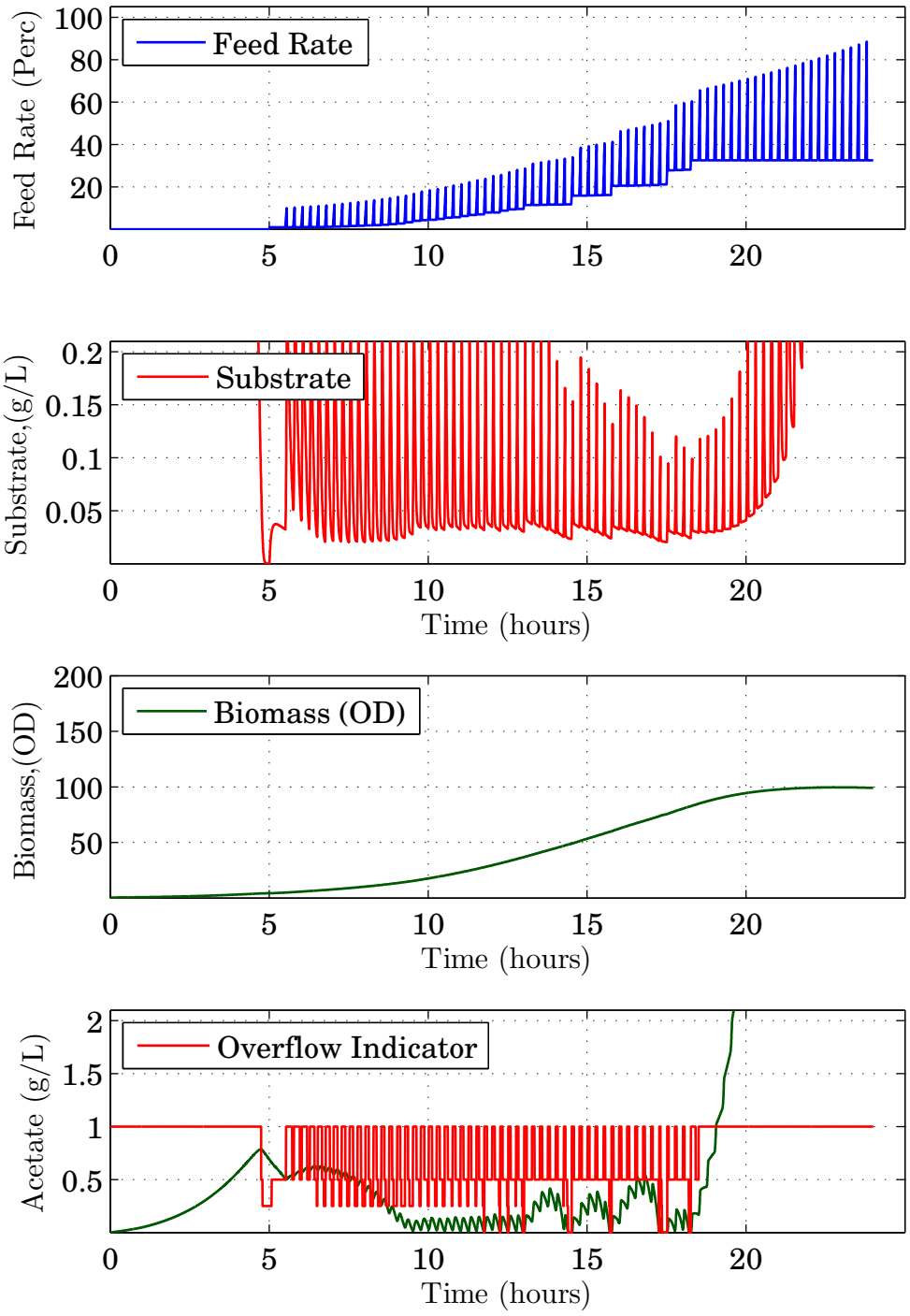


Figure 5.1: Profiles from simulated *E.coli* fermentation B15 using the $\text{BOOM}_{15}$ controller: A) Feed Rate B) Substrate C) Biomass D) Acetate and simulated overflow indicator.

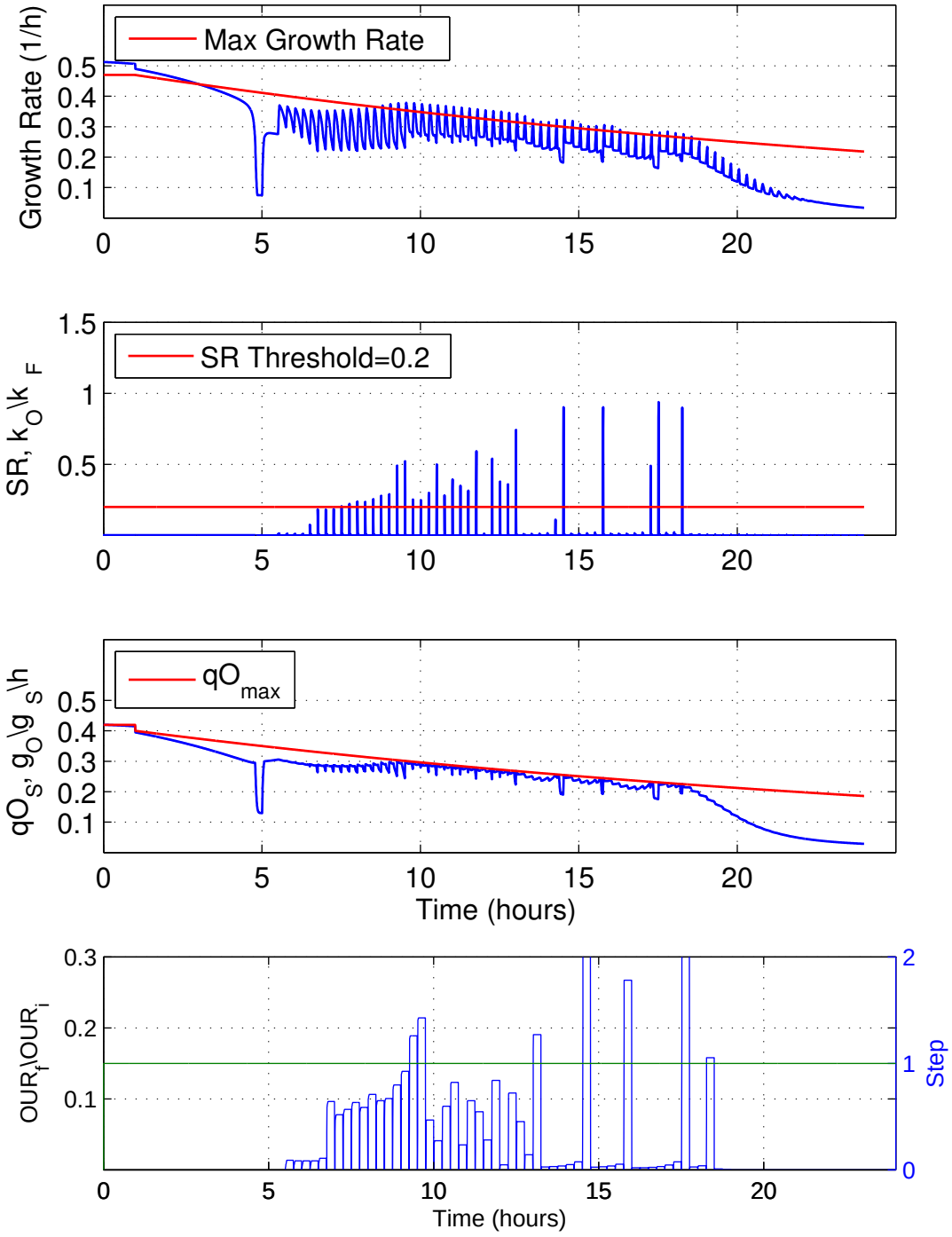


Figure 5.2: Growth rate Profiles from simulated *E.coli* fermentation B15 using the $\text{BOOM}_{15}$ controller: A) Growth Rate and theoretical max growth rate B) $SR$ responses to ramp events and the $SR$ threshold C) the $qO$ profile with the decreasing $qO_{max}$ profile D) the feed rate percentage increases for each ramp event.

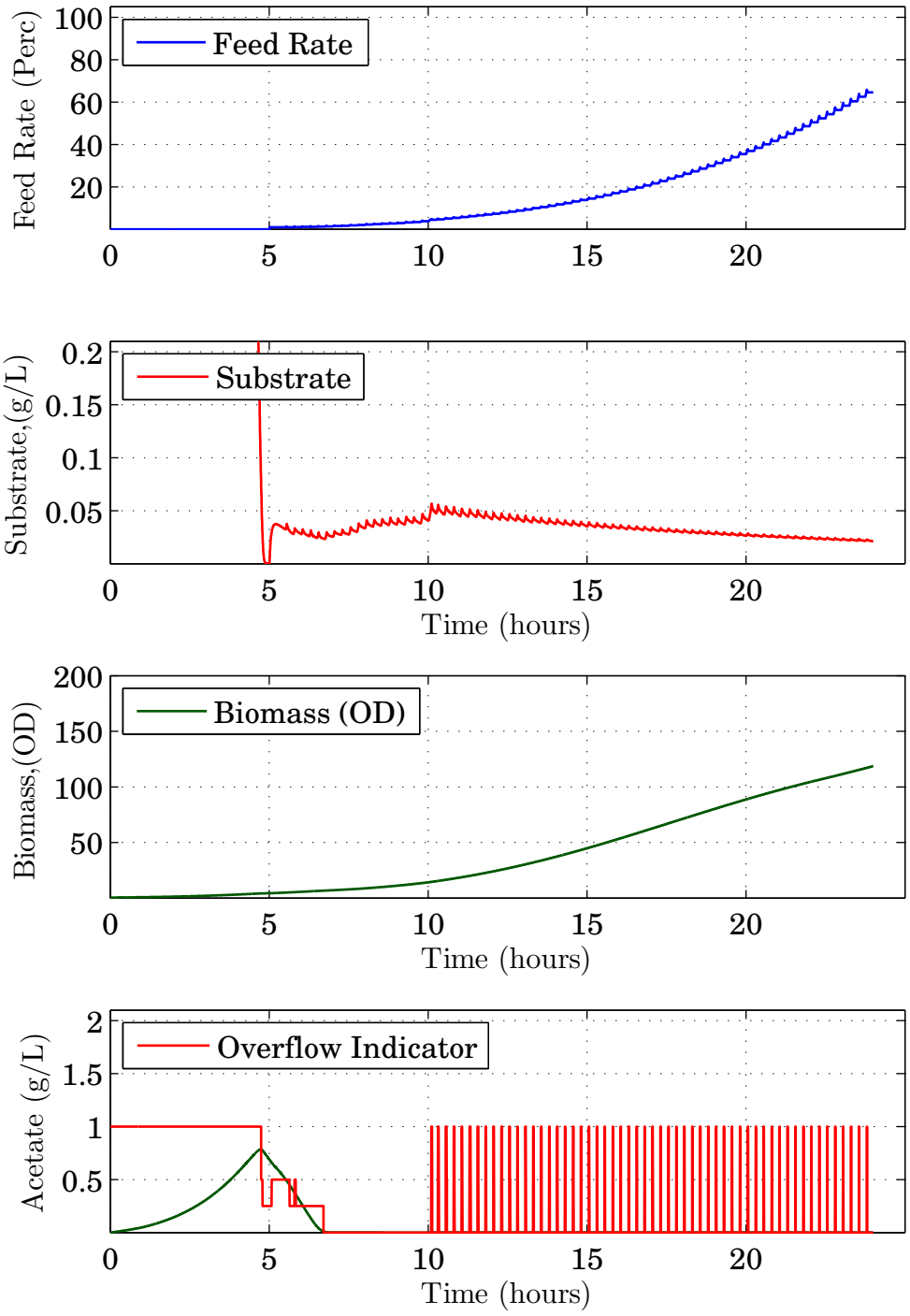


Figure 5.3: Profiles from simulated *E.coli* fermentation B2 using the $\text{BOOM}_{15}$ controller: A) Feed Rate B) Substrate C) Biomass D) Acetate and simulated overflow indicator.

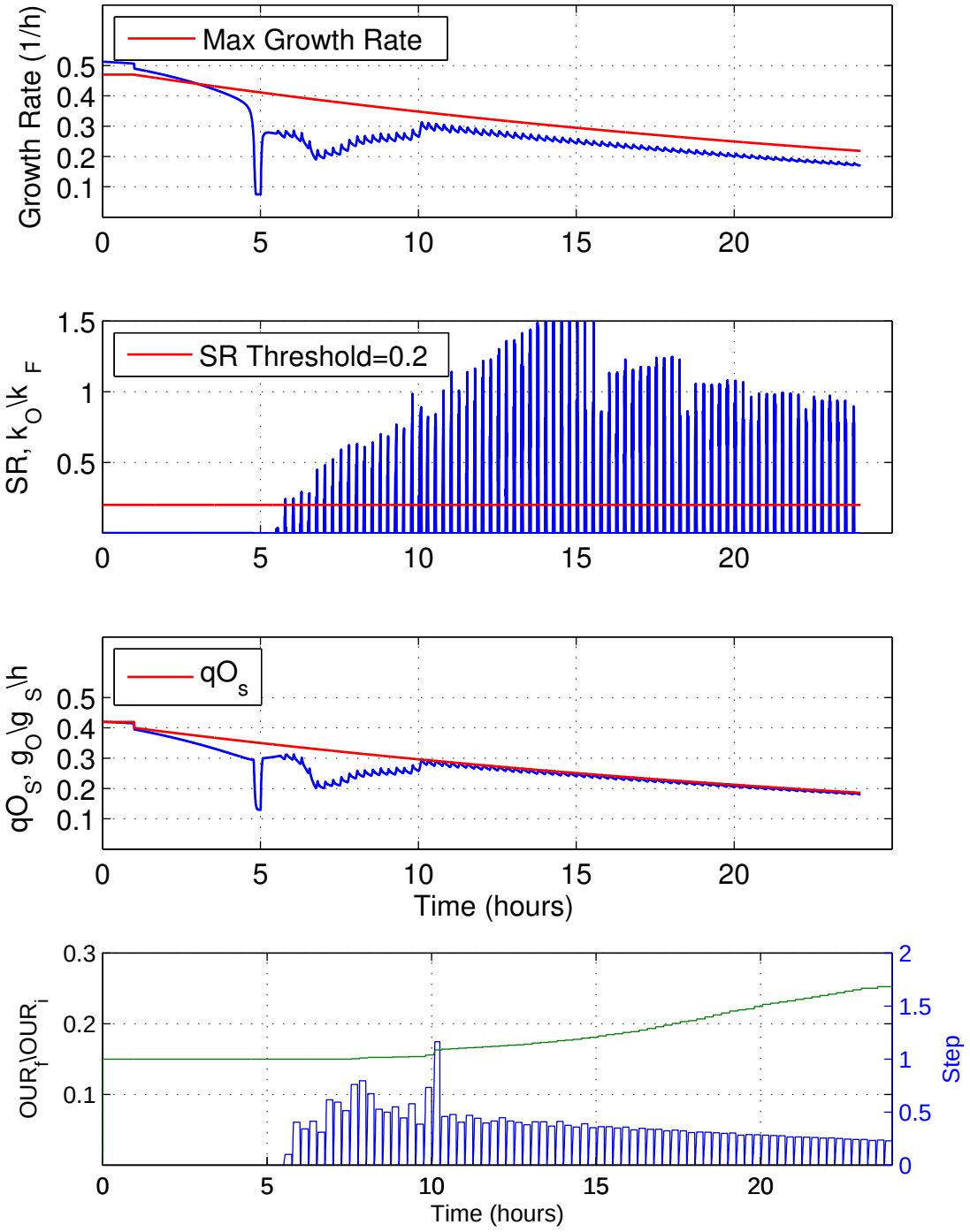


Figure 5.4: Growth rate Profiles from simulated *E.coli* fermentation B2 using the $\text{BOOM}_{15}$ controller: A) Growth Rate and theoretical max growth rate B) $SR$ responses to ramp events and the $SR$ threshold C) the $qO$ profile with the decreasing $qO_{max}$ profile D) the feed rate percentage increases for each ramp event.

# Chapter 6

# Materials & Methods

The *E.coli* cultured in the experiments in this study were MG1655 pTVP1GFP, obtained from the American Type Culture Collection (ATCC). The plasmid pTVP1GFP encodes the VP1 capsid of foot-and mouth disease [Liu et al., 2006] fused to green fluorescent protein (GFP) [Garcia-Fruitos et al., 2007]. The *E.coli* MG1655 were transformed with the pTVP1GFP plasmid. The plasmid including the pBR322 origin, lac I expression, ampicillin- resistance, and isopropyl $\beta$-D-1-thiogalactopyranoside (IPTG) inducibility through a *trc* promoter.

*E.coli* MG1655 pTVP1GFP were cultured in a minimal medium described previously [Korz et al., 1995]. Frozen stock (1 mL, stored at -80°C) were thawed and added to the minimal medium containing 100 mg/mL ampicillin (Sigma). Cells were grown overnight in a shaker incubator (New Brunswick C24, Eppendorf AG, Hamburg, Germany) at 37°CC and 250 rpm to approximately 2.5 OD. ODs were obtained at 600nm with a spectrophotometer (Spectronic 20 Genesys, Thermo Scientific, Suwanee, GA), where 1 OD is equivalent to 0.50 g dry cell weight per liter. Samples were diluted with deionized water to obtain absorbance readings in the linear range (0– 0.5 OD). The overnight cultures were used to inoculate two experimental flasks, which

contained 250 mL medium in a 1000mL shake flasks to obtain a final cell density of 2.5 OD. Before innoculating the bioreactor, a specific volume of the overnight culture (approximately 300 mL) was spun down at 8000g in a Beckman-Coulter Avanti J-26XP ultra centrifuge using a JA-10 rotor. The cells were resuspended in 40 mL of supernatent. The 1.5 L of minimal media in the bioreactor was innoculated and the starting OD was approximately 0.5 OD. Induction was performed using 1.428 g of IPTG suspended in 10 mL of deionized water, for a culture concentration of 4 mM IPTG.

Hourly samples were drawn for off-line analysis. Optical density was measured using the spectrophotometer. Acetate concentration was analyzed using a colorimetric assay at 572 nm (EnzyChrom EOAC-100, BioAssay Systems, Hayward, CA). Samples exceeding the acetate concentration range of 0.118 to 1.18 g/L were diluted and reanalyzed. For protein analysis, each sample was analyzed using Bacterial Protein Extraction Reagent (BPER) (Thermo Scientific, Rockford, IL) and measured by a Tecan GeNiOS spectrophotometer (Tecan Group Ltd. Mannedorf, Switzerland). The pTVP1GFP protein production was measured by the fluorescence signal using 485 nm excitation and 535 nm emission.

## 6.1 Controller Comparison Experiments

Three methods for fed-batch fermenation control were compared: Exponential Feed Rate, DO-stat, and BOOM control. Each control method completed two fed-batch fermentations of *E.coli* MG1655 pTVP1GFP, induced at 1 hour with 4mM IPTG, and the results are shown for the first 13 hours. The total protein production results of these experiments was compared.

### 6.1.1 Exponential Feed Rate Control

In this study, the exponential feed rate control algorithm had the following feed rate (F):

$$\frac{d}{dt}F = \mu_{set}\ F \tag{6.1}$$

with a $\mu_{set}$ value of 0.3 $h^{-1}$ and $F_0$ value of approximately 0.003 L/h, which represents 1% of the coarse feed-pump capacity. After many different experiments, the authors of [Sharma et al., 2007] chose this value of $\mu_{set}$ to achieve high biomass but prevent overflow. Once the Exponential feed rate is started, no modification of the feed rate was allowed. Dissolved oxygen for this experiment was controlled by the DO PID controller on the DCU, which regulated the stir speed to maintain a setpoint of 40%.

### 6.1.2 DO-stat Control

The DO-stat control algorithm was derived from [Chen et al., 1997]. The height of the feed rate pulse was set such that it can provide enough substrate even at high cell densities; for these experiments, that value was approximately 0.058 L/h, which represents 17% of the coarse feed-pump capacity. The dissolved oxygen threshold was chosen at 60%. If the DO probe signal rose above the threshold, the substrate feed rate was activated. Once the signal fell below the threshold, the feed rate was deactivated. The stir speed controller for this algorithm increased the current stir speed by 2% when the DO went below 30%. The initial stir speed was 200 RPM.

### 6.1.3 $\text{BOOM}_{15}$ Controller

The boundary of oxidative and overflow metabolism (BOOM) controller was set to a 15 minute ramp frequency ($\text{BOOM}_{15}$). The 'slope' was set to 0.9%, the

'deltaStep' to 30%, and the 'muGS' to 0.1 $h^{-1}$. The $\text{BOOM}_{15}$ controller used the adaptive $k_L a$ estimator for $OUR$ measurements and the gains on $\alpha_0$ and $\alpha_1$ were set to 0.50 and $50e^{-6}$, respectively.

# Chapter 7

# Results & Discussion

In order to validate the BOOM controller, duplicate *E.coli* fermentations were conducted with the $BOOM_{15}$ controller and two commonly used industrial controllers: Exponential Feed and DO-stat. Figure 7.1A shows the biomass profiles for these six fermentations. All six fermentations were started as batch cultures and lasted approximately 5 hours. The cultures were induced with 4mM IPTG at 1 hour to start the expression of the pTVP1GFP fusion protein. Due to the high innoculum of 0.5 OD, the *E.coli* processed the initial glucose in batch phase 4 to 7 hours sooner than in previous experiments. The final biomass concentrations of 40 OD at 13 hours were comparable to 17 to 20 hours in some papers [Akesson et al., 1997, Xu et al., 1999, Sharma et al., 2007]. The $BOOM_{15}$ and Exponental feed fermentations and the DO-stat fermentations were run for a total of 15 and 17 hours, respectively. Due to some lysing issues later on in some fermentations, only first 13 hours are shown for all results.

An exponential model ($X = X_0\ exp(\mu_{phase}\ t)$) was fit to the first 5 hours of each experiment using SAS 9.3 (SAS Institute Inc.,Cary, NC) and the NLPROC MIXED function. There was significant evidence to say that the exponential growth

term, $\mu_{phase}$, was not different for any of the experiments ($p > 0.05$). After 12 hours of induction, the average final biomass for the $BOOM_{15}$ and Exponential controller fermentations were similar at 29 and 25 respectively, while the average final OD for the DO-stat was 19 OD. The DO-stat had the lowest final biomass due to it having the lowest growth rates, see Figure 7.1C. The growth rates for both DO-stat fermentations were less than 0.2 $h^{-1}$ after hour 10. Statistical analysis of the growth rate profiles of DO-stat from hour 6 to hour 13 showed that the growth rates have a negative slope ($p \leq 0.05$). The analysis for growth trends was performed using JMP (SAS Institute) and the Linear Fit for Bivarate Data. Using ANOVA, the growth rate was tested against a null hypothesis of $h_0 : slope = 0$. While the Exponential feed and $BOOM_{15}$ fermentations had growth rates above 0.2; there was significant evidence to show that the growth rates for the $BOOM_{15}$ fermentations also had a negative slope ($p \leq 0.05$). There was sufficient evidence present to state that the Exponential feed growth rates were constant, with a mean of [0.22, 0.235] for Exp 1 and 2, respectively. Neither Exponential feed fermentation grew at the designated rate of the Exponential feed controller ($\mu_{set} = 0.30\ h^{-1}$). Therefore the fitted growth rates of 0.22 and 0.235 must represent the maximum growth rate for this *E.coli* strain with 4mM induction. The difference between the $\mu_{set}$ and actual growth rates indicates the Exponential feed fermentations must be overfed.

Acetate production is considered a growth inhibitor and a strong inhibitor of recombinant protein production. In Figure 7.1B, the acetate concentration profiles are shown for all six fermentations. The apparently high growth rates of the Exponential feed and $BOOM_{15}$ controllers were very surprising given the extremely high acetate concentrations. At hour 13, the Exponential feed fermentations 1 and 2 had acetate concentrations are 8 and 18 g/L and growth rates of 0.24 and 0.21 $h^{-1}$ respectively. Combined with the $BOOM_{15}$ data, acetate appears to begin to inhibit growth rate

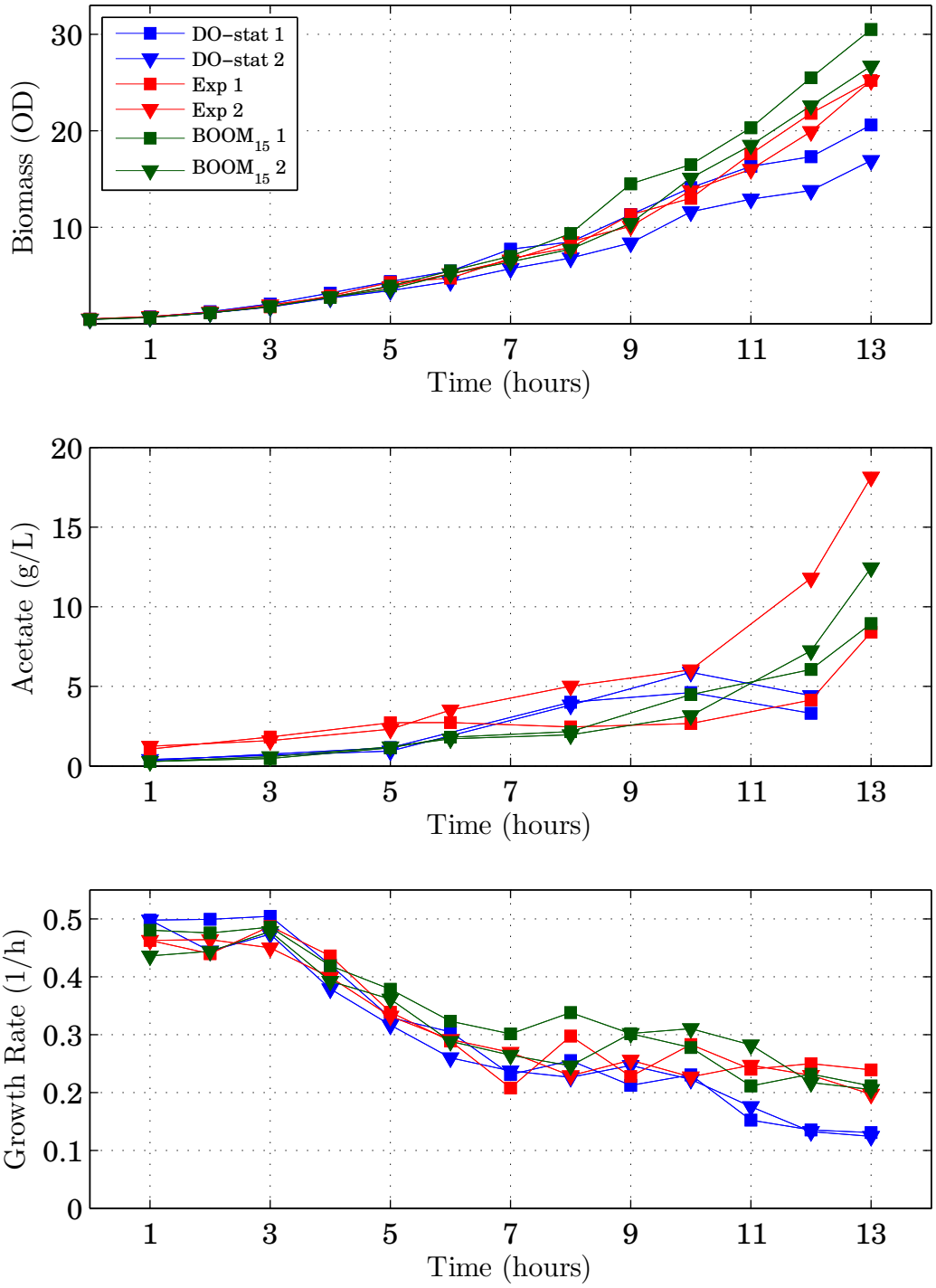


Figure 7.1: The A) Biomass, B) Acetate, and C) Growth rate profiles for all induced *E.coli* MG1655 pTVP1GFP fermentations.

around 8 g/L. Other data (not shown) indicates that the acetate severely inhibits growth rate for induced *E.coli* MG1655 pTVP1GFP above 25 g/L. The acetate levels for the DO-stat fermentations did not rise as high as the other controllers, see Figure 7.1B. The initial rise in acetate was due to the ratio of the feed pulse to the biomass; after hour 10 the culture demonstrated it was able to process all the glucose from the pulse as well the extracellular acetate.

The recombinant protein expression measurements are shown in Figure 7.2. As expected, the increase in protein expression during the batch phase was similar for all fermentations. The measurements show the expression of recombinant protein increased in the cells at similar rates until eight hours. After eight hours, the pTVP1GFP per cell level for all fermentations was not significantly different ($p > 0.05$). Ultimately, what is important is the amount of recmobinant protein produced. In this case the recombinant protein is a fusion protein pTVP1GFP that fluoresces, so a single whole lysate assay was used to quantify the protein production level per cell. Since all the BPER measurement profiles similar, an average profile was created, see Figure 7.3A. In order to compare recombinant protein production, the OD profiles are multipled by the average BPER profile and the total protein production curves are shown in Figure 7.3B. The high levels of acetate did not appear to affect the recombinant protein production in these fermentations. The average final protein production after 12 hours of induction are shown in Figure 7.4; the $\text{BOOM}_{15}$ fermentation protein production amount (428k) was 10% higher than the Exponential feed (377k) and 50% higher than the DO-stat fermentations (281k).

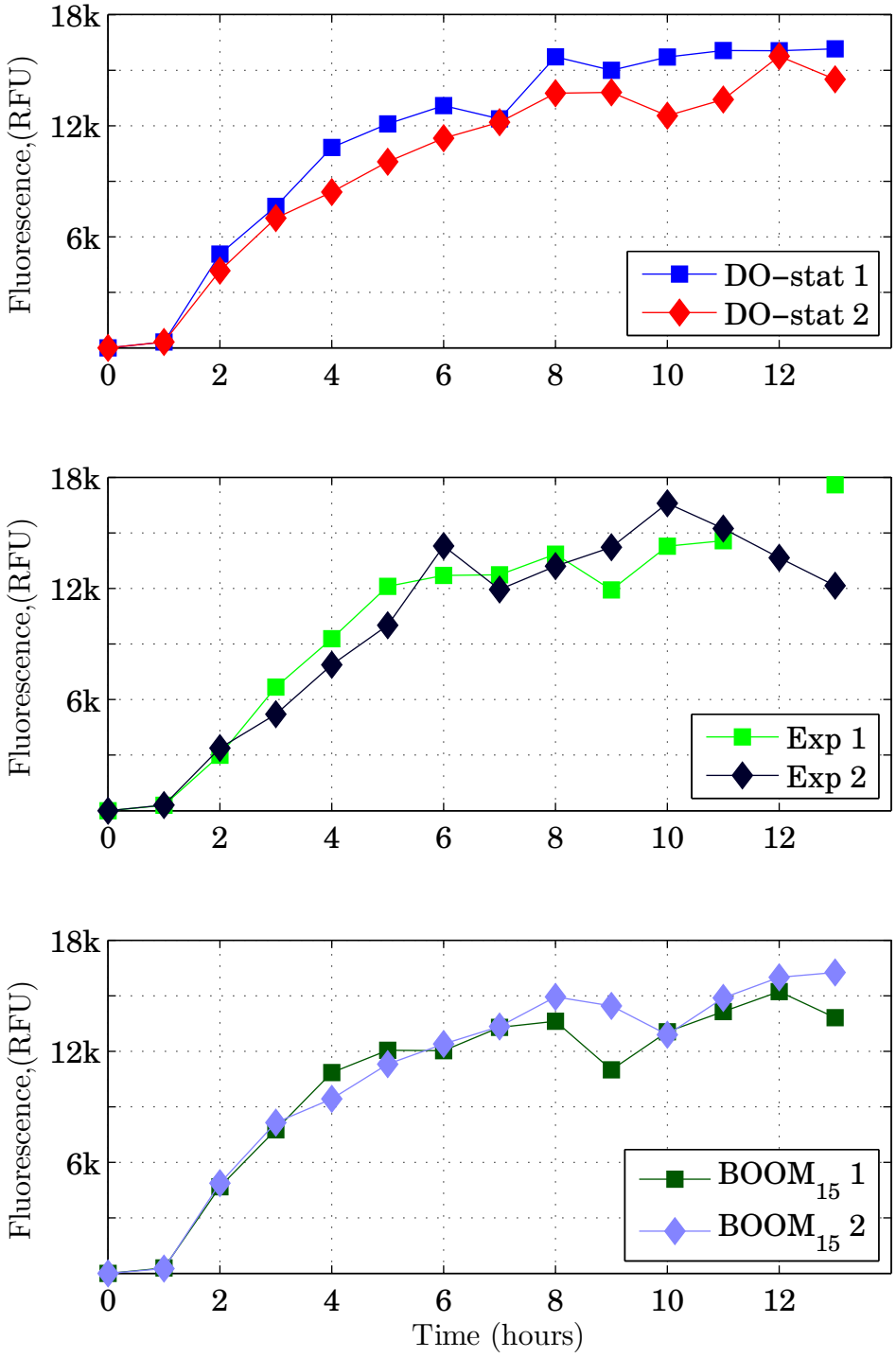


Figure 7.2: The recombinant protein production measured by the BPER flouresence assay for all fermentations. The culture was induced at 1 hour.

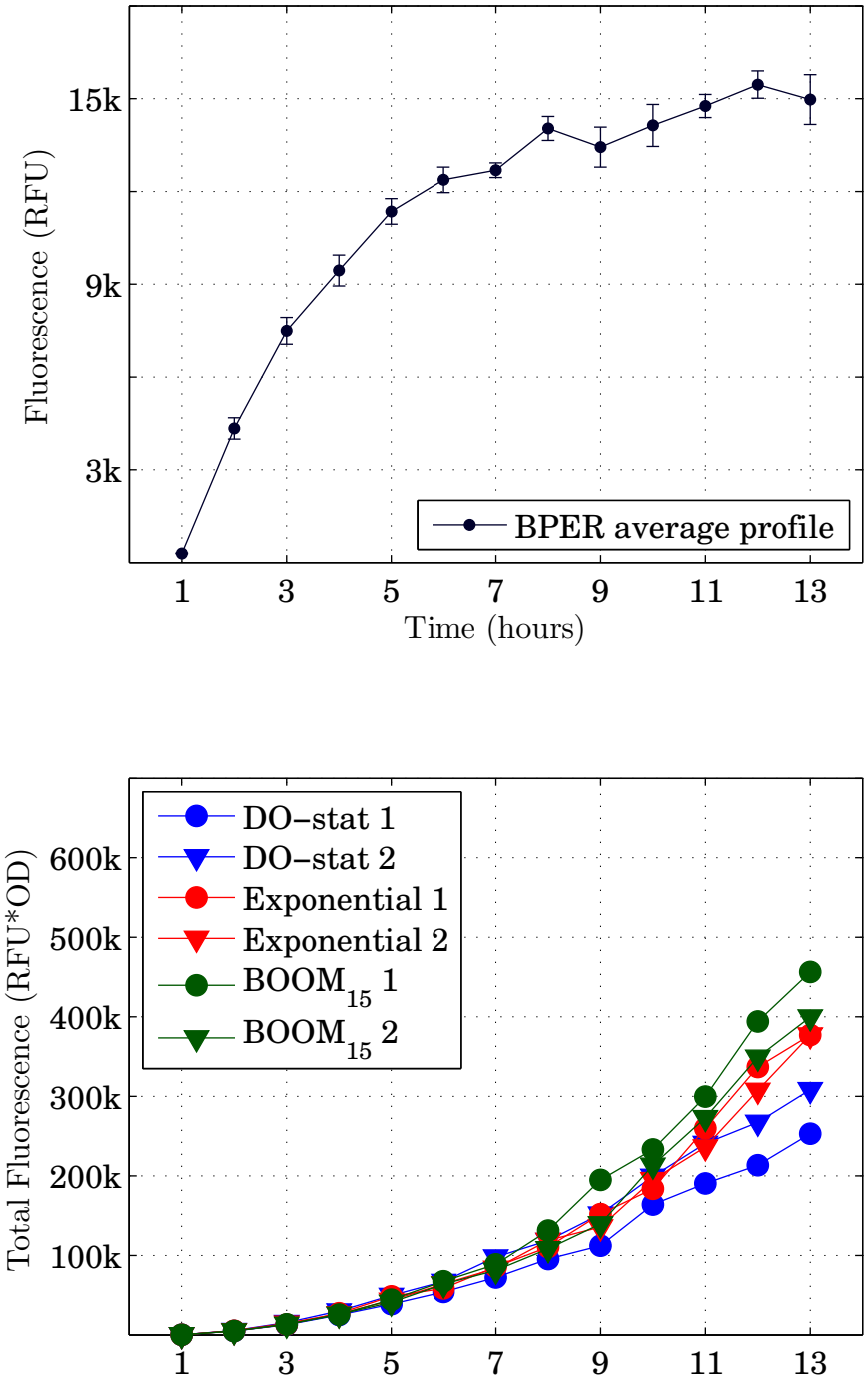


Figure 7.3: A) The total recombinant protein production measurements are averaged for all induced fermentations and shown with error bars. B) The final protein amounts for DO-stat, Exponential feed, and $BOOM_{15}$ are 281k, 377k, and 428k, respectively.

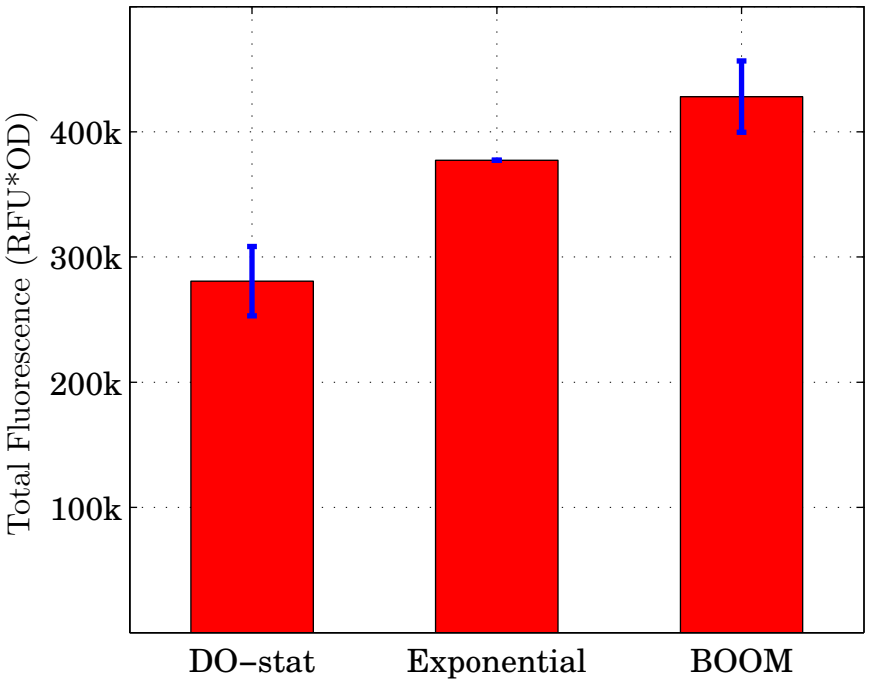


Figure 7.4: The final protein amounts for DO-stat, Exponential feed, and $\text{BOOM}_{15}$ shown with error bars.

## 7.1 $BOOM_{15}$ Controller Performance

The $BOOM_{15}$ controller produced consistent growth rates as well as the highest recombinant protein production at 13 hours. The most surprising result in these fermentations was the acetate buildup. The fundamental assumption of the BOOM algorithm was that the TCA cycle would be balanced with glycolysis thus OUR would not be able to change. The feed rate law,

$$F_{new} = \frac{OUR_{max}}{OUR_{init}} F_{old} \tag{7.1}$$

assumes that the $OUR_{est}$ values would stay fairly constant if acetate was present during a ramp event. This was not true for the induced *E.coli* MG1655 pTVP1GFP strain. At 9 hours in the $BOOM_{15}$ 1 fermentation, Figure 7.5 B and D shows the $SR$ pushed over the oxidative threshold despite the presence of 4 g/L of acetate. The feed law allowed the feed rate to increase 10% for the ramp events in hour 9. The rising acetate concentration did eventually affect the $OUR$ response to the ramp events. By hour 10, the $BOOM_{15}$ controller was unable to drive the $SR$ above the oxidative threshold. The controller correctly identified overflow metabolism; however, the feed rate law still increased the feed rate because the $OUR_{max}/OUR_{init} > 0$. This response was incorrect and similar behavior was seen in the $BOOM_{15}$ 2 fermentation. The feed rate law needs to be modified to decrease the feed rate when the $SR$ does not breach the oxidative metabolism during a ramp event. This modification should help in keeping acetate concentration in check, and would have been helpful in $BOOM_{15}$ 1 in hours 7 and 10 - 13. Despite the high final acetate concentration for $BOOM_{15}$ 1 and 2, the $BOOM_{15}$ controller achieved fast growth, not allowing the acetate concentration to rise to levels that significantly hindered growth rate or protein production.

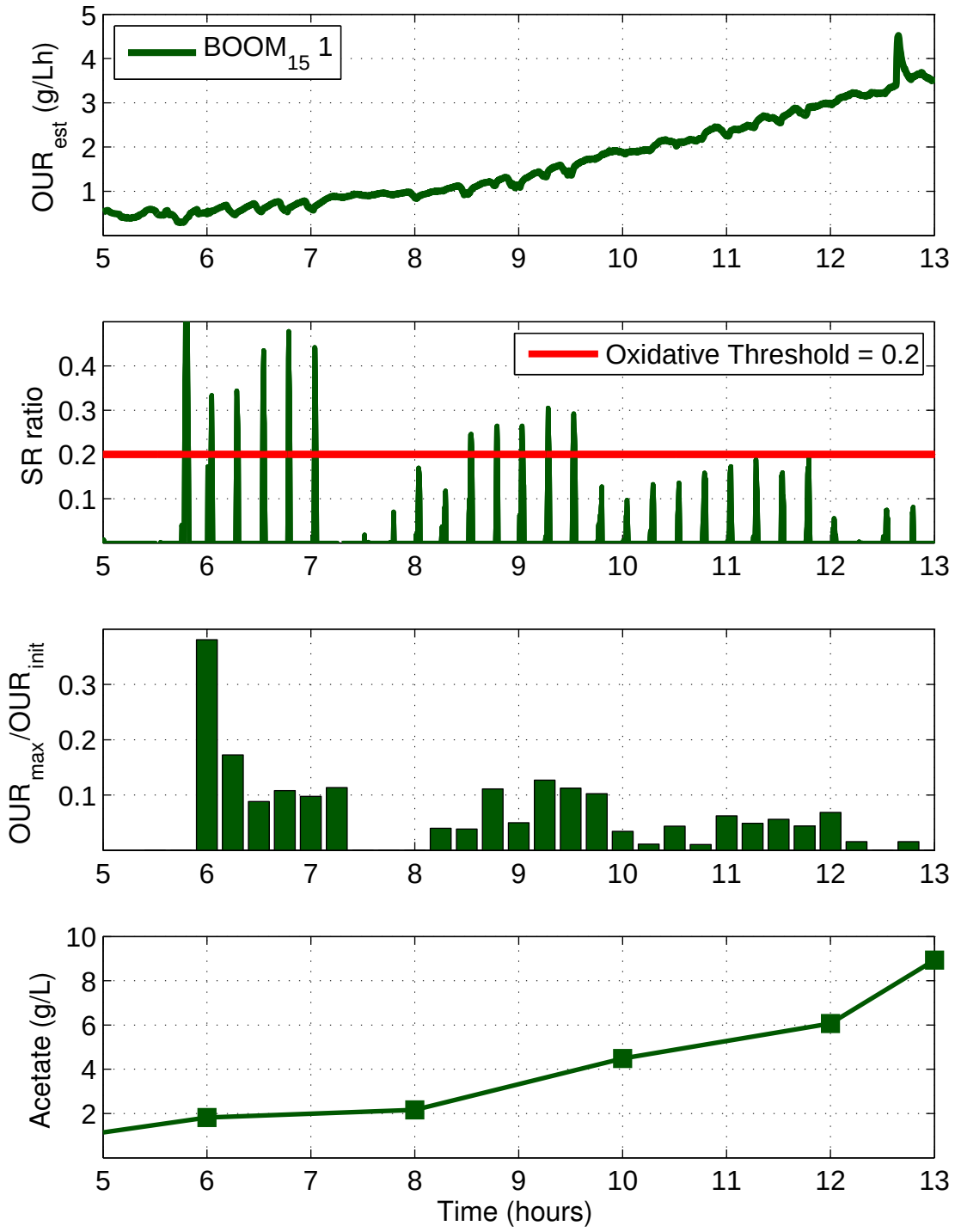


Figure 7.5: The A) $OUR$ responses to the ramp events for $\text{BOOM}_{15}$ 1 are shown along with the B) $SR$. The C) ratio of the $OUR_{max}$ and $OUR_{init}$ is used to make feed rate decisions. The D) acetate concentrations for the fed-batch phase are also shown. The spike in the $OUR_{est}$ at hour 12.5 was the result of antifoam addition and did not affect $\text{BOOM}_{15}$ performance.

## 7.2 $BOOM_{30}$ Controller Fermentation

The buildup of acetate in the $BOOM_{15}$ 1 and 2 did not inhibit the $BOOM_{15}$ controller from achieving its goal of fast growth and maximum protein production. However, if the $BOOM_{15}$ fermentations had continued, the acetate may have reached inhibitory concentrations. A separate fermentation was run in which the ramp frequency of the BOOM controller from decreased from 15 minutes to 30 minutes ($BOOM_{30}$ ). The $BOOM_{30}$ controller had slight changes to the Zig-zag DO control range, from [40 70] to [33 70]. The $BOOM_{30}$ controller also had a slightly different the estimator gain for $a_1$, which changed from [$50e^{-3}$] to [$100e^{-3}$]. The $BOOM_{30}$ fermentation was conducted using the same methods as $BOOM_{15}$ 1 and 2. The *E.coli* MG1655 pTVP1GFP strain induced was induced at 1 hour at 4mM IPTG and run for 13 hours total. The $BOOM_{30}$ controller was started at 5 hours after the batch phase.

The biomass, growth rate, and acetate concentration of the $BOOM_{30}$ fermentation are compared to $BOOM_{15}$ 1 and 2 in Figure 7.6. The $BOOM_{30}$ controller achieved comparable biomass and growth rates to $BOOM_{15}$ 1 and 2, but had significantly lower acetate concentrations, see Figure 7.6 C. The protein production profile (not shown) was consistent with all other fermentations ($p > 0.05$). The total protein production was similar to $BOOM_{15}$ 1 (455k vs 456k). The lower ramp frequency of the $BOOM_{30}$ controller prevented it from adapting as quickly to the end of batch phase as $BOOM_{15}$ . In Figure 7.6 B, the growth rate for $BOOM_{30}$ was lower after the batch phase but eventually rose by hour 10; the $BOOM_{30}$ was not able to drive the growth rate into the BOOM region as quickly as $BOOM_{15}$ . The $BOOM_{30}$ had the lowest acetate concentrations of any induced fermentation, peaking in hour thirteen at only 1.2 g/L. The lower ramp frequency of $BOOM_{30}$ was the major reason

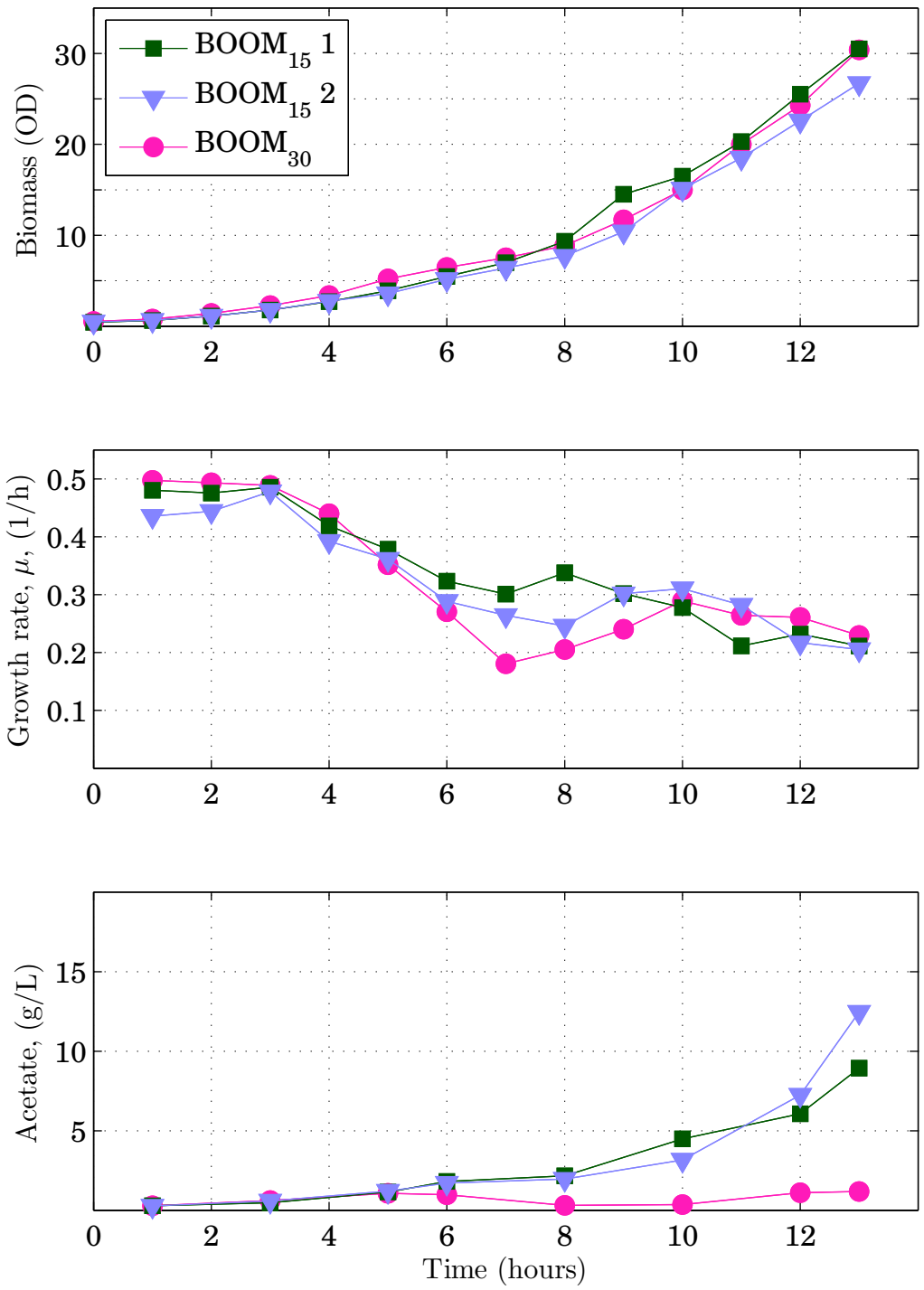


Figure 7.6: The A) Biomass , B) Growth rate, and C) Acetate levels of the $BOOM_{30}$ fermentation are compared to $BOOM_{15}$ 1 and 2.

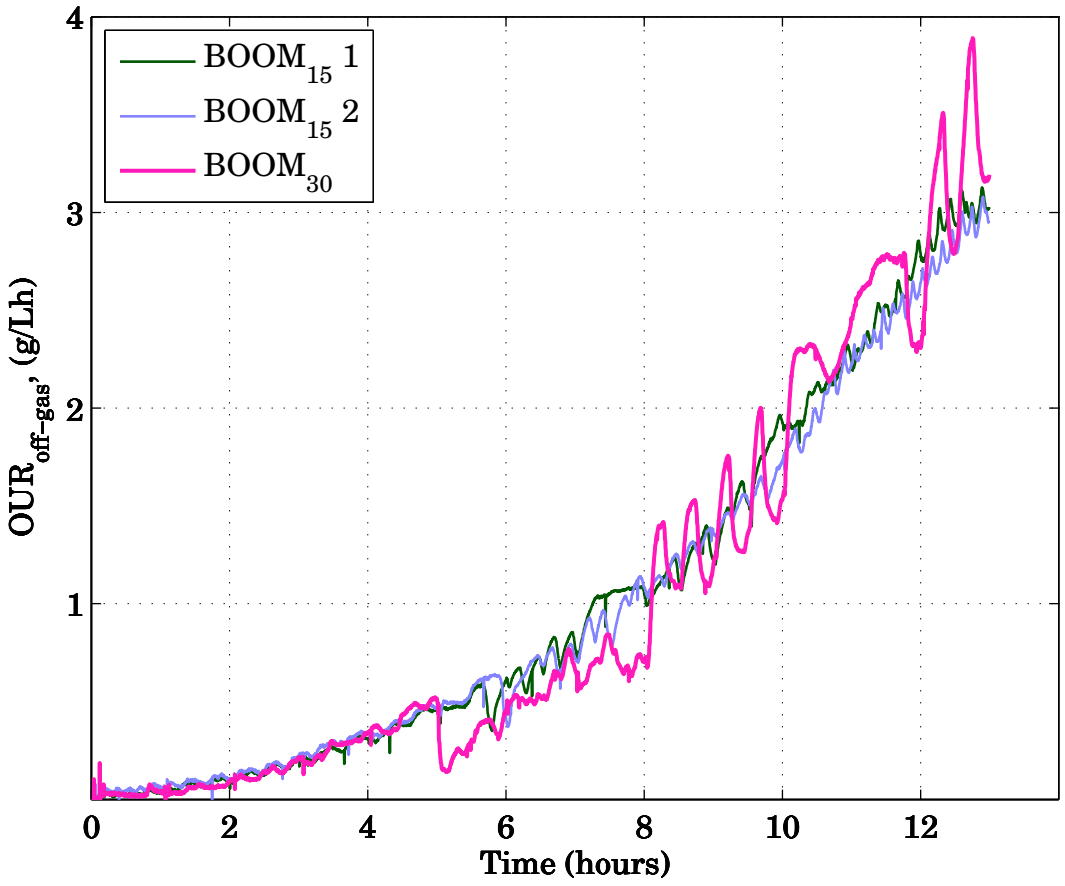


Figure 7.7: The off-gas measurements are compared for $BOOM_{30}$ , $BOOM_{15}$ 1, and $BOOM_{15}$ 2.

the acetate profile was much lower than $BOOM_{15}$ 1 and 2. In order to prevent acetate buildup in a culture, the amount of time that $S < S_{crit}$ in a culture must be greater than the amount of time $S > S_{crit}$. The longer time betwen ramp events in $BOOM_{30}$ allowed the culture to consume excess acetate and maintain $S < S_{crit}$. The effect of the lower acetate concentation had a direct effect on the $OUR$ response in $BOOM_{30}$ versus $BOOM_{15}$ , see Figure 7.7. The magnitude of the change in $OUR$ due to each ramp event is much more pronounced in $BOOM_{30}$ . The ability of the induced *E.coli* MG1655 pTVP1GFP strain to change $OUR$ in the presence of acetate caused the feed rate law to incorrectly raise the feed rate when $BOOM_{15}$ 1 and 2

were in overflow. The shorter ramp frequency did not give the culture time to lower $S$ below $S_{crit}$ and process all the acetate before the next ramp event occurred. In Figure 7.8, the differences in the BOOM controller are examined for $\text{BOOM}_{30}$ and $\text{BOOM}_{15}$ 1. The $\text{BOOM}_{30}$ controller was able to push $SR$ above the oxidative threshold and into the BOOM region more consistently than $\text{BOOM}_{15}$ 1. The difference in $SR$ response between $\text{BOOM}_{30}$ and $\text{BOOM}_{15}$ 1 is due to differences in acetate concentration. If the $SR$ failed to breach the oxidative threshold, e.g in hours 7 and 11, the $OUR_{max}/OUR_{init}$ ratio was small and the $\text{BOOM}_{30}$ controller did not make large adjustments in the feed rate. The largest adjustments in feed occured for both controllers when the acetate was low. For $\text{BOOM}_{30}$ , the larger adjustments in feed at hours 8 and 10 were necessary to drive the growth rate into the BOOM region, but did not result in a buildup of acetate. For $\text{BOOM}_{15}$ , the controller made large adjustments to drive up the growth rate after the end of batch phase. In the latter half of the $\text{BOOM}_{15}$ 1 fermentation, the $OUR_{max}/OUR_{init}$ ratio caused the $\text{BOOM}_{15}$ controller to incorrectly increase the feed rate even when the $SR$ ratio indicated the culture was in overflow. Modifying the controller to hold or decrease the feed rate when overflow is detected may have prevented the acetate buildup seen in $\text{BOOM}_{15}$ 1.

## 7.3 $\text{BOOM}_{15,\Delta T}$ Fermentation

In a separate fermentation, the $\text{BOOM}_{15}$ controller was used to control an uninduced *E.coli* MG1655 pTVP1GFP culture under varying temperature conditions. Temperature can be changed quickly and can increase or decrease metabolism as it rises and falls. Temperature is commonly used by researchers to slow metabolism during induction allow for better protein expression. Varying temperature is good test

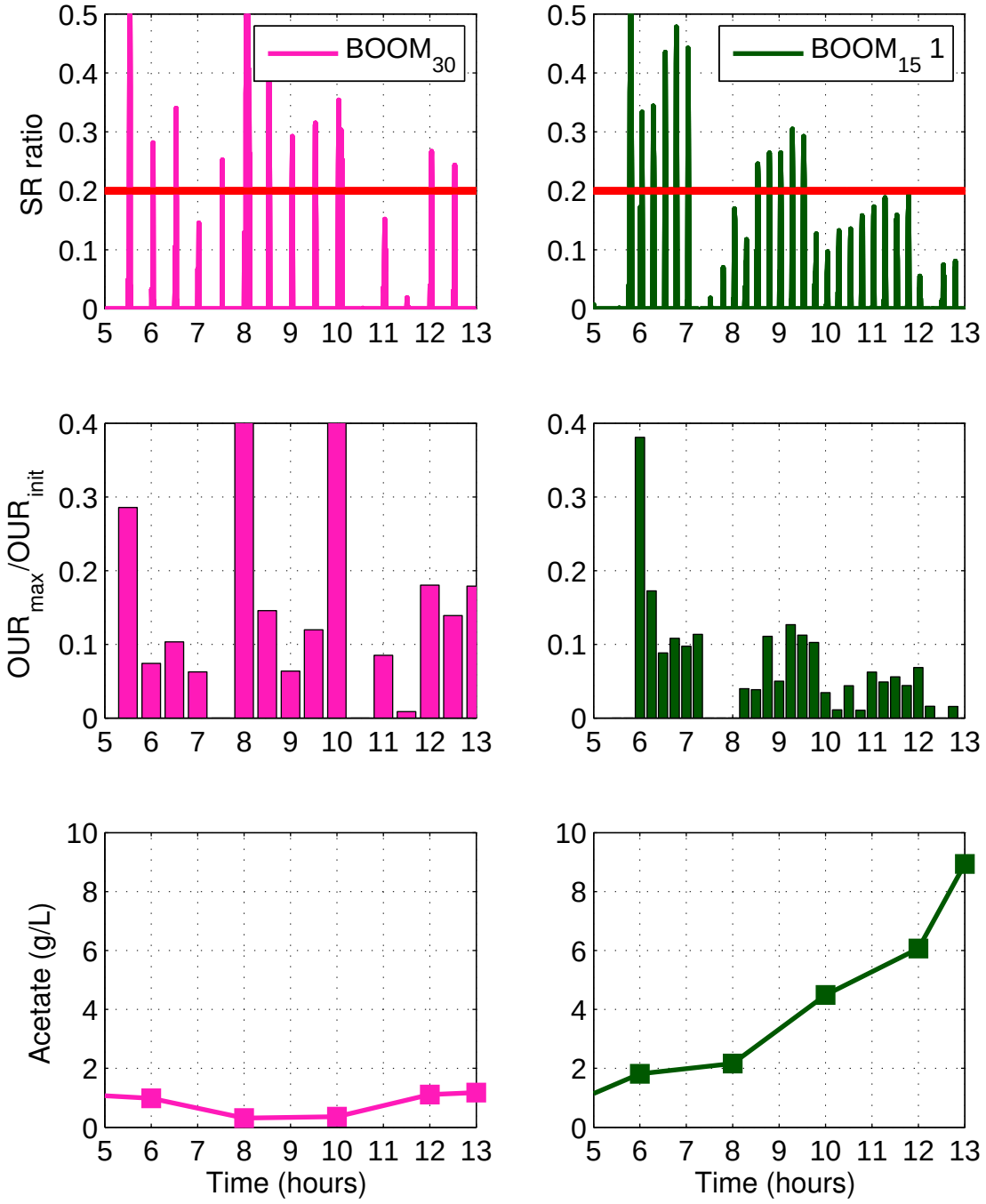


Figure 7.8: The behavior of the $\text{BOOM}_{30}$ and $\text{BOOM}_{15}$ 1 controllers are compared by looking at the $SR$ responses compared to the oxidative threshold at 0.2. The $OUR_{max}/OUR_{init}$ ratio used to make feed rate decisions is shown above the acetate levels.

of the responsiveness of the $\text{BOOM}_{15}$ controller to quick changes in *E.coli* metabolism. The fermentations with induced *E.coli* MG1655 pTVP1GFP were a test of gradual growth suppression due to protein expression. In this fermentation, the metabolism was changed rapidly by lowering temperature from 37°C to 30°C at the eighth hour. The $\text{BOOM}_{15}$ controller had to adapt the feed rate quickly to the new lower growth rate. A set of shake flask experiments run at the same temperature levels established baseline growthrates of $\mu_{37°C} = 0.61\ h^{-1}$ and $\mu_{30°C} = 0.30\ h^{-1}$. The fermentation was prepared and run similarly to the induced *E.coli* MG1655 pTVP1GFP fermentations.

The biomass, growth rates, and acetate profiles are shown for the $\text{BOOM}_{15,\Delta T}$ fermentation in Figure 7.9; the temperature profile is included as well. The fermentation was at a temperature of $37°C$ from the beginning of batch until hour 8. By hour 8, the $\text{BOOM}_{15}$ controller had driven the growth rate near to $\mu_{37°C} = 0.61\ h^{-1}$, which was the assumed maximum growth rate taken from the shake flask data, see Figure 7.9 B. The bioreactor took 24 minutes to cool down the culture from $37°C$ to $30°C$. The growth rate at hour 9 was $0.41\ h^{-1}$, and the growth rate stayed near the $\mu_{30°C} = 0.30\ h^{-1}$ until hour 13. The $\text{BOOM}_{15}$ controller quickly drove the culture to the lower maximum growth rate of $0.30\ h^{-1}$ at $30°C$ without a significant rise in the acetate. At hour 13, the temperature was lowered to $20°C$ in an attempt to maximize bioreactor OTR and lengthen the culture. The $\text{BOOM}_{15}$ controller was unable to adapt to this temperature shift and the acetate rose to 10 g/L. The $\text{BOOM}_{15}$ controller was more successful at minimizing acetate production in this fermentation because the maximum growth rate was not being lowered by induction, see Figure 7.9 C. The metabolism of the *E.coli* at $30°C$ and at $37°C$ drove $S < S_{crit}$ quickly and processed the glucose and any acetate inbetween ramp events. Changing the $\text{BOOM}_{15}$ controller and allowing it to lower the feed rate when overflow was detected might have prevented the acetate buildup at hour 13.

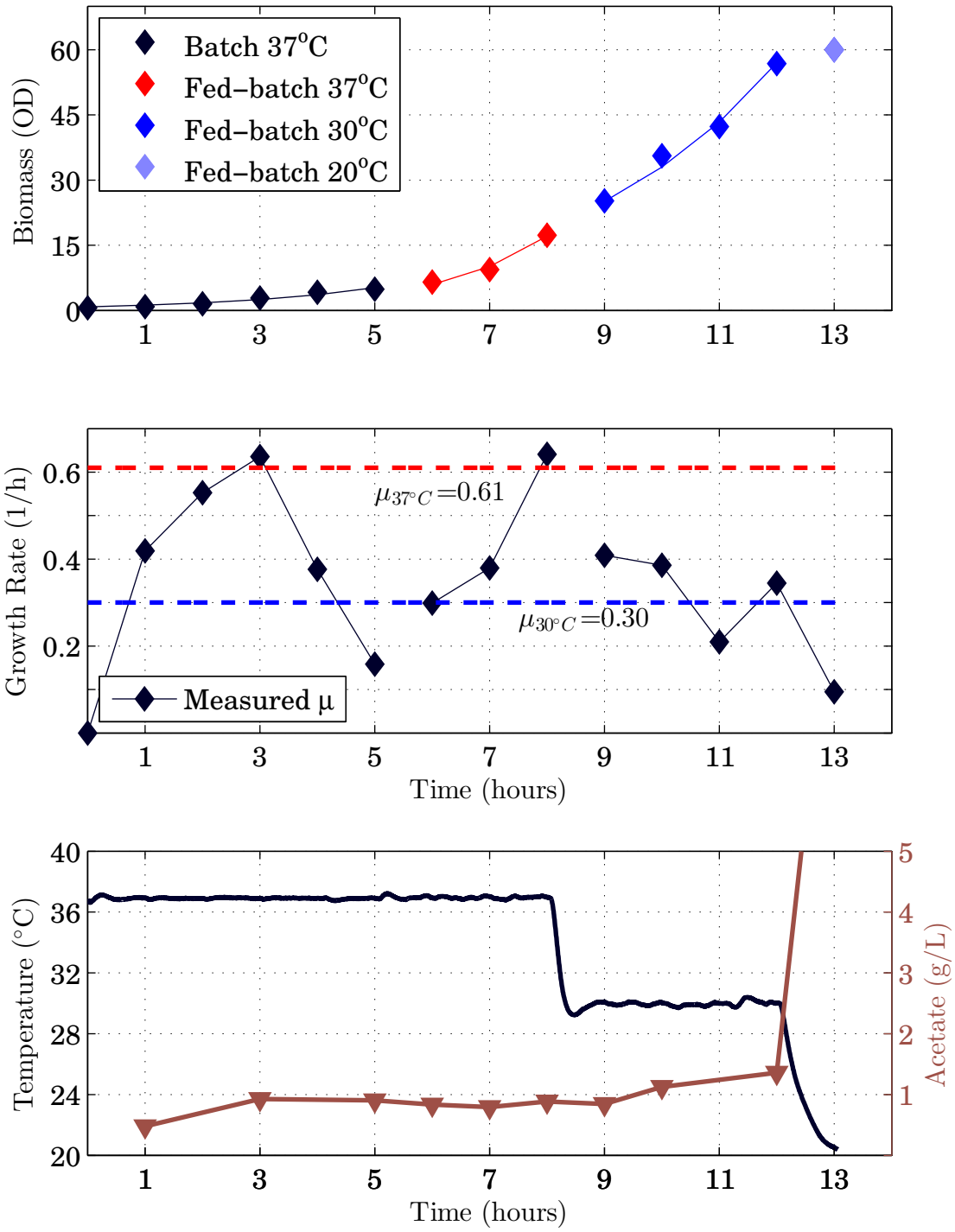


Figure 7.9: The A) Biomass, B) Growth rate, and C) Acetate profiles are shown for the $\text{BOOM}_{15,\Delta T}$ fermentation. The ideal growth rates at each temperature for the uninduced *E.coli* MG1655 pTVP1GFP are shown with the growth rate profile.

## 7.4 BOOM Controller: Simulation & Experiment Comparison

In this section the $BOOM_{15}$ and $BOOM_{30}$ controllers are evaluated in simulation and their performance is discussed with relation to the actual fermentations. For both $BOOM_{15}$ and $BOOM_{30}$ fermentations, the 'slope' was 0.9, the 'stepRatio' was 30, and the 'muGS' was 0.1. The $BOOM_{15}$ fermentations are simulated and the profiles shown in Figure 7.10 and 7.11. At 13 hours, the simulation biomass profile matches the actual fermenation measurement, around 40 OD. In Figure 7.10 D, the acetate concentration is kept low for the entire culture; this may indicate the simulated *E.coli* W3110 have a higher maxmimum acetate consumption flux $qA_{p,max}$ or acetate yield coefficient $Y_{A/X}$ than the MG1655. With low acetate, the $BOOM_{15}$ simulation is able to drive the $SR$ above the oxidative threshold with every ramp event, see Figure 7.11 B. The $BOOM_{15}$ simulation and fermentantion controllers both converge to the maximum growth rate quickly, around 7 hours. The $BOOM_{30}$ simulation was also well behaved, see Figure 7.12. In the simulation, the $BOOM_{30}$ controller converged to the maximum growth rate by hour 8. With the half the ramp frequency, the average growth rate for $BOOM_{30}$ was lower, yielding a slightly lower biomass than $BOOM_{15}$ , 125 vs 138 OD. The $BOOM_{30}$ controller had to take larger adjustments to the feed rate with each ramp, see Figure 7.13 D. In Figure 7.11 D andFigure 7.13 D, neither controller changed the 'step' variable.

The $BOOM_{30}$ and $BOOM_{15}$ controllers do slightly adjust the step values in the fermentations (Figure 7.14). The 'step' variable was larger for $BOOM_{30}$ , the ramp slope needed to be steeper to compensate for the additional biomass growth between each ramp event. The biomass difference was small between each ramp event for $BOOM_{15}$ . In the latter half of the $BOOM_{15}$ 1 fermentation, the gradual

increase due to the 'muGS' term was enough to drive the *E.coli* into overflow with each ramp event. As seen in Table 5.1, the $BOOM_{15}$ controller is more sensitive to the 'slope' variable than $BOOM_{30}$ controller. When the 'slope' variable is set too high and the ramp frequency is also high, the BOOM controller cannot adapt the 'step' value appropriately and possibility of pushing the culture into overflow metabolism is greater. The $BOOM_{30}$ controller performed well in its fermentation, adapted the 'step' variable, and kept the acetate concentration low. The 'slope' variable was set too high for both fermentations and a recommended range of [0.2 to 0.5%] is more appropriate. The 'muGS' should also be lowered to 0.05 $h^{-1}$ from 0.10 $h^{-1}$ since the final maximum growth rate for the 4mM induced *E.coli* MG1655 pTVP1GFP strain was 0.20 to 0.25 $h^{-1}$. Simulations have shown that allowing the feed rate to decrease when overflow metabolism is detected would allow the $BOOM_{15}$ controller to be less sensitive to the 'slope' variable and keep the acetate concentration low.

## 7.5 Algorithm Improvements

Examining the simulation and fermentation data, the 'slope' value for the BOOM controller should be lowered from 0.9% to [0.2 to 0.5%]. In all experiments and simulations, the $SR$ threshold of 0.2 appears to be fairly accurate in indicating overflow metabolism. The reduced ramp frequency of the $BOOM_{15}$ controller pushes the culture into the BOOM region more quickly and adjusts to metabolism changes faster than the $BOOM_{30}$ controller. The *E.coli* MG1655 pTVP1GFP may have a small $Y_{A/X}$ coefficient and consume acetate too slowly for the quarter hour ramp frequency. Another improvement to the algorithm logic would be to allow a negative control input if overflow is detected. The feed law could be set either to $F_{new} = 0$ or $F_{new} = m\ F_{old}$ where $0.9 \leq m < 1.0$. This change would allow the high ramp

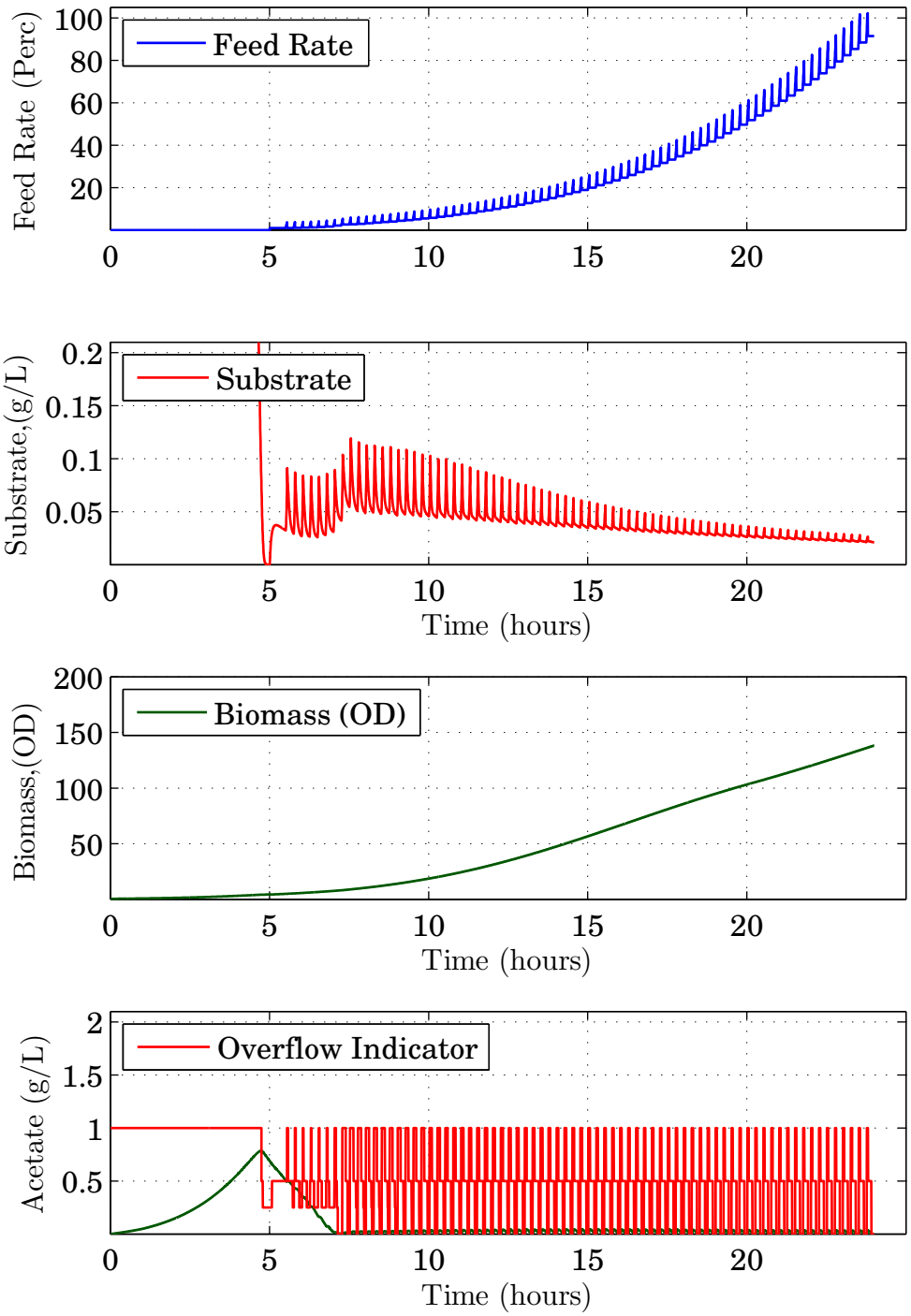


Figure 7.10: The $BOOM_{15}$ controller was simulated using the 'slope', 'step', and 'muGS' parameters used in the fermentations. The A) Feed rate, B) Substrate, C) Biomass, and D) Acetate profiles for this simulation correspond with B14 in Table 5.1.

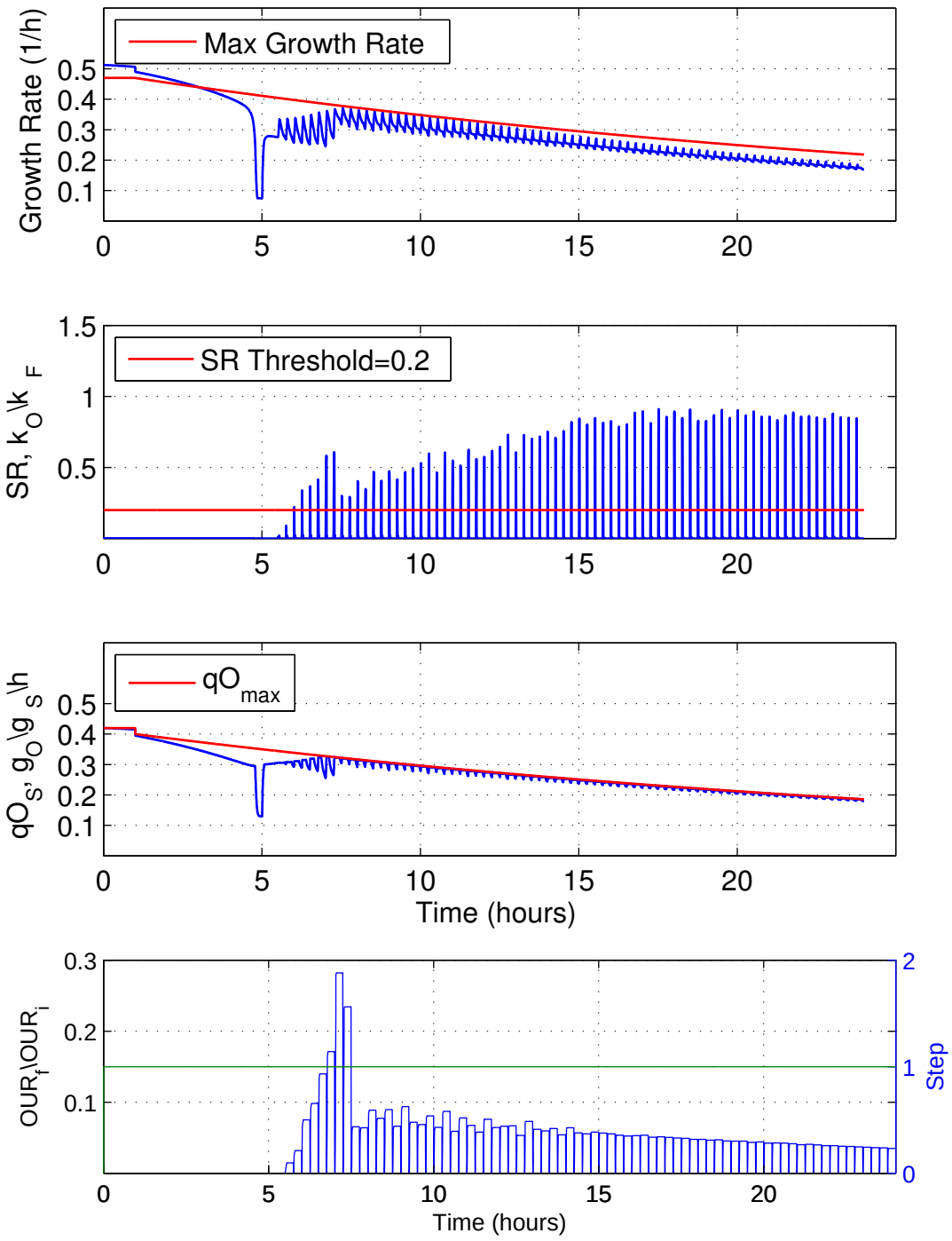


Figure 7.11: The A) maximum growth rate, B) SR, C) $qO_{max}$, and D) $OUR$ ratio profiles are shown for a simulated $\text{BOOM}_{15}$ controller. This controller used the 'slope', 'step', and 'muGS' parameters used in the $\text{BOOM}_{15}$ fermentations.

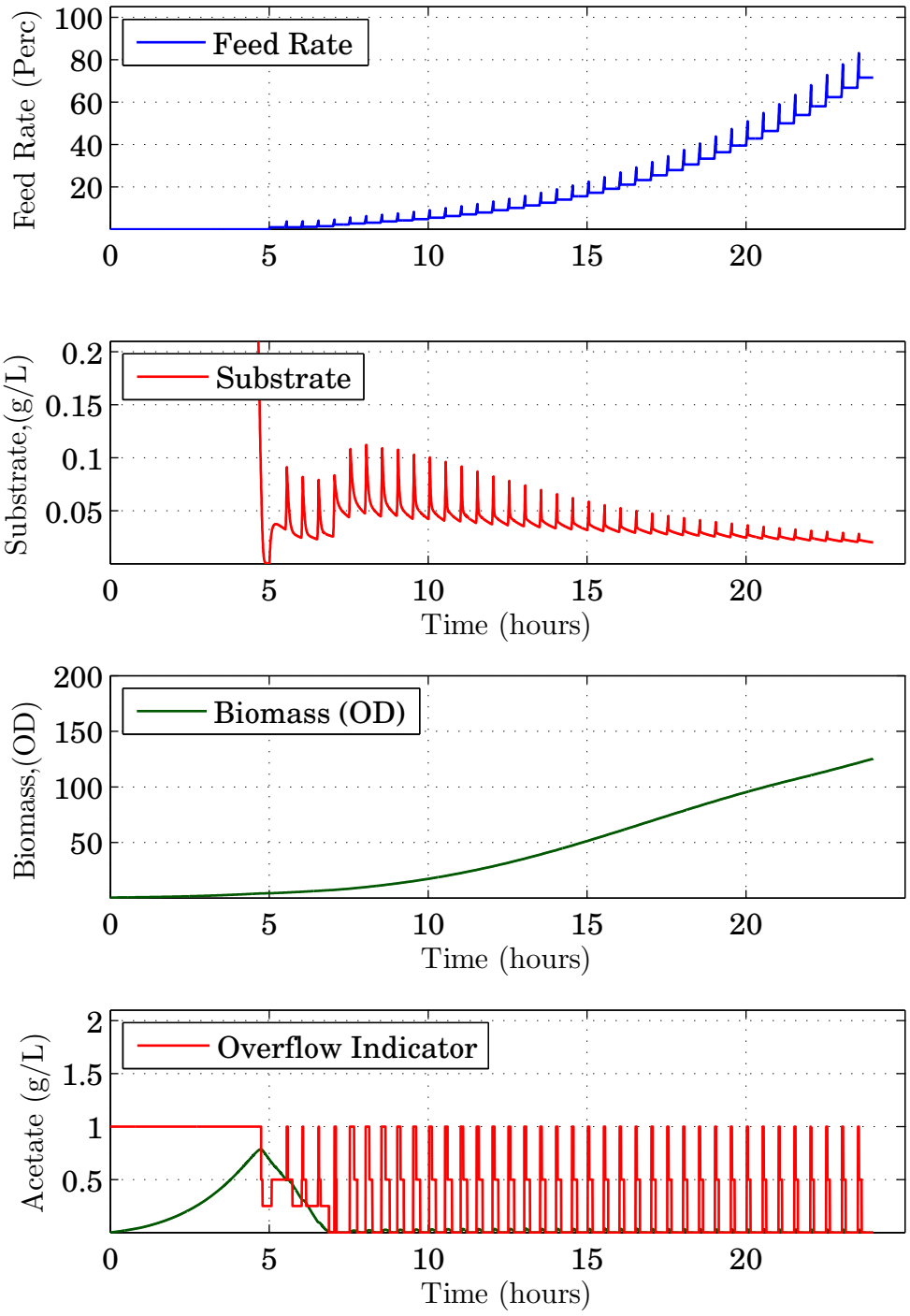


Figure 7.12: The $BOOM_{30}$ controller was simulated using the 'slope', 'step', and 'muGS' parameters used in the fermentations. The A) Feed rate, B) Substrate, C) Biomass, and D) Acetate profiles for this simulation correspond with C4 in Table 5.1.

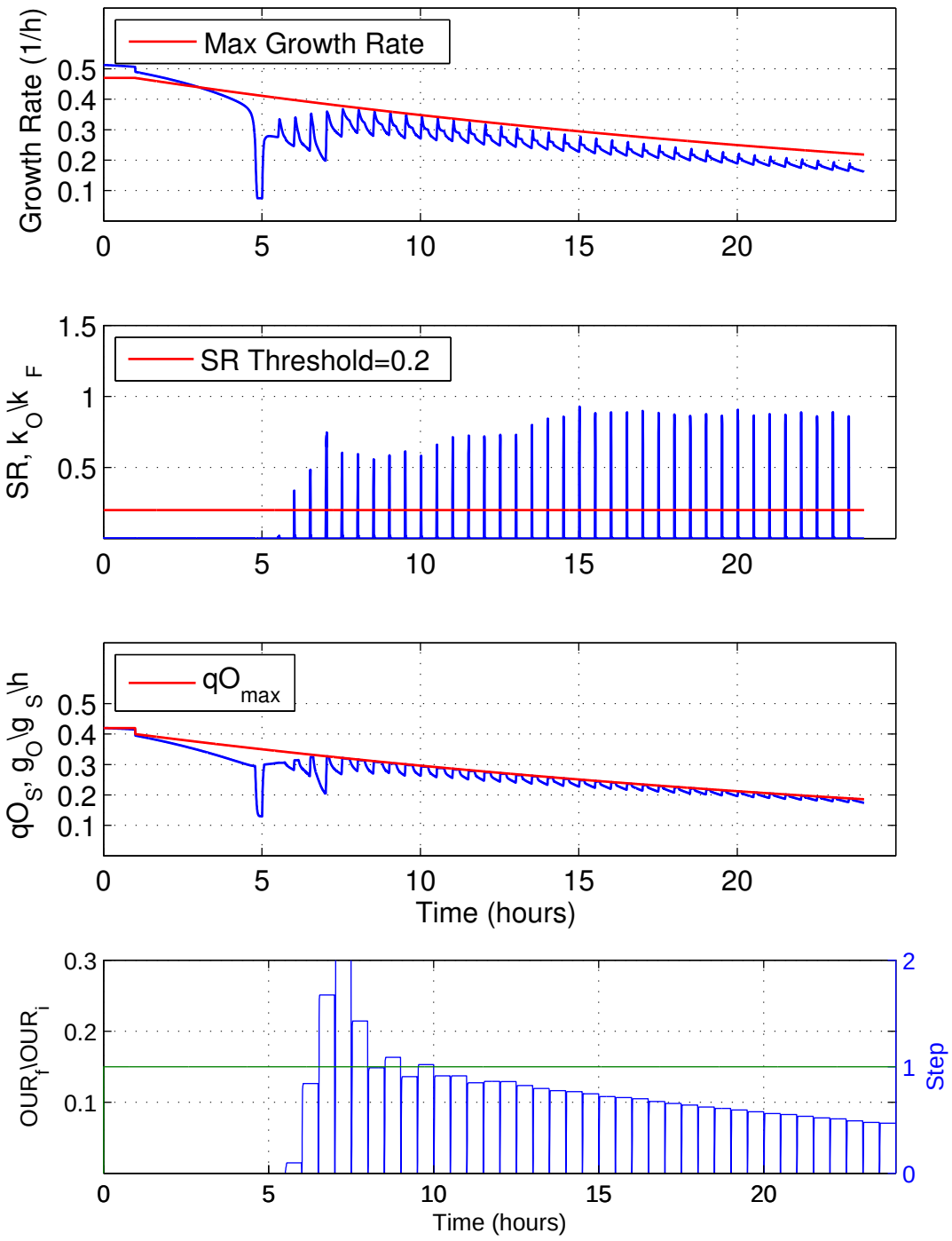


Figure 7.13: The A) maximum growth rate, B) SR, C) $qO_{max}$, and D) $OUR$ ratio profiles are shown for a simulated $BOOM_{30}$ controller. This controller used the 'slope', 'step', and 'muGS' parameters used in the $BOOM_{30}$ fermentations.

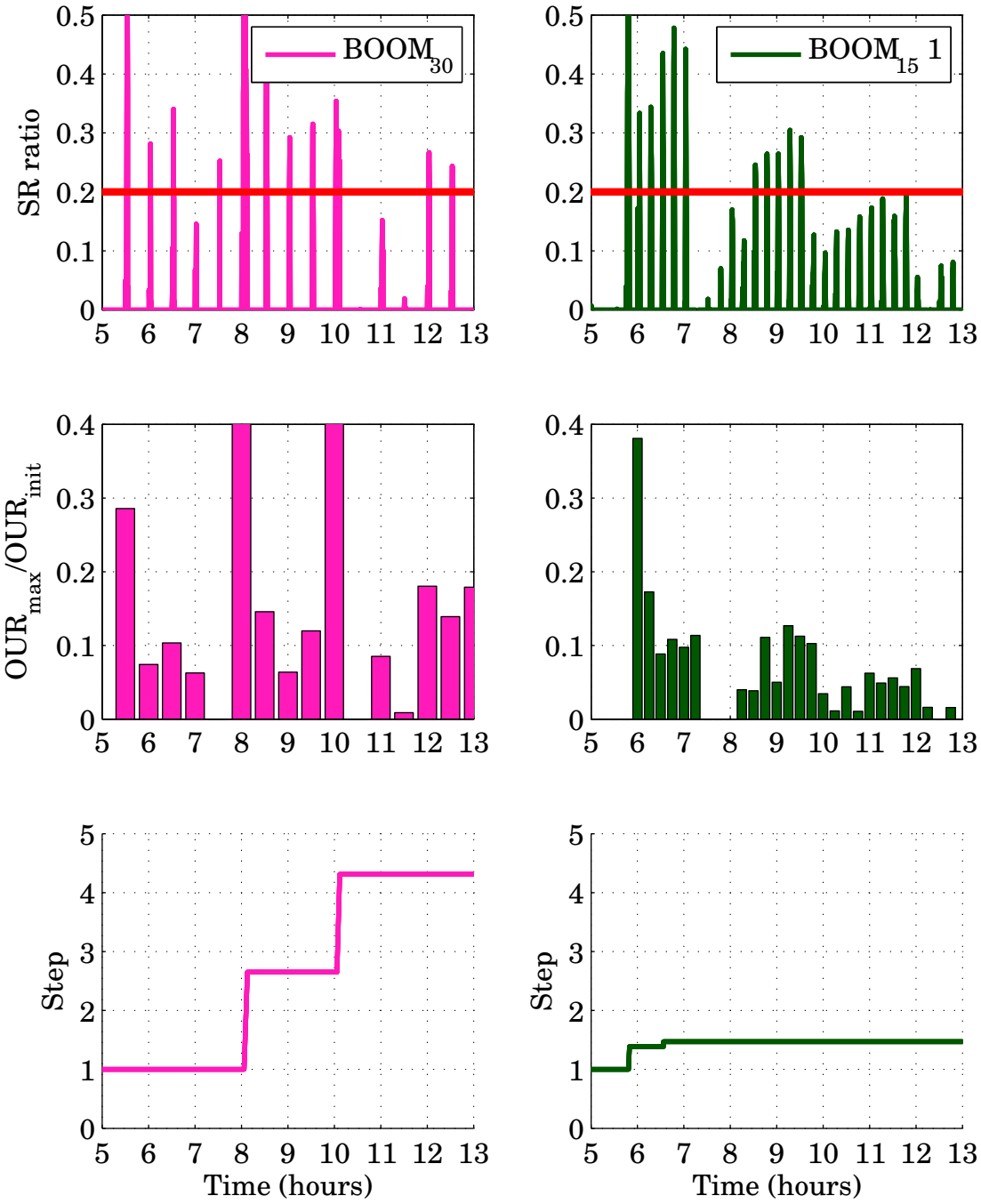


Figure 7.14: The step variable is compared for the $BOOM_{15}$ 1 and $BOOM_{30}$ fermentations.

frequency to be kept, thereby improved responsiveness to changes in cell behavior, while allowing the controller to keep lower the feed rate. Less glucose will drive down $S$ and lengthen the amount of time that $S < S_{crit}$ between ramp events, reducing acetate buildup.

## 7.6 Estimator Performance

The performance of the adaptive $k_La$ estimator and it's ability to provide real-time $OUR$ estimates was crucial for correct performance of the BOOM controller. In Figure 7.15, the fast response of the $OUR$ estimate and filtered response of the $OUR$ based on the off-gas are shown. In the ramp event at 12.5 hours, the change in slope of the $OUR$ estimate signal is clearly seen, indicating overflow metabolism. The BOOM controller would not be able to detect any change in the $OUR$ during the small ramp time frame using only the exhaust-gas sensor.

The $OUR$ estimator exhibited drift in the latter half of all fermentation experiments. In Figure 7.16, the $OUR_{est}$ begins to diverge from the $OUR$ profile based on the off-gas sensor. This behavior needs to studied to ensure that the estimated off-gas measurement is correctly tracking the actual off-gas measurement after 12 hours. Incorrect $OUR$ estimates could lead to overfeeding by BOOM controller.

#### 7.6.0.1 Antifoam addition

The $OUR$ estimate demonstrated its ability to track quick changes in culture $k_La$. After hour 13 in the Exponential feed 1 fermentation, the cells began to lyse and antifoam was added, see Figure 7.16. The purpose of antifoam is to weaken surface tension which inhibits bubble formation, temporarily lowering $kLa$, and shrinking $OTR$. The effect is strong at first, but weakens as the solution is homogenized

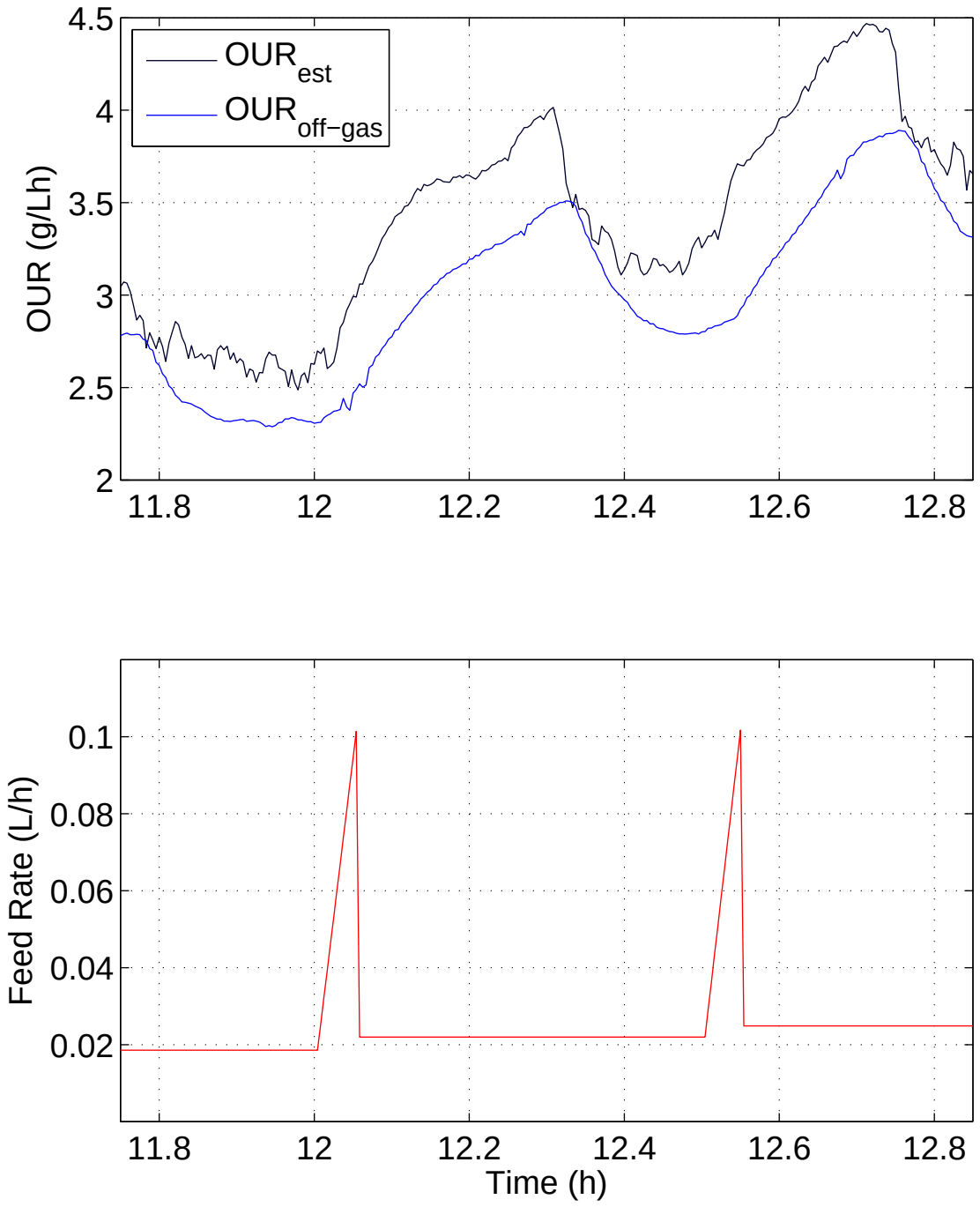


Figure 7.15: The $OUR$ profiles for the off-gas sensor and the $OUR$ estimator during ramp events in the $\text{BOOM}_{30}$ fermentation.

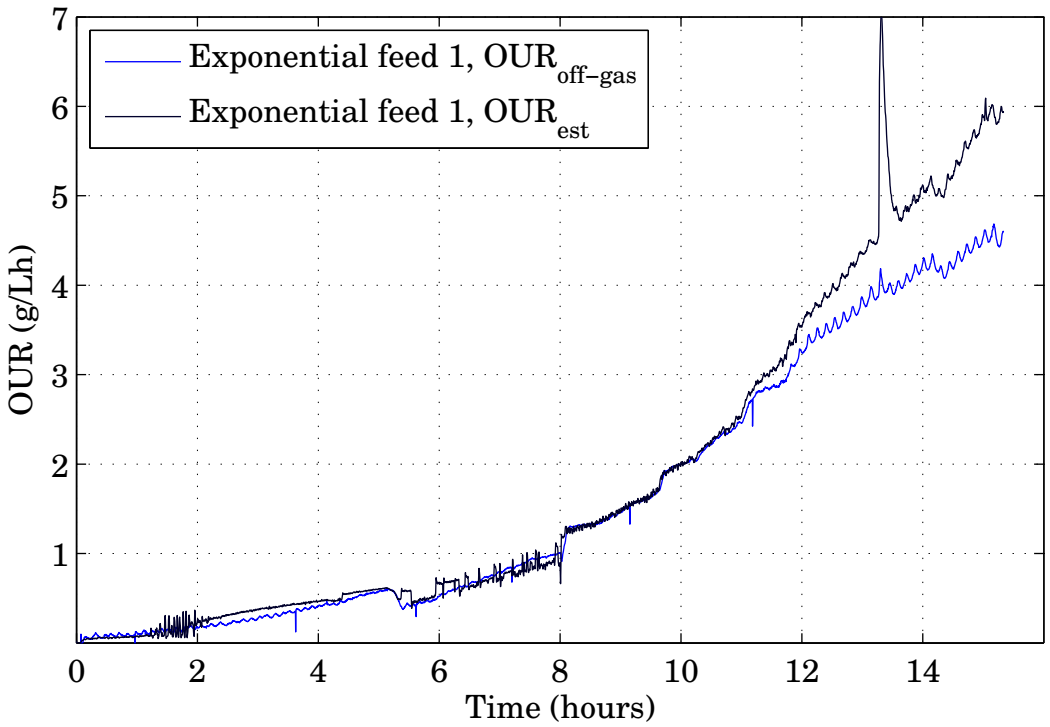


Figure 7.16: The $OUR$ profiles are shown for the off-gas sensor and the $OUR$ estimator for the Exponential feed 1 fermentation.

into the culture, see Figure 7.17 A. By shrinking $OTR$, the DCU dissolved oxygen controller had to increase the stir speed to attempt to maintain the 40% DO setpoint, see Figure 7.17 B. The $\text{OUR}_{est}$ signal uses the off-gas sensor, DO probe ($C$), stir speed ($N$), and mass flow to create an estimate for $k_La$ by estimating parameters $a_0$ and $a_1$. The sudden increase in stir speed caused the $k_La$ estimate and $OUR$ estimate to increase in accordance with their definitions inside the estimator, seen in Equation 7.2 and 7.4.

$$k\hat{L}a = \hat{a_0} + \hat{a_1}(N - N_0) \tag{7.2}$$

$$O\hat{T}R = k\hat{L}a(C^* - C) \tag{7.3}$$

$$OUR_{est} = O\hat{T}R - \dot{C} \tag{7.4}$$

The estimator used the lack of change in the exhaust gas measurement (Figure 7.16, $OUR_{off-gas}$) to conclude that the $k_La$ parameters needed to be adjusted. In Figure 7.18, the estimator quickly dropped the $\alpha_0$ and $\alpha_1$ values and brought the $k_La$ estimate to a slightly lower value than before the antifoam addition. The lower $k_La$ estimate yielded a lower $OTR$ estimate (1% loss in value) which was correct since antifoam lowers $OTR$. The frequency content present in stir speed and DO signals, as controlled by the PID DO control onboard the DCU, appears to be rich enough for fast adaptation of the estimator.

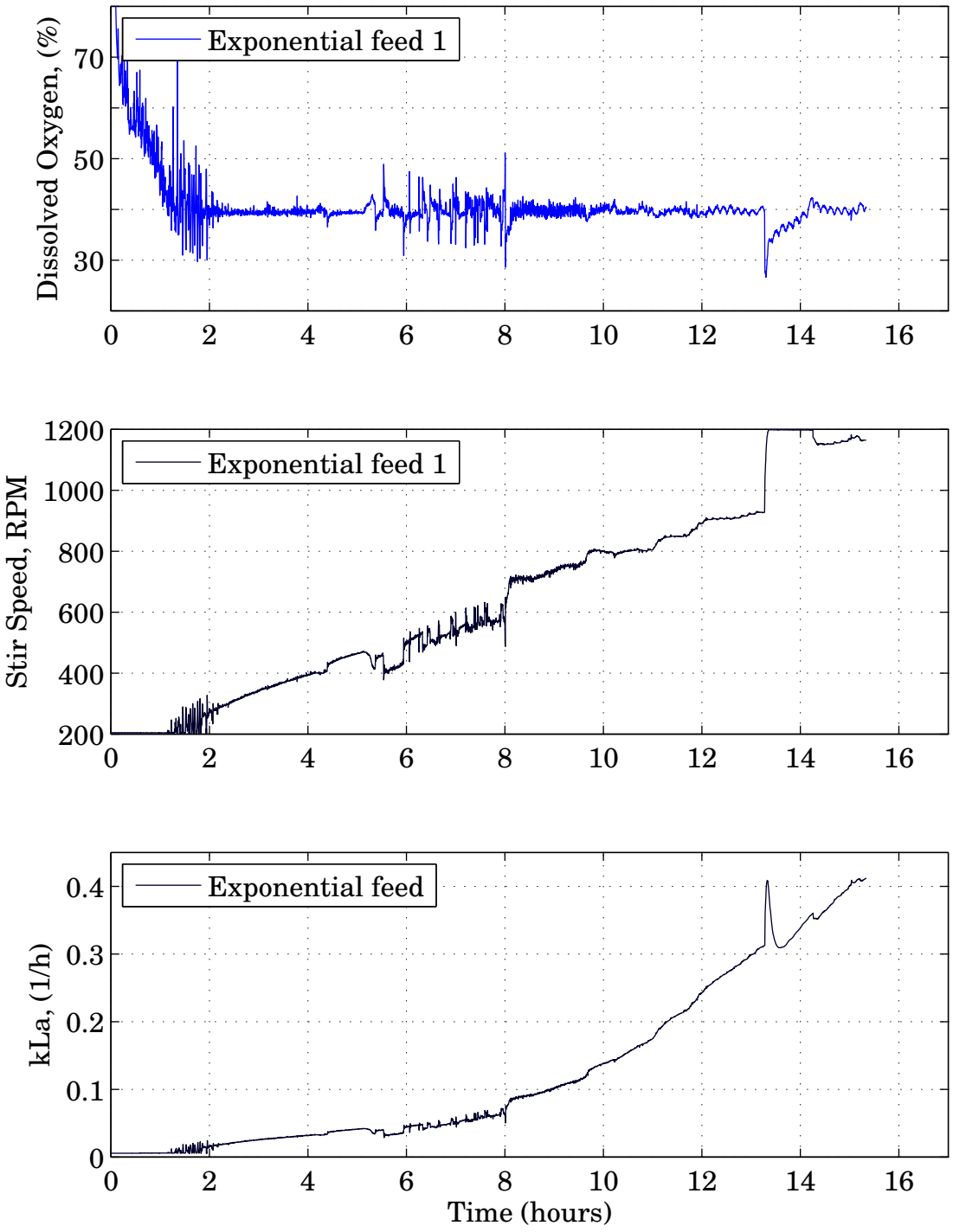


Figure 7.17: The reaction of the DCU dissolved oxygen controller to the antifoam addition at hour 13 is captured in profiles of the A) dissolved oxygen and B) stir speed profiles. The C) estimated $k_L a$ profile is also shown.

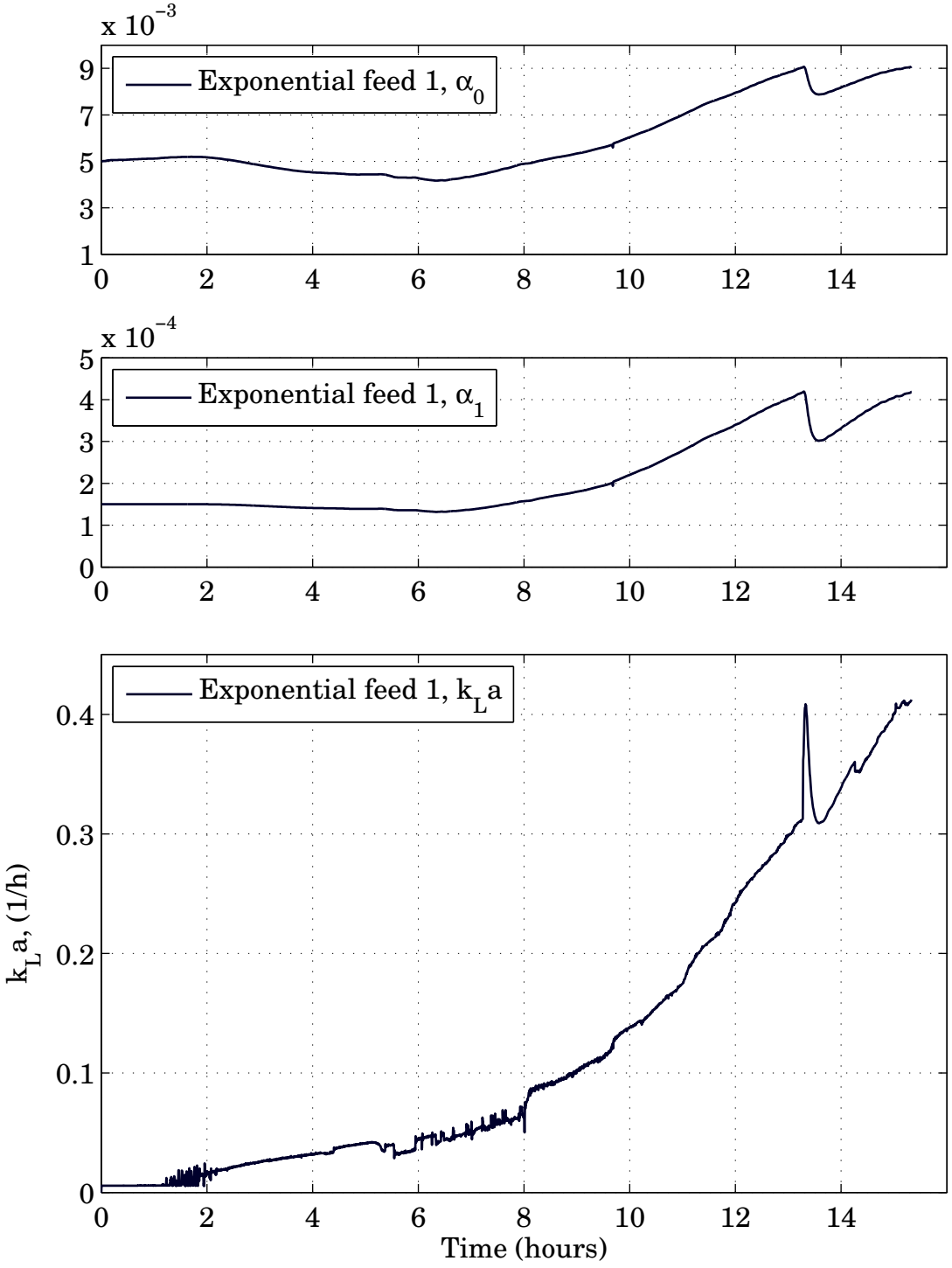


Figure 7.18: The profiles for the estimated $a_0$ and $a_1$ parameters and $k_La$ are shown for Exponential feed 1.

# Chapter 8

# Conclusions and Future Work

## 8.1 Conclusions

A controller was presented that could drive *E.coli* culture to the boundary of oxidative and overflow metabolism (BOOM). By keeping the growth rate in the BOOM region, the fermentations yielded high levels of biomass and recombinant protein while keeping acetate below inhibitory levels. The BOOM controller did not require the *E.coli* to be characterized or need a model of the metabolic changes that could occur during the fermentation. The BOOM controller was based on a basic understanding of the *E.coli* metabolism and the relationships between oxygen and glucose in the three different metabolic phases. The BOOM controller made control decisions using a real-time $OUR$ estimator driven by the DO probe and off-gas sensor. The $OUR$ estimator eliminated any latency in $OUR$ measurement due to headspace mixing or sensor delay.

A small-scale bench-top bioreactor was used to test the effectiveness of this controller. The bioreactor system and sensors were characterized and a simulated system was created to test controller performance. The BOOM control algorithm

relied on a series of periodic ramp events to sense the metabolic state of the culture. A sensitivity ratio, $SR$, was formed based on the $OUR$ estimates and the feed rate. The BOOM controller monitored the $SR$ and $OUR$ estimates during a ramp event and changed the feed rate to drive the culture into the BOOM region. The controller adapted the height and duration of the ramps events based on the response of the culture. The feed rate was kept constant between ramps events to allow the culture to come out of overflow metabolism, process acetate, and stay in the BOOM region. The BOOM controller has four main parameters for adjusting its performance: ramp frequency, slope, deltaStep, and muGS. In general, a higher ramp frequency allows the BOOM controller to adjust more quickly to changes in metabolism; two ramp frequencies were tested: 15 minutes and 30 minutes. The 'slope' and 'muGS' require a minimum of prior knowledge about the organisms substrate uptake and maximum growth rate. Good values for 'slope' were determined to be between [0.1 0.5] and 0.05 for 'muGS'. Setting these parameters conservatively ensures the algorithm will be able to properly adjust the ramp height during a fermentation. The 'deltaStep' parameter determines how quickly the algorithm can adjust the ramp height and drive the culture into the BOOM region, it can be set anywhere between [10 70].

The performance of the BOOM controller was examined in fermentations with both fast (temperature) and slow (induction) metabolism changes. The *E.coli* MG1655 pTVP1GFP strain was induced with 4mM IPTG after 1 hour and run for 13 hours total. The BOOM controller was compared to an Exponential feed and DO-stat controller in terms of total amount of recombinant protein produced. The Exponential feed rate controller was set at a growth rate found in literature to yield high growth and low waste production. The DO-stat controller was adapted from another paper. The $\text{BOOM}_{15}$ controller produced 10% more protein than the Exponential feed controller and 50% more than the DO-stat controller. The $\text{BOOM}_{15}$

controller maintained fast growth and did not let the acetate reach inhibitory levels. A second fermentation was run using the $BOOM_{30}$ controller. The $BOOM_{30}$ and $BOOM_{15}$ controller produced exactly the same amount of protein. The $BOOM_{30}$ controller maintained a lower acetate concentration than the $BOOM_{15}$ fermentations due to its lower ramp frequency. The $BOOM_{15}$ controller also controlled a 13 hour fermentation with uninduced *E.coli* MG1655 pTVP1GFP, in which the temperature was dropped from 37°C to 30°C at hour 8. Growth rate targets were obtained using shake flask experiments at the two temperatures. The $BOOM_{15}$ controller drove the culture growth rate to the $\mu_{max,37°C}$ value of 0.6 $h^{-1}$ by hour 8. After the temperature drop the $BOOM_{15}$ controller correctly modified the feed rate to maintain the culture slightly above the $\mu_{max,30°C}$ value of 0.3 $h^{-1}$ without allowing acetate buildup.

The BOOM controller was able to to adapt to fast and slow metabolism changes in an *E.coli* fermentation and consistently keep culture in the BOOM region, achieving fast growth and preventing acetate from inhibiting growth. The Exponential feed rate controller was set using knowledge gained from many previous experiments. The BOOM controller was able to achieve better results requiring no additional experimentation and only minimal-knowledge about the strain.

## 8.2 Future Work

The BOOM controller kept all *E.coli* in the BOOM region in all *E.coli* fermentations. The only difference between the $BOOM_{15}$ and $BOOM_{30}$ performance was acetate buildup. The induced *E.coli* MG1655 pTVP1GFP was able to change the $OUR$ during ramp events, which was unexpected. More literature needs to reviewed to understand this behavior. The BOOM controller is set up to change the feed rate based on the difference in $OUR$ readings at the beginnging and end of each

ramp event. This setup led to slight overfeeding in the $BOOM_{15}$ fermentations. The $SR$ ratio did correctly identify overflow metabolism. The BOOM controller needs to be modified to decrease the feed rate when the $SR$ ration fails to breach the oxidative threshold during a ramp event. Simulations have shown that this modification decreases acetate buildup even when the control parameters are set aggressively. The BOOM parameters were set too high in the $BOOM_{15}$ fermentations and should be lowered in the future. The ramp event logic could also be modified to stop early if the $SR$ ratio rises then falls below the oxidative threshold within the set ramp period. The feed rate law could be modified to use the $OUR$ value when the $SR$ peaks, rather than the $OUR_{max}$ over the entire ramp event.

The Xu model growth rate, mass balance model, and simulated DCU integrated in FermSim provided an accurate test bed for the BOOM controller. There are many different types of microorganisms that exhibit the same type of metabolic behavior as *E.coli* . Testing the BOOM controller again different microorganism models in literature would provide further insight into its utility and robustness. If the metabolism exhibits the Crabtree effect, the BOOM controller should be able to control it.

The estimator performance needs to be examined closely to ensure the estimated off-gas measurement is tracking the actual measurement. If the estimator is performing correctly, the cause for the divergence of the $OUR$ calculations for the estimator and off-gas sensor needs to be found. Currently, the $OUR$ estimator is not used in fermentations where pure oxygen is added to the house air due to a unknown error in the way $OUR$ is being calculated. Using the $OUR$ estimator for an entire 24 fermentation would allow for a more complete validation of the BOOM controller.

The FermCtrl model is setup to start the BOOM controller at a user specified time for the end of batch phase. The DO signature for batch phase is prominent

enough that it should be able to be automatically detected. The performance of the estimator in adapting to the addition of antifoam indicates that the ZigZag DO algorithm may not be needed and the simpler PID DO controller on the DCU is sufficient to provide rich frequency content. The primary goal of the BOOM controller was to automate the fermentation process and alleviate the need for manual adjustments if the culture metabolism shifted. One area in which the FermCtrl model has no insight is in the buildup of foam. Foam buildup leads to large amounts of the culture leaving through the exhaust port. This event would be catastrophic for the off-gas sensor and measures need to be taken to ensure a foam event would not go through off-gas sensor. The FermCtrl model is running on a computer with battery backup, however, there currently exists no quickly way to initialize the BOOM controller and estimator states to a previous set of values should the model stop running.

Later fermentations exhibited sparger failure. Investigation was performed into the cause and the sterile filter integrity was checked according to the manufacturer protocol. A definitive root cause was not found but a sterile water trap was inserted in the air path between the filter and the sparger which has prevented further failures. The failures have not occured in fermentations without the off-gas sensor and the first dozen fermentations with the off-gas sensor ran nominally.

# Appendices

# Appendix A Bioreactor Primer

This section was written to provide a background knowledge of bioreactors and bioreactor protocol for students those not used to working in a fermentation lab.

## A.1 Stirred-tank Bioreactors

Benchtop systems for culturing cells, such as stirred-tank bioreactors, are vitally important to the biopharmaceautical industry for the research and development of new products. This section will present the equipment used in benchtop culture systems as well as the associated sensors and methods. The history and metabolism of *Escherichia coli* are reviewed briefly.

There are two main types of benchtop culture systems. The first is the shake flask, which consists of a flask filled with media and an innoculum of cells capped by a stopper which allows gas flow. A shake flask is kept inside an incubator on a plate that gently agitates back and forth. Stirred-tank bioreactors consist of a vessel containing a stirrer, oxygen supply, and different probe sensors. Shake flasks are widely used in research because setup is easy, complexity is low, and the results are consistent; however, there is minimal sensing and cell density is limited by oxygen transfer. The ability to achieve much higher density cell cultures gives stirred-tank bioreactors a large advantage in terms of protein production.

This section will assume a generic set of sensors in its description of stirred-tank bioreactors. This sensor set is consistent with the majority of literature and the bioreactor used in this work. A stirred-tank bioreactor consists of three main parts: a glass tank, a metal lid, and a control unit. The glass tank is usually double walled, allowing for water to be circulated around the outside for temperature control. The glass tank has a metal lid with gasket which forms a seal with the rim allowing for

the head pressure inside the bioreactor to be controlled. On top of the lid is a motor which stirs the culture. The motor turns a rod with paddles which extends into the culture. The paddle can have different designs based on the organism that is being cultured. The purpose for the motorized stirrer is to constantly agitate the culture and ensure homogeneity. The sparger is a hollow metal tube which extends from the metal lid into the culture and ends near the bottom of the vessel in a ring containing small holes. The input gas exits the holes in the ring in small bubbles. The paddle works in conjunction with the sparger to break up the bubbles and diffuse the gas throughout the liquid. Together, the sparger and the paddles are used to keep the culture sufficiently oxygenated. Also in the lid are various ports for the insertion of probes, such as dissolved oxygen, temperature, and pH. The digital control unit (DCU) for a bioreactor monitors the various sensors in the culture and varies the inputs into the culture, namely the substrate feed rate, the base addition rate, the stir speed, and the flow of water through the water jacket. The DCU can be remotely commmanded if desired, in which case, additional sensors can be employed to monitor the culture.

## A.2 Sensors

The purpose of sensors in a stirred-tank bioreactor is to monitor the bioprocess and to keep the culture stable and growing. Shake flasks typically are not used with any sensors; however, there are many types of sensors used with stirred-tank bioreactors, see Figure 1. The sensors for monitoring the state of a culture growing in a stirred-tank bioreactor are divided into two types: online and offline sensors.

### A.2.1 On-line Sensors

Online sensors are typically in direct contact with the culture culture and provide almost immediate measurements of different properties of the culture, such as dissolved oxygen concentration, pH, and temperature, see Figure 1. Probes for pH are typically made of glass and contain two electrodes, The anode is kept at a certain reference voltage and the cathode flucuates with the $H^+$ concentration in the solution. The potential difference between the two indicates the pH of the system. A dissolved oxygen probe works in a similar fashion. An electrolyte solution covers the anode and cathode inside the probe while also in contact with the outside solution through a gas permeable membrane. The quantity of oxygen permeating the membrane determines the magnitude of potential difference between the cathode and the anode. This probe must be calibrated beforehand. One particularly useful sensor is the off-gas sensor; this sensor measures the oxygen and/or carbon dioxide composition of the gas leaving the top of the bioreactor. Off-gas sensors have only just recently transitioned from being expensive units ($100,000) capable of monitoring multiple experiments to cheaper single culture units ($6000) [Aehle et al., 2011a]. Another popular sensor is a balance. A balance weighs the bottles containing the culture inputs such as the substrate or base solution and provides increased accuracy when calculating the amount of mass delivered to the system. Some very specialized online sensors can measure cellular by-products such as acetate or ethanol directly, but implementation of those is rare. Online biomass sensors are also available, but are prone to fouling and rarely used.

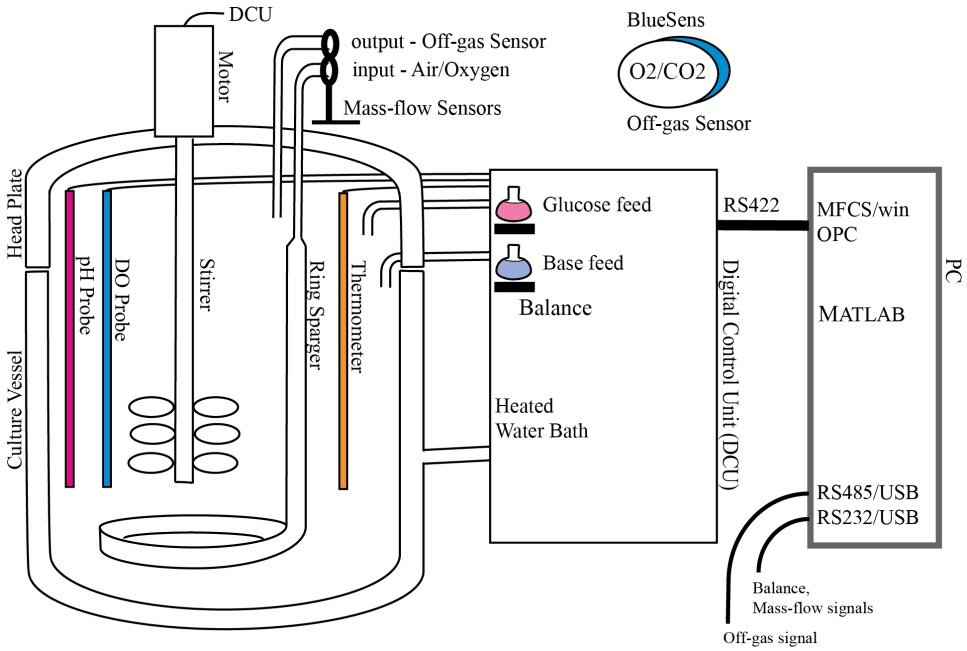


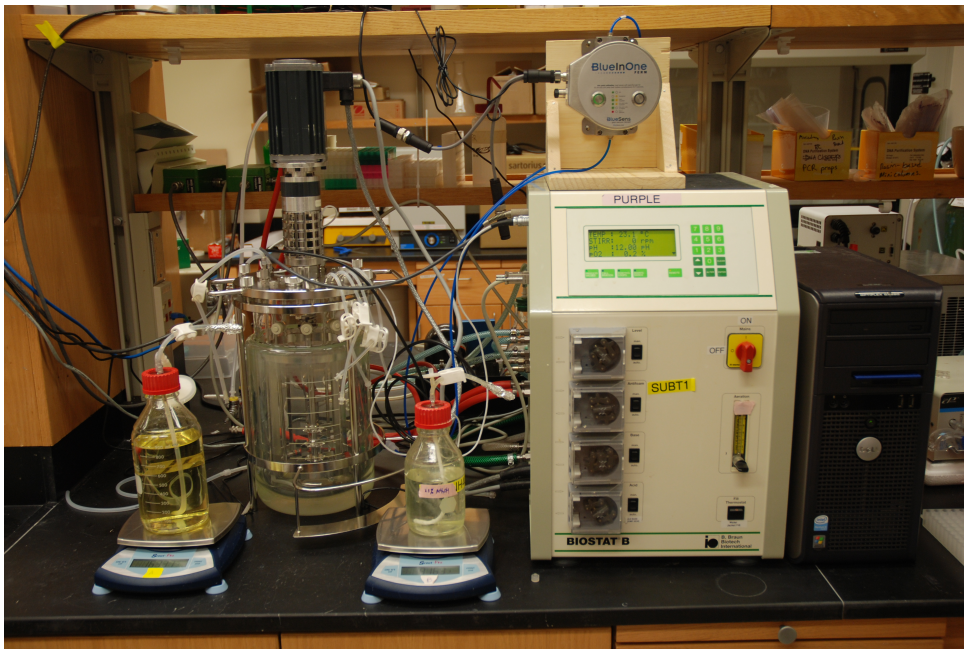


Figure 1: The bioreactor systen and standard sensor set are shown above. The system includes additional online sensors, an Off-gas sensor and the balances for the glucose input and base input bottles. The bioreactor vessel, DCU, and additional sensors used for fermentations is shown below.

### A.2.2 Off-line Sensors

Offline sensors measure properties of a culture sample removed from a running bioreactor experiment; unlike online measurements, offline measurements may take a few minutes or a couple hours to calculate [Tatiraju et al., 1998]. The most popular property to measure off-line is biomass concentration. This is done by measuring the optical density (OD) of a culture sample with a spectrophotometer. The spectrophotometer measures the absorbance of the sample using a specific wavelength of light (e.g. 600nm). As the density of the culture grows, the sample must be diluted for accuracy. The procedure only takes a few minutes. The OD of a sample is proportional to the biomass concentration in the culture. To establish the porportionality constant, a more lengthy off-line measurement process is used to determine the dry culture weight (DCW). To determine the DCW, the culture sample is spun down in a centrifuge, the supernatent is poured out, and the wet cell pellet is weighed. This pellet is dried in an oven or desiccator and then weighed again. The weight of the dried sample is compared to weight of the wet sample and the ratio calculated, usually 0.5g DCW to 1 OD. The concentration of acetate can be read using a chemical assay and an absorbance microplate reader. Enyzmes are added to a small volume of the culture and that sample is then exposed to a particular wavelength of light by the microplate reader. The strength of absorbance corresponds to the amount of acetate in the sample. The measurement is compared to a set of controls to obtain the actual concentration. The levels of the glucose, ammonia, lactate, and various other cell by-products can be measured by instruments such as liquid/gas chromatographs or biochemistry analyzers or chemical assays.

Table 1: The available DCU control algorithms and corresponding culture variables.

| Signal Name | Sensor | Control Input | Controller | Closed Loop |
|---|---|---|---|---|
| Dissolved Oxygen (DO) | DO Probe | Stir Speed | PID | x |
| Hydronium Level (pH) | pH Probe | Base Addition | PID | x |
| Temperature (T) | Thermometer | Water Bath | PID | x |
| Glucose Level (S) | N/A | Feed Pump | Setpoint | |

### A.2.3 Sensor Usage & Basic Bioreactor Control

A typical bioreactor setup will have on-line sensors for pH, DO, temperature, and off-gas as well as off-line sensors for optical density and metabolite concentration. The use of a balance is somewhat less common. On-line biomass or metabolite sensors are very rare, not regarded as reliable, and thus rarely used in research or industry [Johnston et al., 2002].

The online bioreactor sensors are usually connected to independent proportional-integral-derivative (PID) controllers on the DCU, see Table 1. For example, the pH probe indicates when the addition of a base solution is needed; the temperature probe indicates when to circulate water from a water bath; the dissolved oxygen probe indicates when increase or decrease the stir speed and when to change the composition of the input gas. The substrate feed controller on the DCU is capable of changing speeds based on a user-defined time-varying profile or of accepting commands from an external source.

## A.3 The Fed-batch protocol

The focus of this secton will be on the protocol for stirred-tank bioreactors taken from a few papers in literature [Xu et al., 1999, Akesson et al., 2001, Voisard et al., 2002, Pinsach et al., 2006]. The challenge of designing a fed-batch protocol will

also be reviewed.

A frozen sample of bacteria is taken from a -80°C freezer and grown to a certain density in a shake flask in an incubator. After the cells have reached a desired density, usually an OD of 0.4 to 1.0 [Voisard et al., 2002, Babaeipour et al., 2008], they are harvested, spun down with a centrifuge, and resuspended in a much smaller volume. The innoculum is then introduced into a bioreactor which has already been filled with fresh media, heated to the proper temperature, and at the correct pH. There are several different types of fermentation protocols: batch, fed-batch, and continuous. In a batch culture, no additional glucose is added beyond what is initially present in the growth media when it is innoculated with cells. After the cells grow and deplete the surrounding glucose, the experiment is done. In a continuous culture, there is a constant feed of fresh medium into the bioreactor and a certain volume of medium and cells is removed in return to allow for more biomass growth.

Experiments focused on growing high density cell cultures use the fed-batch culture protocol. A fed-batch culture has two phases: batch and fed-batch. The culture initially operates in batch mode, in which the cells grow rapidly and consume the surrounding glucose. The amount of glucose needed in the batch phase is dependent on the researcher to know the substrate-to-biomass coefficient of the cell, $Y_{X/S}$. The $Y_{X/S}$ represents how many grams of biomass are produced per gram of substrate. This value is different for each strain. Adding the correct amount of glucose will ensure the culture will reach some specific biomass density (OD). The cells need to reach a certain minimium density in order for the bioreactor to be able to control the growth. The feed rate for the fed-batch phase is usually set to follow some predetermined time-varying profile using an equation like (1) found in [Durany et al., 2005]:

$$F = \frac{\mu_{set} X_0 V_0}{S_f Y_{X/S}} \, exp(\mu_{set}) \tag{1}$$

where $\mu_{set}$ represents the desired growth rate, $X_0$ the initial biomass, $V_0$ the initial culture volume, $S_f$ the input glucose concentration. Once again, the researcher must know these different parameters for this strain in order to control it correctly. This calculation assumes substrate-to-biomass yield coefficient stays constant for the entire experiment.

The primary metabolism for the *E.coli* uses oxygen to process glucose and create biomass. The sparger and paddle ensure the supply of oxygen into the culture is greater than the culture requirements. With ample oxygen supply, the rate of the *E.coli* metabolism is controlled by the external feed rate. The feed rate is the primary control for the growth rate of the cells, and keeps them growing only as quickly as substrate is avaliable; this is known as being substrate-limited. Cultures are controlled in a substrate-limited fashion to prevent overflow metabolism and excess metabolite production which can inhibit growth and/or protein production.

The DCU is uses its online sensors to control the environment variables of the bioreactor. The pH is kept at a setpoint, usually 6.9 - 7.0, via the addition of a base. The dissolved oxygen (DO) is kept constant by the stir speed and the composition and flow of the input gas. The sparger is supplied with atmosphere, pure oxygen, or a mixture of both. A typical flow rate is between 1 to 2 volume of air by volume of liquid per minute (v.v.m) [Jobe et al., 2003, Durany et al., 2005]. In this work, the mass flow rates were 3 liters per minute for 1.5L of media or 2 v.v.m . A fed-batch experiment must end when the volume of the biomass, the added base, and the added substrate have filled the tank; fed-batch experiments typically last no longer than 24 hours. The operator can also terminate the fed-batch culture if the oxygen uptake rate (OUR) of the culture becomes too large. Careful attention must be paid to the DO levels later in the culture as it is possible for the OUR of the cells to become larger than the oxygen transfer rate (OTR) of the system, causing the DO to drop

rapidly below acceptable levels, usually below 25%. Optional DO controllers can step in and decrease the feed rate accordingly to stabilize the DO [Oliveira et al., 2005].

## A.4 Protocol Development

Bioprocesses are very complex with thousands of reactions happening continuously in the cells [Pomerleau and Perrier, 1990]. As the biopharmaceutical industry continues to modify the genome of *E.coli* to increase its productivity or make new products, current bioreactor protocols are modified to attain desired cell behavior. Many variables can be changed in a fermentation protocol and these changes are usually done incrementally in order to keep the culture stable. One of the most basic variables is definition of the cell growth medium. There are two main types of growth medium, complex and defined [Akesson et al., 2001]. Complex media usually contains extract from an animal, such as bovine growth serum, thus it's chemical composition is not exactly known. Defined media is composed of off-the-shelf growth factors, antibiotics, fungicides, etc; it's composition is exactly known and provides the nutritional requirements for organism growth. Typically, defined media yields the most consistent cell behavior.

The next variable to set is the feed rate. As previously mentioned, researchers rely on previous experience and characterization of the strain to calculate how much to feed a culture at any given time. However, these calculations are approximate at best if the strain is not exactly that used in previous experiments. Different strains of *E.coli* may behave differently with the same protocol. The differences stem from slight differences in metabolism which affect the uptake rates of glucose and oxygen. A conservative growth profile for one strain may send another into overflow metabolism.

The last major variable that can effect growth behavior is induction strength.

Induction is the process by which a chemical is added to the culture and the *E.coli* begins to transcibe a protein encoded by an inserted piece of foreign DNA. The fragment of DNA is known as the plasmid. A plasmid contains a promotor, which is the 'light switch' for protein production. During a culture experiment, a chemical known as an inducer is added, which activates the promotor, causing protein production to begin [Harrison et al., 2003]. An example of a common inducing agent is Isopropylthio-$\beta$-galactoside (IPTG). Induction strength refers to the molarity of the inducing agent in the culture. Some strains require much less inducing agent, 100$\mu$M, to grow stably and produce protein, while others require more, 1mM. By genetically altering these organisms, changes have been introduced into their biochemical network [Diaz et al., 1999] that can make their behavior unpredicatable. In [Durany et al., 2005], they say that "depending on the fixed production system (recombinant protein to be expressed, host strain and vector for recombinant production and operational mode), the metabolic burden associated to recombinant expression can affect in a different manner culture growth, sometimes by drastically collapsing normal cell metabolism and leading to quick culture growth interruption".

As previously mentioned, protocols are developed in order to tightly constrain cells to a desired behavior. Finding the exact combination of culture variables that yields the desired outcome is time consuming given the amount of variation that can occur from only small changes [Durany et al., 2005]. In [Durany et al., 2005], they present data from multiple experiments in which they analyze different inductions times of a fed-batch experiment. Durany points out that this is work is connected to a string of preceding papers in the which experiments were performed to find the best media composition and the best induction strength [Durany et al., 2004]. Researchers have to vary strains, culture media, and other conditions to find protocols that will achieve desired behavior and stable growth. One of the main goals of a metabolic-

state sensing controller is to deliver stable growth regardless of the unknown dynamics imposed by a variable such as induction strength. The researcher can instead focus on the other culture variables, hopefully minimizing the number of experiments necessary to find an appropriate growth protocol.

# Appendix B Fermentation Preparation

## B.1 Solution Preparation

Some of the elements in the defined mimial media for the *E.coli* cannot be autoclaved and thus it is prepared separately and is added the morning of the experiment. The first set of elements are known as the batch additives and consist of all elements needed in 1.5 L of mimimal media outside of water and the pH buffer, these are glucose, magnesium sulfate, trace metals, and iron III citrate. In addition to these, antifoam is also added as protein production can cause foaming in the reactor. The day of the experiment, the batch additives are added to the vessel before the calibration of the DO probe. The next set of elements is the fed-batch additives and these are added to 250 mL of 50% glucose solution used to feed the culture; this consists of different concentrations of magnesium sulfate, trace metals, and iron III citrate. This solution is known as the feed solution and is prepared in a sterile 1000mL bottle with a feeding tube cap. The last solution that is needed to culture the *E.coli* is the 7% w/v (3.4M) Ammonia Hydroxide solution used as base addition for pH control. This solution is placed in a 500mL bottle with feeding tube cap.

Both of these solutions are connected to the peristaltic pumps on the DCU using #14 MasterFlex (R) Tygon tubing (Holland Applied Technologies, Chicago, IL). This tubing has an average flow rate of 5.6 mL/min. Two sets of tubing are

used for each solution. Each tubing is 150cm long and intended for three to four uses. Each tubing is threaded into its respective pump, substrate and base, and then dH2O is pumped through it for two minutes. The amount of water pumped is measured using the balances and the mL/min value is input into the corresponding 'Calibration' section on the DCU menu. The tubing for the vernier substrate pump is #12 Masterflex tubing with an average flow rate of 0.133 mL/min. This tubing is used in 100 cm lengths and a new section is prepared every experiment. The #12 tubing interfaces with normal luer lock hardware by being inserted into a section of autoclaved #14 tubing.

## B.2 System Preparation

This section will discuss the various systems including the Biostat B DCU, vessel, probes, and sensors that need to be checked and readied for an *E.coli* experiment. All experiments were performed using the BioStat B fermentation system, balances, mass flow sensors, BlueSens off-gas sensor, and a computer running Matlab/Simulink 2012a. A more detailed checklist for the preparation of th reactor can be found in the appendices.

### B.2.1 Reactor

The glass vessel for Biostat B must be disinfected with bleach, scrubbed with soap, and then rinsed thoroughly before each experiment. This typically happens immediately following the previous experiment. If the stainless steel cage, stir shaft, and paddles appear free of cell debris and the vessel had no appreciable odor, it is assumed ready for preparation. The day before the experiment, Water and pH buffer are added to the reactor in addition to the DO and pH probes. The headplate is

tightened down and all ports are plugged. A set of four input lines is located on the headplate for substrate, base, or antifoam. These lines are capped and wrapped with blue cheesecloth and foil for the autoclave. One port is left open for emergency pressure relief. The line to the sample port is also wrapped. The sparger input port is clamped and the sterial filter line attached and wrapped. Lastly another sterile filter is attached to the exhaust port line. All lines and hoses are coiled on top of the headplate. The entire vessel is autoclaved using a liquid cycle which pressurizes the autoclave chamber with 20 psi of steam and keeps the vessel at a temp of 121°C for 45 minutes. The vessel is allowed to cool for 1.5 hours or to a temp of 65°C before water lines for the water jacket and exhaust cooling tower are connected. A water bath supplies 12°C water to the DCU for vessel temperature control. A previous experiment showed the thermometers to be off by $\approx$ 1°C, thus to achieve 37°C, the temperature controller on Purple is set to 35.9°C and on Orange to 36°C. The temperature controller is activited the evening before to allow it to stabilize before the experiment.

### B.2.2 Sensor Calibration

There are a number of probes and sensors that are part of the bioreactor system and must be recalibrated or at least checked every experiment. The pH probe is connected to the DCU and two calibrating solutions at pH 4.0 and 7.0 are used in conjunction with the temperature probe. Inserted the day before with the pH probe, the DO probe is filled with 1.5mL of electrolyte solution and inserted into the headplate. The DO probe must be connected to the DCU 2-4 hours before calibration to allow the probe to polarize. The day of the experiment, with the bioreactor heated to the correct temperature, $N_2$ and dry house air are used to establish 0% and 100% reference values for the DCU. The two-point calibration yields a slope

which is recorded and compared to the nominal values (60-80 nA) to track probe health. No calibration is performed on the Ohaus balances. The mass flow sensors and controller need to be calibrated once every year or two and came with 3-point calibration documents equating flow rate to voltage output. These calibrations were input into 'Lookup Table' blocks in Matlab. Additionally, the two mass flow sensors were hooked up in serial and their 'Lookup Table' blocks slightly modified to ensure agreement between the two sensors. Relative accuracy is slightly more important that overall accuracy. Finally, the exhaust-gas sensor is only calibrated as needed. When the sensor is up to temperature and the bioreactor is fully pressurized and the flow is ≈3.1 Lpm, it should read 0.2096 for $O_2$ and 0.0034 for $CO_2$. If the reading are off by more than 1 thousandth, the BlueSens is recalibrated using the front two buttons in a few minutes.

## B.3 Software

For each experiment, a Matlab model controls the feed-rate and sometimes the stir speed of the DCU. Before the experiment, the feed-rate and DO control algorithms are developed using the FermSim model. Once the proper behavior is achieved in simulation, them COMMAND portion of the FermSim model is replaced, turning it into a FermCtrl model. The day before the experiment, the FermCtrl model is run to test communication and stability of the model. All functionality is checked before the experiment, especially off-gas sensor connectivity and mass flow meter readings, which are checked to ensure they are around 3.1 LPM. During an experiment, the Matlab model should run autonomously, starting after batch phase (5 hours) and controlling the feed rates; no gains or other adjustments are made.

# Appendix C PseudoCode

This section contains the pseudocode for the BOOM control algorithm.

```
INPUTS:
time
batch end time
current feed rate command
current SR reading
step

OUTPUTS:
Fs - the feed rate assignment
Fdot - the rate of change for 'Fs'
stepDot - change in 'step'

Tuning Parameters:
frequency - desired ramp frequency, in hours
slope - initial slope defined as, desired pump change per minute
deltaStep - desired 'step' change per minute
OverflowCkTimer - number of seconds allowed for culture to react
sensitivity - SR threshold for overflow determination
Fstart - initial pump value, used for starting the algorithm
muGS - a minimum growth rate that continually scales the 'slope'
```

```
1  **********Algorithm Start **********
2  If the time is greater than t_batch
3      start an initial small feed rate with magnitude, Fstart
```

```
4
5   If the time is greater than t_batch
6     slope equals a slowly growing exponential with rate, muGS
7     deltaStep equals a slowly growing exponential with rate, muGS
8
9   If the time is greater than t_batch
10
11      % Start Ramp
12      If the time can be divided evenly by the desired ramping freq and a
            ramp is not in progress
13          set the 'rampStartTime' to the current time
14          set the overflow indicator to off
15          capture the current 'F_cmd' and save it to 'F_init'
16          set ramp length to 0
17          set the initial OUR to the current OUR
18          set the final OUR to the current OUR
19
20      % Ramp Logic
21      if the overflow indicator is off and the ramp length is 0
22          FDot_cmd equals the slope times the step
23          change the feed rate by the value FDot_cmd
24          turn on the ramp indicator variable
25          capture the max OUR
26          set OURf to the max OUR
27
28      % Good Ramp Test
29      if the ramp indicator is on and the SR is greater than sensitivity
30          set 'goodRamp' to on
31
32      % Overflow Test
```

```
33      if 'goodRamp' is off and the rampIND is on and ramp has been active
            for 'OverflowCkTimer' seconds
34          set the overflow indicator to on
35          turn off the ramp indicator
36          set the ramp length to the 'OverflowCkTimer' value
37          set the new feed rate to equal the ratio of OURf/OURi times
                the initial feed rate
38
39      % Increase Ramp Slope
40      if the ramp indicator is on and the ramp has been active for longer
            than 'OverflowCkTimer'
41          increase the value of the rate of change of step from zero to
                the deltaStep term
42          the step value will begin to grow, which should change the
                FDot_cmd value
43
44
45      % Stop Ramp event, culture not in overflow
46      if the SR is less than sensitivity and the goodRamp indicator is on
            and the ramp indicator is on and at least OverflowCkTimer number
             of seconds has passed
47          turn the ramp indicator to zero;
48          set the ramp length to the difference bewteen currentTime and
                the rampStartTime
49          set the new feed rate to equal the ratio of OURf/OURi times the
                initial feed rate
50          turn the good ramp indicator off
```

# Appendix D Acronyms

ANN - artificial neural networks

BAR - base addition rate

BOOM - boundary of oxidative and overflow metabolism

CER - carbon dioxide execretion rate

DCW - dry culture weight

DO - dissolved oxygen

DSD - DCU Serial Device

GUI - graphical user interface

GUR - glucose uptake rate

OBE - observer based estimator

OD - optical density

OTR - oxygen transfer rate

OUR - oxygen uptake rate

PID - proportional-integral-derivative

stb - stirred tank bioreactor

v.v.m - volume per volume per minute

# Bibliography

[Aehle et al., 2012] Aehle, M., Bork, K., Schaepe, S., Kuprijanov, A., Horstkorte, R., Simutis, R., and Lubbert, A. (2012). Increasing batch-to-batch reproducibility of cho-cell cultures using a model predictive control approach. *Cytotechnology*, 64(6):623–634.

[Aehle et al., 2011a] Aehle, M., Kuprijanov, A., Schaepe, S., Simutis, R., and Lubbert, A. (2011a). Simplified off-gas analyses in animal cell cultures for process monitoring and control purposes. *Biotechnology Letters*, 33(11):2103–2110.

[Aehle et al., 2011b] Aehle, M., Schaepe, S., Kuprijanov, A., Simutis, R., and Lubbert, A. (2011b). Simple and efficient control of cho cell cultures. *Journal of Biotechnology*, 153(1-2):56–61.

[Akesson and Hagander, 2000] Akesson, M. and Hagander, P. (2000). A simplified probing controller for glucose feeding in escherichia coli cultivations. In *Decision and Control, 2000. Proceedings of the 39th IEEE Conference on*, volume 5, pages 4520–4525.

[Akesson et al., 1997] Akesson, M., Hagander, P., and Axelsson, J. P. (1997). A pulse technique for control of fed-batch fermentations. In *Control Applications, 1997., Proceedings of the 1997 IEEE International Conference on*, pages 139–144.

[Akesson et al., 1999a] Akesson, M., Hagander, P., and Axelsson, J. P. (1999a). A probing feeding strategy for escherichia coli cultures. *Biotechnology Techniques*, 13(8):523–528.

[Akesson et al., 2001] Akesson, M., Hagander, P., and Axelsson, J. P. (2001). Avoiding acetate accumulation in escherichia coli cultures using feedback control of glucose feeding. *Biotechnology and bioengineering*, 73(3):223–230.

[Akesson et al., 1999b] Akesson, M., Karlsson, E. N., Hagander, P., Axelsson, J. P., and Tocaj, A. (1999b). On-line detection of acetate formation in escherichia coli cultures using dissolved oxygen responses to feed transients. *Biotechnology and bioengineering*, 64(5):590–598.

[Babaeipour et al., 2008] Babaeipour, V., Shojaosadati, S. A., Khalilzadeh, R., Maghsoudi, N., and Tabandeh, F. (2008). A proposed feeding strategy for the overproduction of recombinant proteins in escherichia coli. *Biotechnology and applied biochemistry*, 049(2):141–147.

[Babaeipour et al., 2007] Babaeipour, V., Shojaosadati, S. A., Robatjazi, S. M., Khalilzadeh, R., and Maghsoudi, N. (2007). Over-production of human interferon by hcdc of recombinant escherichia coli. *Process Biochemistry*, 42(1):112–117.

[Bastin and Dochain, 1990] Bastin, G. and Dochain, D. (1990). *On-line Estimation and Adaptive Control of Bioreactors*. Elsevier Science, Amsterdam, Netherlands.

[Charbonnier and Cheruy, 1994] Charbonnier, S. and Cheruy, A. (1994). Estimation of state variables and kinetic parameters in an enzyme production process by using minimal modelling. In *Control Applications, 1994., Proceedings of the Third IEEE Conference on*, volume 3, pages 1923–1928.

[Chen et al., 1997] Chen, W., Graham, C., and Ciccarelli, R. (1997). Automated fed-batch fermentation with fed-back controls based on dissolved oxygen (do) and ph for production of dna vaccines. *J. Ind. Microbiol. Biotechnol.*, 18:43–48.

[Cornet et al., 1993] Cornet, I., Dochain, D., Ramsay, B., and Perrier, M. (1993). Adaptive linearizing inferential control of a phb producing process. In *Control Applications, 1993., Second IEEE Conference on*, volume 1, pages 481–485.

[Dabros et al., 2010] Dabros, M., Schuler, M. M., and Marison, I. W. (2010). Simple control of specific growth rate in biotechnological fed-batch processes based on enhanced online measurements of biomass. *Bioprocess and Biosystems Engineering*, 33(9):1109–1118.

[Diaz et al., 1999] Diaz, C., Lelong, P., Dieu, P., Feuillerat, C., and Salome, M. (1999). On-line analysis and modeling of microbial growth using a hybrid system approach. *Process Biochemistry*, 34(1):39–47.

[Dorresteijn et al., 1994] Dorresteijn, R., Gooijer, C. D., Tramper, J., and Beuvery, E. (1994). A simple dynamic method for on-line and off-line determination of kla during cultivation of animal cells. *Biotechnology techniques*, 8(9):675–680.

[Dowd et al., 1999] Dowd, J. E., Kwok, K. E., and Piret, J. M. (1999). Predictive modeling and loose-loop control of perfusion bioreactors. In *Electrical and Computer Engineering, 1999 IEEE Canadian Conference on*, volume 3, pages 1596–1597.

[Durany et al., 2004] Durany, O., Caminal, G., de Mas, C., and Lopez-Santin, J. (2004). Studies on the expression recombinant fuculose-1-phosphate aldolase in e.coli. *Process Biochemistry*, 39:1677–1684.

[Durany et al., 2005] Durany, O., de Mas, C., and Lopez-Santin, J. (2005). Fed-batch production of recombinant fuculose-1-phosphate aldolase in e. coli. *Process Biochemistry*, 40(2):707–716.

[Food and Association, 2004] Food, U. S. and Association, D. (2004). Guidance for industry process analytical technology (pat) - a framework for innovative pharmaceutical development, manufacturing, and quality assurance.

[Garcia-Fruitos et al., 2007] Garcia-Fruitos, E., Martinez-Alonso, M., Gonzalez-Montalban, N., Valli, M., Mattanovich, D., and Villaverde, A. (2007). Divergent genetic control of protein solubility and conformational quality in escherichia coli. *J. Mol. Biol.*, 374:195–205.

[Harrison et al., 2003] Harrison, R. G., Todd, P., Rudge, S., and Petrides, D. P. (2003). *Bioseparations Science and Engineering*. Oxford University Press, Inc., New York, New York.

[Hocalar and Turker, 2010] Hocalar, A. and Turker, M. (2010). Model based control of minimal overflow metabolite in technical scale fed-batch yeast fermentation. *Biochemical engineering journal*, 51(1-2):64–71.

[Jayaraj and Smooker, 2009] Jayaraj, R. and Smooker, P. (2009). So you need a protein - a guide to the production of recombinant proteins. *Open Veterinary Science Journal*, 3:28–34.

[Jenzsch et al., 2006a] Jenzsch, M., Gnoth, S., Beck, M., Kleinschmidt, M., Simutis, R., and Lubbert, A. (2006a). Open-loop control of the biomass concentration within the growth phase of recombinant protein production processes. *Journal of Biotechnology*, 127(1):84–94.

[Jenzsch et al., 2006b] Jenzsch, M., Simutis, R., and Luebbert, A. (2006b). Generic model control of the specific growth rate in recombinant escherichia coli cultivations. *Journal of Biotechnology*, 122(4):483–493.

[Jobe et al., 2003] Jobe, A. M., Herwig, C., Surzyn, M., Walker, B., Marison, I., and von Stockar, U. (2003). Generally applicable fed-batch culture concept based on the detection of metabolic state by on-line balancing. *Biotechnology and bioengineering*, 82(6):627–639.

[Johnston et al., 2002] Johnston, W., Cord-Ruwisch, R., and Cooney, M. (2002). Industrial control of recombinant e. coli fed-batch culture: new perspectives on traditional controlled variables. *Bioprocess and Biosystems Engineering*, 25(2):111–120.

[Johnston et al., 2003] Johnston, W. A., Stewart, M., Lee, P., and Cooney, M. J. (2003). Tracking the acetate threshold using do-transient control during medium

and high cell density cultivation of recombinant escherichia coli in complex media. *Biotechnology and bioengineering*, 84(3):314–323.

[Karakuzu et al., 2006] Karakuzu, C., Turker, M., and Ozturk, S. (2006). Modelling, on-line state estimation and fuzzy control of production scale fed-batch baker's yeast fermentation. *Control Engineering Practice*, 14(8):959–974.

[Keulers, 1993] Keulers, M. (1993). Structure and parameter identification of a batch fermentation process using non-linear modelling. In *American Control Conference, 1993*, pages 2261–2265.

[Kiran and Jana, 2009] Kiran, A. U. and Jana, A. (2009). Control of continuous fed-batch fermentation process using neural network based model predictive controller. *Bioprocess and Biosystems Engineering*, 32(6):801–808.

[Korz et al., 1995] Korz, D., Rinas, U., Hellmuth, K., Sanders, E., and Deckwer, W. (1995). Simple fed-batch technique for high cell-density cultivation of escherichia coli. *J. Biotechnology*, 39:59–65.

[Kudva and Narendra, 1973] Kudva, P. and Narendra, K. (1973). Synthesis of an adaptive observer using lyapunov's direct method. *Int. J. Control*, 18(6):1201–1210.

[Levisauskas et al., 1999] Levisauskas, D., Galvanauskas, V., Simutis, R., and Lubbert, A. (1999). Model based calculation of substrate/inducer feed-rate profiles in fed-batch processes for recombinant protein production. *Biotechnology Techniques*, 13(1):37–42.

[Liu et al., 2006] Liu, Y., Hu, R., Zhang, S., Zhang, F., Li, Z., Wei, X., and Chen, L. (2006). Expression of the foot-and-mouth disease virus vp1 protein using a replication-competent recombinant canine adenovirus type 2 elicits a humoral antibody response in a porcine model. *Viral Immunol.*, 19(2):202–209.

[Ljubenova and Ignatova, 1994] Ljubenova, V. and Ignatova, M. (1994). An approach for parameter estimation of biotechnological processes. *Bioprocess Engineering*, 11(3):107–113.

[Lubenova et al., 1993] Lubenova, V., Ignatova, M., and Tsonkov, S. (1993). On-line estimation of specific growth rate for a class of aerobic batch processes. *Chem.Biochem.Eng.*, 7(2):101–106.

[Mare et al., 2005] Mare, L., Velut, S., Ledung, E., Cimander, C., Norrman, B., Karlsson, E. N., Holst, O., and Hagander, P. (2005). A cultivation technique for e. coli fed-batch cultivations operating close to the maximum oxygen transfer capacity of the reactor. *Biotechnology Letters*, 27(14):983–990.

[Mohseni et al., 2009] Mohseni, S. S., Babaeipour, V., and Vali, A. R. (2009). Design of sliding mode controller for the optimal control of fed-batch cultivation of recombinant e. coli. *Chemical Engineering Science*, 64(21):4433–4441.

[Montesinos et al., 1995] Montesinos, J. L., Lafuente, J., Gordillo, M. A., Valero, F., Sola, C., Charbonnier, S., and Cheruy, A. (1995). Structured modeling and state estimation in a fermentation process: Lipase production by candida rugosa. *Biotechnology and bioengineering*, 48(6):573–584.

[Mosier and Ladisch, 2009] Mosier, N. S. and Ladisch, M. R. (2009). *Modern Biotechnology: Connecting Innovations in Microbiology and Biochemistry to Engineering Fundamentals*. John Wiley & Sons, Inc., Hoboken, New Jersey.

[Oliveira et al., 2005] Oliveira, R., Clemente, J. J., Cunha, A. E., and Carrondo, M. J. T. (2005). Adaptive dissolved oxygen control through the glycerol feeding in a recombinant pichia pastoris cultivation in conditions of oxygen transfer limitation. *Journal of Biotechnology*, 116(1):35–50.

[Oliveira et al., 2002] Oliveira, R., Ferreira, E. C., and de Azevedo, S. F. (2002). Stability, dynamics of convergence and tuning of observer-based kinetics estimators. *Journal of Process Control*, 12(2):311–323.

[Pepper et al., 2013] Pepper, M., Wang, L., Padmakumar, A., Burg, T., Harcum, S., and Groff, R. (2013). A real-time adaptive oxygen transfer rate estimator for metabolism tracking in escherichia coli cultures. In *BlueSens Report No.3*, pages 6–11. BlueSens gas sensors GmbH.

[Perrier et al., 2000] Perrier, M., de Azevedo, S. F., Ferreira, E. C., and Dochain, D. (2000). Tuning of observer-based estimators: theory and application to the on-line estimation of kinetic parameters. *Control Engineering Practice*, 8(4):377–388.

[Pico-Marco and Pico, 2003] Pico-Marco, E. and Pico, J. (2003). Partial stability for specific growth rate control biotechnological fed-batch processes. In *Control Applications, 2003. CCA 2003. Proceedings of 2003 IEEE Conference on*, volume 1, pages 724–728.

[Pinsach et al., 2006] Pinsach, J., de Mas, C., and Lopez-Santin, J. (2006). A simple feedback control of escherichia coli growth for recombinant aldolase production in fed-batch mode. *Biochemical engineering journal*, 29(3):235–242.

[Pomerleau and Perrier, 1990] Pomerleau, Y. and Perrier, M. (1990). Estimation of multiple specific growth rates in bioprocesses. *AIChE Journal*, 36(2):207–215.

[Pomerleau and Perrier, 1992] Pomerleau, Y. and Perrier, M. (1992). Estimation of multiple specific growth rates: Experimental validation. *AIChE Journal*, 38(11):1751–1760.

[Psichogios and Ungar, 1992] Psichogios, D. C. and Ungar, L. H. (1992). Process modeling using structured neural networks. In *American Control Conference, 1992*, pages 1917–1921.

[Rahman et al., 2010] Rahman, A. F. N. A., Spurgeon, S. K., and Yan, X. (2010). A sliding mode observer for estimating substrate consumption rate in a fermentation process. In *2010 11th International Workshop on Variable Structure Systems*, pages 172–177.

[Riesenberg et al., 1990] Riesenberg, D., Menzel, K., Schulz, V., Schumann, K., Veith, G., Zuber, G., and Knorre, W. (1990). High cell-density fermentation of recombinant escherichia coli expressing human interferon. *Appl. Microbiol. Biotechnol.*, 34:77–82.

[Rocha and Ferreira, 2002] Rocha, I. and Ferreira, E. C. (2002). An integrated system for advanced monitoring and control of fed-batch fermentations of recombinant e.coli. *Computer Applications in Biotechnology*, 2001:349–354.

[Rocha et al., 2008] Rocha, I., Veloso, A., Carneiro, S., Ferreira, E. C., and Costa, R. (2008). Implementation of a specific rate controller in a fed-batch e.coli fermentation. In *Proceedings of the 17th World Congress of The International Federation of Automatic Control (IFAC)*, volume 17, pages 15565–15570.

[Rocha et al., 2006] Rocha, I., Veloso, A., and Ferreira, E. C. (2006). Design of estimators for specific growth rate control in a fed-batch e.coli fermentation. In *Proceedings 5th MATHMOD Vienna - 5th Vienna Symposium on Mathematical Modelling, vol. 2: full papers CD*, ARGESIM report 30, pages 1.1–1.9. ARGESIM.

[Santos et al., 2010] Santos, L. O., Dewasme, L., Hantson, A. L., and Wouwer, A. V. (2010). Nonlinear model predictive control of fed-batch cultures of micro-organisms exhibiting overflow metabolism. In *Control Applications (CCA), 2010 IEEE International Conference on*, pages 1608–1613.

[Schaepe et al., 2011] Schaepe, S., Kuprijanov, A., Aehle, M., Simutis, R., and Lubbert, A. (2011). Simple control of fed-batch processes for recombinant protein production with e. coli. *Biotechnology Letters*, 33(9):1781–1788.

[Sharma et al., 2007] Sharma, S. S., Blattner, F. R., and Harcum, S. W. (2007). Recombinant protein production in an escherichia coli reduced genome strain. *Metabolic Engineering*, 9(2007):133–141.

[Simon and Karim, 2001] Simon, L. and Karim, M. N. (2001). Identification and control of dissolved oxygen in hybridoma cell culture in a shear sensitive environment. *Biotechnology progress*, 17(4):634–642.

[Simon and Karim, 2002] Simon, L. and Karim, M. N. (2002). Modeling and control of amino acid starvation-induced apoptosis in cho cell cultures. In *American Control Conference, 2002. Proceedings of the 2002*, volume 2, pages 1579–1584 vol.2.

[Tatiraju et al., 1998] Tatiraju, S., Soroush, M., and Mutharasan, R. (1998). Multi-rate nonlinear state and parameter estimation in a bioreactor. In *American Control Conference, 1998. Proceedings of the 1998*, volume 4, pages 2324–2328 vol.4.

[V., 1996] V., L. (1996). On-line estimation of biomass concentration and non stationary parameters for aerobic bioprocesses. *Journal of Biotechnology*, 46(3):197–207.

[Veloso et al., 2009] Veloso, A. C. A., Rocha, I., and Ferreira, E. C. (2009). Monitoring of fed-batch e. coli fermentations with software sensors. *Bioprocess and Biosystems Engineering*, 32(3):381–388.

[Velut et al., 2007] Velut, S., de Mare, L., and Hagander, P. (2007). Bioreactor control using a probing feeding strategy and mid-ranging control. *Control Engineering Practice*, 15(2):135–147.

[Vemuri et al., 2006] Vemuri, G. N., Altman, E., Sangurdekar, D. P., Khodursky, A. B., and Eiteman, M. A. (2006). Overflow metabolism in escherichia coli during steady-state growth: transcriptional regulation and effect of the redox ratio. *Appl Environ Microbiol*, 72(5):3653–61.

[Voisard et al., 2002] Voisard, D., Pugeaud, P., Kumar, A. R., Jenny, K., Jayaraman, K., Marison, I. W., and von Stockar, U. (2002). Development of a large-scale biocalorimeter to monitor and control bioprocesses. *Biotechnology and bioengineering*, 80(2):125–138.

[Wang et al., 2014] Wang, L., Pepper, M., Padmakumar, A., Burg, T., Harcum, S., and Groff, R. (2014). A real-time adaptive oxygen transfer rate estimator for metabolism tracking in escherichia coli cultures. In *Engineering in Medicine and Biology Society (EMBC), 2014 36th Annual International Conference of the IEEE*, pages 6191–6194.

[Wolfe, 2005] Wolfe, A. J. (2005). The acetate switch. *Microbiology and Molecular Biology Reviews*, 69(1):12–50.

[Xu et al., 1999] Xu, B., Jahic, M., and Enfors, S. O. (1999). Modeling of overflow metabolism in batch and fed-batch cultures of escherichia coli. *Biotechnology progress*, 15(1):81–90.